Chapter 11

The mitochondrion: from genome to proteome

Patrice P. Hamel[1,2], Thalia Salinas-Giegé[3], Jonathan Przybyla-Toscano[4,5], Anna Caccamo[5], Nitya Subrahmanian[6], Nicolas Rouhier[4], Laurence Drouard[3], Pierre Cardol[5], Diego Gonzalez-Halphen[7] and Claire Remacle[5]

[1]*Department of Molecular Genetics, The Ohio State University, Columbus, OH, United States,* [2]*Department of Biological Chemistry Pharmacology, The Ohio State University, Columbus, OH, United States,* [3]*Institut de biologie moléculaire des plantes, CNRS, Université de Strasbourg, Strasbourg, France,* [4]*Université de Lorraine, INRAE, IAM, Nancy, France,* [5]*Genetics and Physiology of Microalgae, InBios/Phytosystems Research Unit, University of Liège, Liège, Belgium,* [6]*Department of Neurology, College of Medicine, University of Florida, Gainesville, FL, United States,* [7]*Instituto de Fisiología Celular, Universidad Nacional Autónoma de México, México D.F., Mexico*

11.1 The mitochondrial genome

11.1.1 Replication, transcription, and translation

11.1.1.1 Genome structure, organization, and content

The *Chlamydomonas reinhardtii* (*Chlamydomonas* throughout) mitochondrial (mt) genome is 99% linear, and the remaining 1% corresponds to open and closed circular DNA molecules (Ryan et al., 1978). Physical mapping using restriction endonucleases and in vitro labeling of mtDNA confirmed that the genome is linear and has unique ends (Grant & Chiang, 1980). Each vegetative haploid cell contains ∼130 copies of mtDNA (Gallaher et al., 2018) organized into about 20−30 nucleoids (Hiramatsu et al., 2006; Nishimura et al., 1998). The nucleoids change in size and shape during the cell cycle while mitochondria appear as sinuous or highly branched structures extending throughout the cytoplasm, sometimes resembling a single large mitochondrion (Ehara, Osafune, & Hase, 1995; Hiramatsu et al., 2006).

The *Chlamydomonas* mt genome of 15.8 kb is characterized by low gene content, very short intergenic sequences, no introns, and a GC content of 45% on average. It contains seven protein-coding genes of the respiratory chain (*nad1*, *nad2*, *nad4*, *nad5*, *nad6*, *cob*, and *cox1*), a reverse transcriptase-like protein (*rtl*), three tRNAs (*trnW*, *trnQ*, and *trnM*), and 14 rRNA fragments (*LSU* and *SSU*) (Boer & Gray, 1988a, 1988b, 1988c; Gallaher et al., 2018; Gray & Boer, 1988; Michaelis, Vahrenholz, & Pratje, 1990; Salinas-Giegé et al., 2017). The ends of the mitochondrial genome, the telomeres, have been studied in detail (Ma et al., 1992; Michaelis et al., 1990; Vahrenholz et al., 1993). The left and the right telomeres are 532 and 530 bp, respectively. They are arranged in an inverted repeat orientation with 3′-overhangs of 40 nt. An intriguing feature is that the outermost 86 bp at each end are identical to an mtDNA internal sequence (Vahrenholz et al., 1993) (Fig. 11.1A).

11.1.1.2 Replication

The *Chlamydomonas* mtDNA replication mechanism remains to be elaborated. One proposed mechanism would involve the *rtl* gene (Boer & Gray, 1988a; Vahrenholz et al., 1993). In this model, the transcription of an internal 86 nucleotide (nt) sequence of the mtDNA (at the end of the *L2b* rRNA sequence) that matches the outermost 86 nt of the two telomeres is hypothesized to prime DNA synthesis at the ends of the genome. The reverse transcriptase-like protein would synthesize the nearly complete mtDNA molecules by copying the RNA primers associated with the parental strands (Fig. 11.1B). Interestingly, the analysis of linear mtDNAs of close relatives of *Chlamydomonas* shows that all the genomes possess an *rtl* gene located between the *L3* and *L8* rRNA coding modules and an internal repeat identical to the

The *Chlamydomonas* Sourcebook. DOI: https://doi.org/10.1016/B978-0-12-821430-5.00011-0
© 2022 Elsevier Inc. All rights reserved.

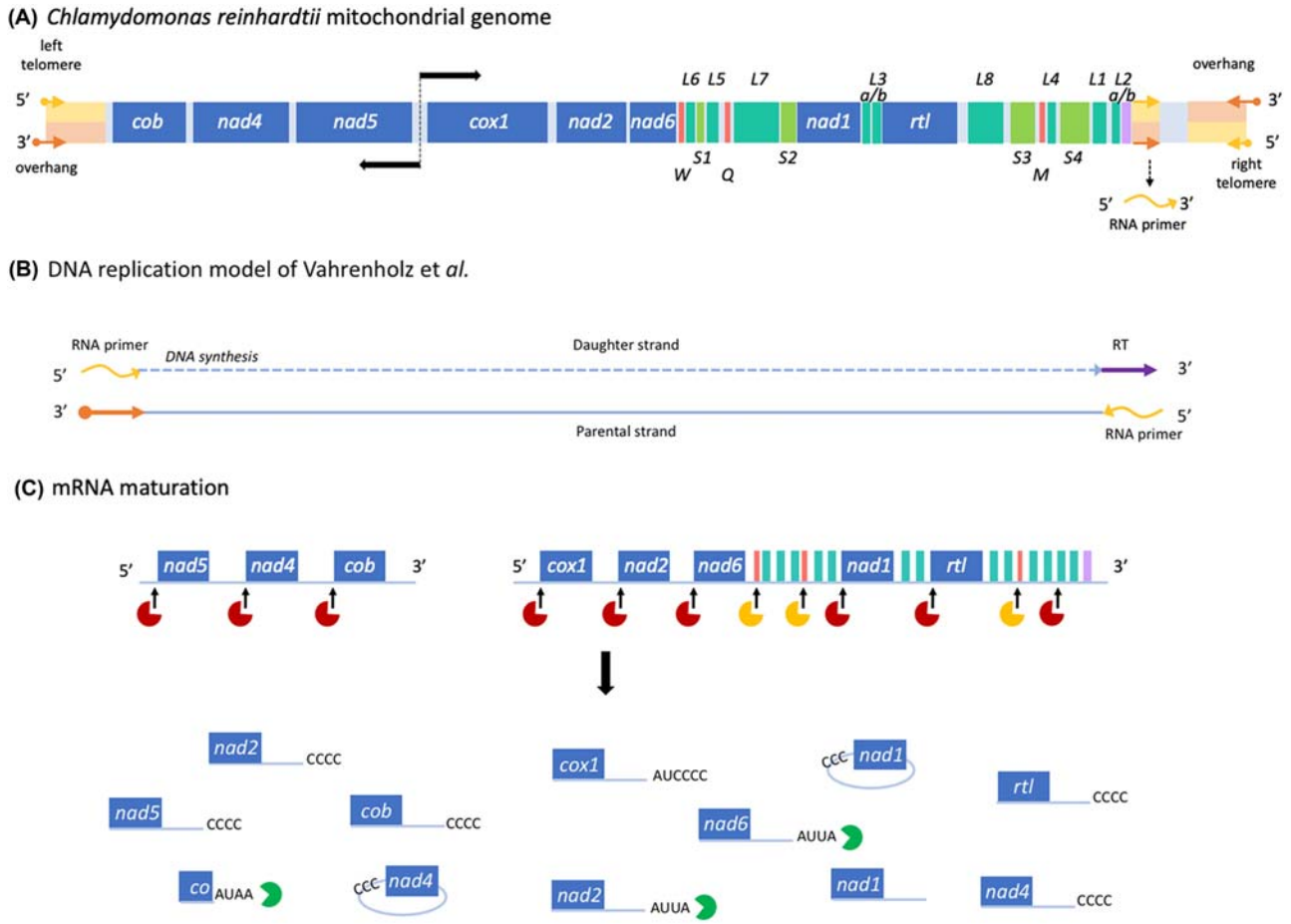

FIGURE 11.1 Mitochondrial genome of *Chlamydomonas*. (A) Physical map of the 15.8 kb linear mitochondrial genome (GenBank accession EU306622). Horizontal black arrows indicate the bidirectional transcription origin. The blue boxes represent the eight protein-coding genes: *cob* (apocytochrome *b* of complex III), *cox1* (subunit 1 of cytochrome *c* oxidase or complex IV), *nad1*, *2*, *4*, *5*, and *6* (subunits of NADH:ubiquinone oxidoreductase or complex I) and *rtl* (reverse transcriptase-like protein). The *nad1*, *2*, *4*, *5*, and *6* genes were previously named *nd1*, *2*, *4*, *5*, and *6*. The boxes in two shades of green represent *LSU* (*L1*−*L8*) and *SSU* (S1−S4) genes encoding the structural ribosomal RNA fragments. The dark pink boxes correspond to the 3 tRNA genes designated by the one-letter code (*W*, *Q*, and *M*). Bicolor orange and yellow boxes at each end of the genome represent the inverted terminal repeats, and the orange and yellow arrows denote the three copies of the 86 bp repeats (Vahrenholz et al., 1993). The yellow squiggle arrow represents the RNA primer generated for mitochondrial replication according to the model shown on B. Notably, the *Chlamydomonas* mitochondrial DNA lacks several of the genes usually present in mitochondrial genomes: *atp6*, *atp8, cox2*, *cox3*, *nad3*, and *nad4L*. (B) Replication model of the mitochondrial genome. The RNA primers (yellow squiggle arrows) will hybridize to the 86 nt of the telomeres (orange arrow). The reverse transcriptase-like protein will then synthesize (purple arrow) a complete mtDNA molecule by copying the RNA primer. (C) Transcription of the mtDNA generates two polycistronic primary transcripts. Unknown endoribonuclease(s) (red "pacman" symbols) cut each mRNA just upstream of its AUG start codon and the rRNA extremities. The only endoribonuclease identified to date is PRORP that cleaves at the 5′ ends of the tRNAs (yellow pacman symbols). The leaderless mRNAs with 3′ UTRs are then posttranscriptionally modified at their 3′ extremity by A/U-rich tails or C-rich tails. The A/U-rich tail may be a platform for 3′−5′ exoribonucleases degradation (green circular sectors), whereas the C-rich tails may constitute protection by stabilizing the longer transcript. Circularized full-length transcripts are observed according to Cahoon and Qureshi (2018). *For (B) Adapted from Vahrenholz, C., Riemen, G., Pratje, E., et al. (1993). Mitochondrial DNA of* Chlamydomonas reinhardtii*: The structure of the ends of the linear 15.8-kb genome suggests mechanisms for DNA replication.* Current Genetics, 24*, 241*−*247.*

extreme termini. The internal repeat location is consistently adjacent to the right telomere with an orientation suitable for DNA synthesis initiation (Smith & Craig, 2021). Although attractive, this hypothesis requires experimental confirmation.

11.1.1.3 Transcription

Both strands of *Chlamydomonas* mtDNA encode genetic information. Transcription starts in the short intergenic region between *nad5* and *cox1* genes and generates two divergent polycistronic transcripts (Gray & Boer, 1988). Two potential

promoter sequences for the bidirectional transcription initiation were identified. The first one, TTATTACAT, is located 3 nt upstream of the ATG codon of the *cox1* gene, and the second one, TTATTATTT, is located 3 nt upstream of the ATG codon of the *nd5* gene (Duby et al., 2001). The *Chlamydomonas MOC1* gene encodes a member of the mTERF (mitochondrial transcription termination factor) family targeted to mitochondria and whose expression is increased in response to light. MOC1 binds specifically to an octanucleotide sequence within the *S3* rRNA, and the loss of MOC1 in the mutant *stm6* increases readthrough transcription at the *S3*-binding site, thereby causing elevated antisense RNA levels. The impaired transcription termination in the *stm6* mutant alters the mitochondrial transcriptome and affects the physiological state of the plastid, causing an increased light sensitivity of the mutant (Schönfeld et al., 2004; Wobbe & Nixon, 2013).

11.1.1.4 RNA maturation

11.1.1.4.1 Endonucleolytic cleavage

After transcription, polycistronic RNAs are subsequently processed into individual transcripts by endonucleolytic cleavage. An extensive analysis showed that most of the time, the endonucleolytic cleavage generates both the 3′ end of a mature upstream RNA and the 5′ end of the downstream RNA. All protein-encoding transcripts start at the AUG initiation codon; they are leaderless mRNAs and possess 3′ UTRs with sizes corresponding to the downstream intergenic regions (between 14 and 275 nt) (Boer & Gray, 1988b; Gray & Boer, 1988; Salinas-Giegé et al., 2017) (http://chlamy-organelles.ibpc.fr).

The mtDNA encodes only three tRNAs. Therefore the "tRNA punctuation" model, where primary transcripts are processed by precise endonucleolytic cleavages by RNases P and Z before and after each tRNA to release mature RNAs, as for human mitochondria (Ojala et al., 1980), does not apply to *Chlamydomonas* mitochondrial transcripts. A unique RNase P protein, PRORP (protein-only RNase P), is targeted to the nucleus, the chloroplast, and mitochondria (Bonnard et al., 2016). This protein processes the 5′ end of tRNAs by endonucleolytic cleavage. For the moment, PRORP is the only endoribonuclease known in *Chlamydomonas* mitochondria. Thus the identity of the endonuclease(s) that cleave at the AUG initiation codon of mRNAs and at the rRNA extremities remains to be determined (Fig. 11.1C).

11.1.1.4.2 Posttranscriptional modification of mitochondrial RNAs

Three types of untemplated 3′ nucleotide additions have been reported in *Chlamydomonas* mitochondria: adenylation, uridylation, and cytidylation (Cahoon & Qureshi, 2018; Gallaher et al., 2018; Salinas-Giegé et al., 2017; Zimmer et al., 2009) (Fig. 11.1C). The addition of A-rich and U-rich tails in *Chlamydomonas* RNAs appears to be part of the RNA degradation pathway in mitochondria, like in land plants (Levy & Schuster, 2016). These additions are postulated to play the role of a "platform" to guide degradation by 3′−5′ exoribonucleases (Zimmer et al., 2009). In contrast to the A/U-rich tails, the C-rich tails are not present in truncated RNAs (Gallaher et al., 2018). Instead, they are primarily present in mRNAs and are more frequent at or near the initial endonucleolytic cleavage site (Cahoon & Qureshi, 2018; Gallaher et al., 2018; Salinas-Giegé et al., 2017). The C-rich tail function is unknown, but they could constitute a means of protecting/stabilizing translatable mRNAs (Salinas-Giegé et al., 2017). This polycytidylation process represents a previously undescribed early maturation event restricted to the members of the Chlorophyceae lineage (Salinas-Giegé et al., 2017).

The location of such added tails at the 3′ end of transcripts suggests that ribonucleotides are incorporated in a template-independent manner by a nucleotidyltransferase (NTR) (Martin & Keller, 2007). A phylogenetic analysis of the 13 NTRs of *Chlamydomonas* shows that 4 of them, namely, PAP2, PAP4, PAP6, and PAP10, are specific to Chlorophyceae and thus constitute good candidates to carry out this activity (Salinas-Giegé et al., 2017), and in particular PAP4 which is a mitochondria-targeted protein (Zimmer, Fei, & Stern, 2008).

11.1.1.5 Translation

11.1.1.5.1 Mitoribosomes

Mitoribosomes, composed of small and large subunits (SSU and LSU, respectively) perform mt translation. They have a bacterial origin, and their catalytic core composed of rRNAs resembles that of bacterial ribosomes. However, they evolved separately in different eukaryotic lineages and acquired specific features (Waltz & Giegé, 2020). Our knowledge of *Chlamydomonas* mitoribosomes was sparse (Atteia et al., 2009; Boer & Gray, 1988c; Denovan-Wright & Lee, 1995; Nedelcu, 1997). Analysis of *C. reinhardtii* and *C. eugametos* mitoribosomes indicated that they sediment at

approximately 60−66S (Denovan-Wright & Lee, 1995). This trait is different from what is observed for land plant mitoribosomes (around 80S) and bacterial ribosomes (70S).

It is only recently that the *Chlamydomonas* mitoribosome structure was described (Waltz et al., 2021). It was resolved by combining biochemistry, genetics, single-particle cryo-electron microscopy (cryo-EM), and in situ cryo-electron tomography (cryo-ET). This structure confirmed the uniqueness of the *Chlamydomonas* mitoribosome with an overall architecture distinct from the bacterial ancestor and the land plant mitoribosomes. According to the available mitoribosome structures of diverse organisms, ribosomal proteins (r-proteins) can be divided into proteins derived from the ancestral bacteria (ancestral r-proteins) and specific proteins (mitoribosome r-proteins) recruited during evolution in eukaryote lineages. The *Chlamydomonas* mitoribosome contains 47 r-proteins in the LSU and 36 in the SSU, making a total of 83 r-proteins compared to the 54 r-proteins in bacterial ribosomes. Among these r-proteins, 54 are ancestral r-proteins, 18 are mitoribosome r-proteins shared with other mitoribosomes, and 11 are specific to *Chlamydomonas*. Most of the latter group protein members are helical repeat proteins, that is, 1 mTERF protein, 6 OctotricoPeptide Repeat (OPR) proteins, and 2 PentatricoPeptide Repeat (PPR) proteins. The structure shows that these proteins interact with rRNA fragments to stabilize them in the mitoribosome. In *Chlamydomonas*, the 23S-like and 16S-like rRNA sequences of mitochondrial LSU and the SSU, respectively, are scrambled and interspersed with one another and with both protein-coding and tRNA genes (Fig. 11.1A). In 1998 Boer and Gray postulated a secondary modeling structure in which fragmented rRNAs are mainly stabilized by base pairing, making the *Chlamydomonas* system one of the first to show that an rRNA does not have to be covalently continuous to be functional (Boer & Gray, 1988c; Denovan-Wright & Lee, 1995). Indeed, the mitoribosome structure confirmed this, and it also showed that among all the rRNA pieces predicted to be integrated into the mature mitoribosome, all but one (*L2b*) were present. Therefore the 23S-like rRNA comprises 8 modules (*L1*, *L2a*, *L3b*, *L4*, *L5*, *L6*, *L7*, *L8*) and the 16S-like rRNA, 4 modules (*S1*, *S2*, *S3*, and *S4*). The *L2b* fragment is expressed and accumulates in mitochondria, but its function remains to be elucidated (see Section 11.1.2). The gene encoding the third rRNA, the 5S rRNA, which associates with the LSU, was thought to be absent from the mtDNA (Boer & Gray, 1988c; Nedelcu, 1997). However, the mitoribosome structure allowed its identification as the *L3a* fragment. This *L3a* RNA was likely derived from an ancestral bacterial 5S rRNA that has become highly diverged, with only a 6 consecutive nt consensus that confirmed its origin (Waltz et al., 2021).

11.1.1.5.2 tRNAs

The *Chlamydomonas* mitochondrial genome encodes only three tRNA genes, foreshadowing the import from the cytosol of the vast majority of tRNAs, which ensures the proper functioning of the mitochondrial translational machinery. Studies carried out to date on organisms in which there is mitochondrial import of tRNAs have shown that the imported tRNAs are of nuclear origin. However, previous studies strongly suggested that chloroplasts could also supply tRNAs to mitochondria (Bennoun & Delosme, 1999). An in-depth study of the *Chlamydomonas* mitochondrial tRNA population demonstrated that it was exclusively composed of imported tRNAs from the cytosol. The analysis of the 49 isoacceptor tRNA families encoded by the nuclear genome indicates that mitochondrial tRNA import is very selective: quantification by Northern blots of each nucleus-encoded tRNA isoacceptor in both the cytosolic and the mitochondrial fractions showed an import rate for each cytosolic tRNA ranging from 0.2% to 95% (Cognat et al., 2008; Vinogradova et al., 2009). Remarkably, the observed steady-state distribution of an imported tRNA reflects the frequency of occurrence of the cognate codon in both mitochondrial and the nuclear genes. This fine-tuning between tRNA import and codon usage appears to originate from a coevolution process rather than from a dynamic adaptation of cytosolic tRNA import into mitochondria (Salinas et al., 2012).

11.1.1.5.3 Aminoacyl-tRNA synthetases

All organellar aminoacyl-tRNA synthetases (aaRSs) are nucleus-encoded. As protein synthesis occurs in three subcellular compartments (cytosol and the two organelles), a minimum of 60 nucleus-encoded aaRS genes is a priori required. However, only 33 aaRS genes have been identified in *Chlamydomonas* (Cognat et al., 2013). From the 33 aaRS genes identified, there are two genes for which 13 amino acids are substrates, and a single gene for which 7 amino acids are substrates. Some aaRS-encoding genes probably escaped detection, but the reduced number of aaRS strongly suggests an extensive sharing of such enzymes among subcellular compartments in algae. Such a result has been observed in *Arabidopsis thaliana*, where it was demonstrated that at least 15 aaRSs are shared between mitochondria and chloroplasts, and 5 between mitochondria and the cytosol (Duchêne, Pujol, & Maréchal-Drouard, 2009). This observation raises several intriguing questions of how the same aaRS can recognize tRNAs of different origins.

11.1.1.5.4 Translation

Like in plant mitochondria, *Chlamydomonas* mitochondria use the universal genetic code, but in contrast to plants, there is no C to U editing in mitochondrial transcripts. The codon usage is biased, and nine codons are never used. All mRNAs have an AUG initiation codon and a UAA or UAG stop codon (Boer & Gray, 1988b; Kück & Neuhaus, 1986; Michaelis et al., 1990).

Bacterial translation initiation depends on a Shine-Dalgarno (SD) sequence located around eight bases upstream of the start codon. In *Chlamydomonas*, leaderless mRNAs do not have an SD sequence. Hence, the mechanisms for mRNA recruitment to the SSU and for the correct positioning of start codons are unclear. Years before showing that mt mRNAs do not possess 5′ UTRs, the compilation of the eight protein-coding genomic sequences allowed the definition of a putative ribosome-binding site (RBS), ATTTTATTA, or ATAATTTA, upstream of the AUG codon (Colleaux et al., 1990). Now we know that this putative RBS is, in fact, present in the 3′ UTR of the upstream mRNAs. Elements within the 3′ UTRs may play an essential role in the processing, stability, or translation of these mRNAs. Indeed, the mitochondrial mutants *dum24* and *dum5*, which have missing stem-loop secondary structure and a single nucleotide deletion in the 3′ UTR of *nd5*, respectively, show a severe reduction of the processed *nd5* mRNA levels (Cardol, Matagne, & Remacle, 2002; Duby et al., 2001). Cahoon and colleagues reported that circularized mRNAs associated with ribosomes were detected in *Chlamydomonas* mitochondria. They propose that mRNAs circularization creates leader sequences upstream of mRNAs for translation initiation (Cahoon & Qureshi, 2018). This is an attractive hypothesis that requires further experimental testing to be validated.

Finally, virtually nothing is known about *Chlamydomonas* mitochondria translation regulation. However, extensive genetic studies on *Chlamydomonas* chloroplast revealed various factors involved in chloroplast translation regulation, mainly through interactions with the 5′ UTR of the transcript. Many of these regulatory factors belong to the Octatricopeptide Repeat (OPR) family, which is composed of more than 120 members (Boulouis et al., 2015). As mentioned above, eight OPR proteins belong to the mitoribosome. Still, many others are predicted to be mitochondrially targeted and it is possible that they are involved in mitochondrial translation (Vol. 2, Chapter 13), potentially through interactions with the 3′ UTR.

11.1.1.6 Respiratory-deficient mutants

Respiratory-deficient mutants have been reviewed in Cardol & Remacle (2009) and Salinas et al., (2014) and are briefly described in the following section. Identification of such mutants is easy because of their null or slow growth phenotype that is evident under conditions where growth only relies on respiration, for example, in the dark when acetate is supplied in the medium (heterotrophic conditions). Both the respiratory chain and the glyoxylate cycle (Durante et al., 2019; Lauersen et al., 2016; Plancke et al., 2014) are required for acetate assimilation and the generation of energy in the dark; mutants strongly compromised for either of these pathways are “dark-diers” (Plancke et al., 2014).

Mutants of mitochondrial genes exhibit uniparental inheritance that is associated with the mitochondrial genome from the mating-type minus parent (Matagne et al., 1989). Biolistic transformation of mutants displaying a large deletion of one of the ends of the mitochondrial genome has been achieved, while site-directed mutants of specific respiratory subunits have been generated (Larosa et al., 2012; Remacle et al., 2006; Salinas et al., 2012). Null mutants include mutations in the mitochondrial *cob* gene encoding apocytochrome *b* (complex III) or in the mitochondrial *cox1* gene encoding subunit 1 of cytochrome *c* oxidase (complex IV). Strains compromised for nucleus-encoded mitochondrial/respiratory proteins obtained by RNA interference (*COX3* and *COX17* genes, see section on complex IV) have also been isolated (Remacle et al., 2010). These mutants have lost the cytochrome-based respiratory pathway because the activities of complexes III and IV work sequentially. The loss of these two proton-pumping enzymes is probably the reason why these mutants cannot grow under heterotrophic conditions. These mutants are thus obligate phototrophs.

Mutants affected in complex I (the mitochondrial genes *nd1*, *nd4*, *nd5*, and *nd6* or nuclear genes *ND3*, *ND4L*, *ND7*, *ND9*, *PSDW*, *NUO5*, *NUOFAF3*, *AMC1*) (see Section 11.2.1.1), exhibit reduced growth in the dark probably because they retain only two of the three oxidative phosphorylation (OXPHOS) sites that are operational when electron transfer proceeds through the whole respiratory chain. Complex I mutants also show a less severe phenotype compared to complex III and complex IV mutants in the light under mixotrophic conditions (light + acetate) for the same reason (Barbieri et al., 2011; Massoz et al., 2014; Massoz et al., 2017; Remacle et al., 2001). As a consequence, their proteome does not show many differences compared to that of wild-type cells (Senkler, Senkler, & Braun, 2017a).

Complex III deficiencies and to a lesser degree complex I deficiencies have an impact on photosynthesis activity (Cardol et al., 2003). This is the reason why complex I or complex III mutants, when combined with mutations affecting the regulation of photosynthesis (*stt7* and *pgrl1*), display a decreased photosynthetic efficiency. These characteristics allow for easy identification of complex I and complex III mutants using fluorescence measurements after mutagenesis of *sst7* or *pgrl1* mutants (Massoz et al., 2015, 2017).

11.2 Mitochondrial proteome

11.2.1 Oxidative phosphorylation complexes

OXPHOS is defined as an electron transfer chain driven by substrate oxidation that is coupled to the synthesis of ATP through an electrochemical transmembrane gradient. The major components are schematically represented (Fig. 11.2).

11.2.1.1 Complex I

With more than 40 subunits and a size of 1 MDa, mitochondrial NADH:Ubiquinone oxidoreductase (complex I) is the largest respiratory enzyme. Complex I, the main entry point of the electrons in OXPHOS, catalyzes the oxidation of NADH and the reduction of ubiquinone (Q) coupled to the pumping of four protons from the matrix side to the intermembrane space (IMS) (Senkler et al., 2017a). Complex I contains 14 subunits of bacterial origin conserved among all eukaryotes and referred to as core subunits. A set of accessory/supernumerary or noncore subunits, whose number varies between 31 and 35 is present in mitochondrial complex I (Table 11.1) (Cardol et al., 2004; Carroll et al., 2003; Dang et al., 2020; Peters, Belt, & Braun, 2013). Among the noncore subunits, 24 appear conserved in all mitochondrial complex I and the remaining constitute a signature of a specific lineage (Cardol et al., 2004; Elurbe & Huynen, 2016). Noncore subunits are not *stricto sensu* required for enzymatic function but when missing or mutated, disruption of complex I assembly and/or activity is a commonly observed consequence (Dang et al., 2020). With two arms, one protruding in the matrix and the other embedded in the inner mitochondrial membrane, the complex I L-shaped structure is conserved from bacteria to eukaryotes. The matrix arm is further separated into the N-module that catalyzes NADH oxidation and the Q module which is the site of ubiquinone reduction. Five core subunits in the matrix arm carry the redox prosthetic groups (eight Fe-S clusters and one FMN, Table 11.1) transferring the electrons from NADH to ubiquinone. In the membrane arm, often divided into a proximal module (P_P) and a distal module (P_D), the reduction of ubiquinone drives proton translocation by a mechanism presumed to rely on a long range propagation of conformational modifications (Kampjut & Sazanov, 2020). The conformational changes involve four separate proton channels, three of them are located in the ND2, ND4, and ND5 subunits while the fourth one comprises at least ND1 and ND3 (Berrisford, Baradaran, & Sazanov, 2016; Cabrera-Orefice et al., 2018; Zickermann et al., 2015). Additional conformational rearrangements associated with an active-to-de-active transition have been mapped to a region of the quinone-binding site (Babot et al., 2014; Kampjut & Sazanov, 2020). Such changes in conformation appear

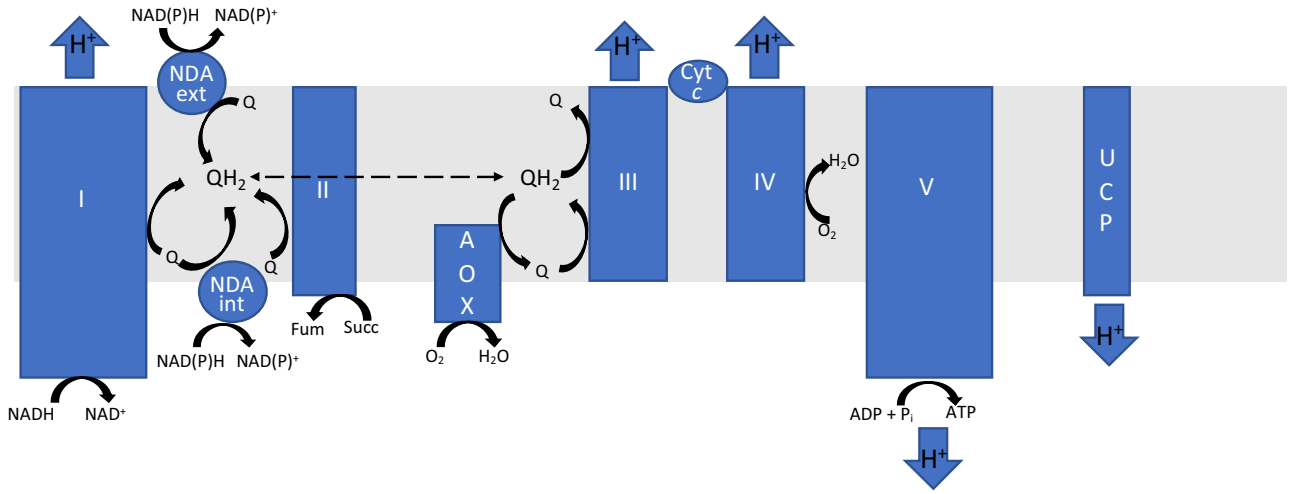

FIGURE 11.2 Schematic representation of the OXPHOS of *Chlamydomonas* mitochondria. *Adapted from Cardol, P., & Remacle, C. (2009). The mitochondrial genome. In The* Chlamydomonas *sourcebook, Organellar and* metabolic processes *(pp. 445–467). San Diego: Elsevier Inc.*

TABLE 11.1 Complex I subunits and biogenesis factors in *Chlamydomonas* and other organisms.

Complex I constituents and expression/assembly factors					
Constituents (subunits)					
Gene	**Phytozome accession number #**	**Common protein product name**	***Arabidopsis* accession #**	***Homo sapiens***	**Cofactor(s) / lipids**
NUO6	Cre10.g422600	51 kDa	At5g08530	*NDUFV1*	NAD^+, FMN, (4Fe-4S)
NUO5	Cre10.g450400	24 kDa	At4g02580	*NDUFV2*	(2Fe-2S)
NUOS1	Cre12.g535950	75 kDa	At5g37510	*NDUFS1*	(2Fe-2S) (4Fe-4S (4Fe-4S)
NUO8	Cre12.g496750	TYKY / 23 kDa	At1g16700 / At1g79010	*NDUFS8*	(4Fe-4S) (4Fe-4S)
NUO10	Cre12.g492300	PSST / 20 kDa	At5g11770	*NDUFS7*	(4Fe-4S), PC
NUO9	Cre07.g327400	NAD9 / 30 kDa	AtMg00070	*NDUFS3*	
NUO7	Cre09.g405850	NAD7/ 49 kDa	AtMg00510	*NDUFS2*	
Core bacterial subunits—membrane arm					
nad1	CreMt.g802343	Nad1	AtMg00516 / AtMg01120 / AtMg01275	*MT-ND1*	
nad2	CreMt.g802341	Nad2	AtMg00285 / AtMg01320	*MT-ND2*	2 × PC
NUO3	Cre08.g378900	NAD3	AtMg00990	*MT-ND3*	
NUO11	Cre09.g402552	NAD4L	AtMg00650	*MT-ND4L*	
nad4	CreMt.g802338	Nad4	AtMg00580	*MT-ND4*	
nad5	CreMt.g802339	Nad5	AtMg00513 / AtMg0060 / AtMg00665	*MT-ND5*	
nad6	CreMt.g802342	Nad6	AtMg00270	*MT-ND6*	
Conserved eukaryotic accessory subunits—matrix arm					
NUOS4	Cre03.g146247	18 kDa	At5g67590	*NDUFS4*	
NUOS6	Cre03.g178250	13 kDa	At3g03070	*NDUFS6*	Zn^{2+}
NUOB8	Cre16.g679500	B8	At5g47890	*NDUFA2*	
NUO13	Cre11.g467767	DAP13 / B17.2	At3g03100	*NDUFA12*	
NUOB13	Cre13.g568800	B13	At5g52840	*NDUFA5*	
NUOA7	Cre12.g484700	B14.5a	At5g08060	*NDUFA7*	
NUOA9	Cre10.g434450	39 kDa	At2g20360	*NDUFA9*	NADPH
ACP1	Cre16.g673109	SDAP-1 / SDAP-2	At1g65290 / At2g44620	*NDUFAB1*	
–	–	–	–	*NDUFA10*	
–	–	–	–	*NDUFV3*	
Conserved eukaryotic accessory subunits—membrane arm					
NUOA1	Cre10.g459750	MWFE	At3g08610	*NDUFA1*	1 × PC
NUOA3	Cre12.g537050	B9	At2g46540	*NDUFA3*	
NUOB14	Cre12.g555250	B14	At3g12260	*NDUFA6*	
NUOA8	Cre07.g333900	PGIV-1/PGIV-2	At3g06310 / At5g18800	*NDUFA8*	
NUOA11	Cre14.g617826	B14.7	At2g42210	*NDUFA11*	

(*Continued*)

TABLE 11.1 (Continued)

Complex I constituents and expression/assembly factors					
Constituents (subunits)					
Gene	**Phytozome accession number** [#]	**Common protein product name**	***Arabidopsis* accession** [#]	***Homo sapiens***	**Cofactor(s) / lipids**
NUOB16	Cre16.g664600	B16.6 / GRIM-19	At1g04630 / At2g33220	*NDUFA13*	
NUO21	Cre06.g267200	20.9 kDa / MNLL	At4g16450	*NDUFB1*	
–	–	AGGG	At1g76200	*NDUFB2*	
NUOB12	Cre05.g244901	B12–1 / B12–2	At2g02510 / At1g14450	*NDUFB3*	
NUOB4	Cre03.g204650	B15	At2g31490	*NDUFB4*	
–	–	SGDH[a]	At1g67785[a]	*NDUFB*[a]	
NUOB18	Cre06.g278188	B18	At2g02050	*NDUFB7*	
NUO18	Cre01.g007850	ASHI	At5g47570	*NDUFB8*	
NUOB22	Cre11.g467668	B22	At4g34700	*NDUFB9*	
NUOB10	Cre12.g555150	PDSW-1 / PDSW-2	At3g18410 / At1g49140	*NDUFB10*	
NUO17	Cre05.g240800	ESSS-1 / ESSS-2	At2g42310 / At3g57785	*NDUFB11*	
NUOC1	Cre17.g725400	KFYI	At4g00585	*NDUFC1*	
NUOP1	Cre13.g571150	B14.5b	At4g20150	*NDUFC2*	
NUOS5	Cre12.g511200	15 kDa-1/15 kDa-2	At3g62790 / At2g47690	*NDUFS5*	
ACP1	Cre16.g673109	SDAP-1/ SDAP-2	At1g65290/At2g44620	*NDUFAB1*	
–	–	–	–	*NDUFA10*	
–	–	–	–	*NDUFB6*	
Carbonic anhydrase domain					
CAG1	Cre12.g516450	CA3	At5g66510	–	Zn^{2+}, HCO_3^-, 2 × PI, 1 × CL
CAG2	Cre06.g293850	CAL2	At3g48680	–	
CAG3	Cre09.g415850	CA2	At1g47260	–	
–	–	CA1	At1g19580	–	
–	–	CAL1	At5g63510	–	
Plant-specific subunits					
–	–	P1 / 11 kDa	At1g67350		–
–	–	P2 / 16 kDa	At2g27730		–
NUOP3	Cre02.g100200	NUOP3	At3g07480		–
NUOP4	Cre08.g378550		–	–	–
NUOP5	Cre08.g378050		–	–	–
Expression and assembly factors					
AMC1[b]	Cre16.g688900	AMC1	–	–	
NUOFAF1	Cre02.g076750	CIA30	At1g72420 / At1g17350	*NDUFAF1*	
NDUFAF2	Cre09.g401150	B17.2L / mimitin	At4g26965	*NDUFAF2*	
NDUFAF3[b]	Cre12.g496800	C3ORF60	At3g60150 / At2g44525	*NDUFAF3*	
–	–	C6ORF66	At3g21400	*NDUFAF4*	

(*Continued*)

TABLE 11.1 (Continued)

Complex I constituents and expression/assembly factors

Constituents (subunits)

Gene	Phytozome accession number [#]	Common protein product name	*Arabidopsis* accession [#]	*Homo sapiens*	Cofactor(s) / lipids
NDUFAF5	Cre13.g584750	–	At1g22800	*NDUFAF5*	
NDUFAF6	Cre03.g194300	C8ORF38	At1g62730	*NDUFAF6*	
NDUFAF7	Cre02.g096400	C20ORF7	At3g28700	*NDUFAF7*	
–	–	C17ORF89	–	*NDUFAF8*	
TIM17	Cre10.g452650	TIMMDC1	At1g20350	*TIMMDC1*	
–	Cre06.g296400	ACAD9	At3g45300	*ACAD9*	
–	–	ECSIT	–	*ECSIT*	
		TMEM126A		*TMEM126A*	
–	–	TMEM126B	–	*TMEM126B*	
FAO12	Cre16.g671450	FOXRED1	At2g24580	*FOXRED1*	
–	–	ATP5SL	–	*ATP5SL / DMAC2*	
–	–	TMEM261	–	*DMAC1 / TMEM261*	
INDH1	Cre10.g427050	INDH/IND1	At4g19540	*NUBPL*	
GLDH1	Cre13.g567100	GLDH	At3g47930	–	
CPLD69	Cre01.g028150	CIAF1	At1g76069	–	
–	–	–	–	*AIF*	
OXA1 *OXA3*	Cre03.g198150 Cre16.g690200	OXA1	At5g62050 At2g46470	*OXAIL*	
–	–	TMEM186	–	*TMEM186*	
–	–	TMEM242	–	*TMEM242*	
–	Cre12.g540051	TMEM70	At2g35790 / At2g32450	*TMEM70*	
COCA1	Cre05.g232752	COA1	At2g20390	*COA1*	

The accession numbers for *Chlamydomonas* genes are provided from the Phytozome *Chlamydomonas* genome database v5.6 and v6.1. The accession numbers for *Arabidopsis thaliana* genes are provided from TAIR (The Arabidopsis Information Resource) as a comparison to vascular plant orthologs and human proteins for a reference to mammalian orthologs (Stroud et al., 2016). Notably, the NAD3 and NAD4L subunits are nucleus-encoded in *Chlamydomonas* (Cardol et al., 2006). A majority of the vascular plant orthologs have been confirmed as *bona fide* complex I subunits based on the proteomic analyses of *Arabidopsis* complex I and structural analyses of *Brassica oleracea* (cauliflower) and *Vigna radiata* (mung bean)complexes (Soufari et al., 2020; Maldonado et al., 2020; Klusch et al., 2021).

[a]*This subunit initially assigned to complex I (Peters et al., 2013) was not identified in plant complex I structures (Klusch et al., 2021; Maldonado et al., 2020; Soufari et al., 2020). The* Chlamydomonas *complex I subunit orthologs were identified based on sequence similarity and proteomic analyses (Cardol et al., 2004, 2005, 2008). Complex I consists of one FMN molecule and eight Fe-S clusters as cofactors required for its oxidoreductase activity, bound by specific subunits detailed in the last column. In addition, structural analyses have revealed the presence of several lipids in the complex I structure (PC: phosphatidylcholine, PI: phosphatidylinositol, CL: cardiolipin), one* Zn^{2+}*, and one NADPH (Klusch et al., 2021; Maldonado et al., 2020; Soufari et al., 2020). The final section of this table also lists potential factors controlling the biogenesis of the* Chlamydomonas *holoenzyme. A total of 23 biogenesis factors have been identified to date for mammalian complex I (Carroll et al., 2021; Formosa et al., 2018; Formosa et al., 2020; Formosa et al., 2021; Sánchez-Caballero et al., 2020; Thompson et al., 2018). All* Arabidopsis *and* Chlamydomonas *orthologs presented in this table were identified by similarity searches such as BLASTp, PSI-BLAST, and DELTA-BLAST. Among these, only NUBPL ortholog has been functionally confirmed with a role in complex I biogenesis in plants (Wydro et al., 2013). In addition, GLDH and CIAF1 have been determined as plant-specific biogenesis factors through studies of* Arabidopsis *complex I (Ivanova et al., 2019; Schertl et al., 2012; Schimmeyer et al., 2016). Orthologs of mammalian complex I biogenesis factors were identified based on similarity using BLAST.*

[b]*In* Chlamydomonas*, only two factors AMC1 and NDUFAF3, have been confirmed as biogenesis factors (Massoz et al., 2017; Subrahmanian et al., 2020). Some accessions have entries in several tables due to their role in different pathways.*

[#]*# = number.*

to be absent in bacterial and vascular plant complex I but have been documented in several, but not all, fungal and animal complexes I that have been experimentally investigated. Atomic-resolution X-ray or cryo-EM structures of complex I at 3−5 Å are now available from the bacterium *Thermus thermophilus* (Baradaran et al., 2013), the fungus *Yarrowia lipolytica* (Parey et al., 2018; Parey et al., 2019; Zickermann et al., 2015), *Ovis aries* (sheep) and *Bos taurus* (cattle) (Fiedorczuk et al., 2016; Vinothkumar, Zhu, & Hirst, 2014; Zhu, Vinothkumar, & Hirst, 2016), *Brassica oleracea* (cauliflower), *Vigna radiata* (mung bean), *A. thaliana* and the colorless green alga *Polytomella* (Klusch et al., 2021; Maldonado et al., 2020; Soufari et al., 2020).

In plants, complex I is best characterized in *A. thaliana* (Braun et al., 2014; Meyer, Welchen, & Carrie, 2019; Subrahmanian, Remacle, & Hamel, 2016). From biochemical and structural studies in plants, *Chlamydomonas* complex I is estimated to comprise a total of 45 subunits (Table 11.1). From the 45 subunits, 29 have been biochemically confirmed to be *bona fide* complex I subunits and four additional subunits have been assigned based on genetic evidence (Cardol et al., 2004) (Table 11.1). Among the lineage-specific noncore subunits, two (NUOP4 and NUOP5) appear to be restricted to the Chlorophyceans, one is plant-specific (NUOP3), and three (CAG1, CAG2, CAG3) are found in all eukaryotes except mammals and fungi (Cardol et al., 2004). In plant complex I, the membrane and soluble arms of the enzyme are connected by a bridge consisting of complex I-FDX (NUOP3 in *Chlamydomonas*), an unusual ferredoxin subunit specific to the plant lineage (Klusch et al., 2021).

The CAG subunits are isoforms of gamma carbonic anhydrases (γ-CA) forming a matrix-exposed spherical domain attached to the P_P module of the membrane domain of complex I (Klusch et al., 2021; Maldonado et al., 2020; Schimmeyer, Bock, & Meyer, 2016; Soufari et al., 2020; Sunderhaus et al., 2006) (Fig. 11.3). *Chlamydomonas* CAG subunits are still present in complex I intermediates lacking the P_D module, indicating that the location of the γ-CA module is with the P_P module, like in land plants (Cardol et al., 2004; Cardol et al., 2008). One cardiolipin coordinated by two phosphatidylinositol molecules is positioned at the interface between the γ-CAs and the membrane arm, suggesting that the lipid provides a docking site for this domain onto the rest of the enzyme (Soufari et al., 2020). The γ-CAs are a class of metalloenzymes catalyzing the reversible hydration of CO_2 to HCO_3^- (Ferry, 2010). A canonical γ-CA trimer is characterized by three active sites, each formed by Zn^{2+}-coordinating histidine residues at the interface of two protomers (Giachin et al., 2016). In vascular plant complex I γ-CAs also assemble as a trimer and one of the three interfaces of the trimeric domain is formed by subunits containing the critical Zn-binding histidines. Accordingly, one Zn^{2+} and a density tentatively assigned to HCO_3^- were detected in this interface of the γ-CA trimer (Meyer et al., 2019; Subrahmanian et al., 2016). The other two interfaces of the trimeric γ-CA do not display all the essential metal-coordinating histidines and, expectedly, no bound Zn^{2+} is detected (Maldonado et al., 2020; Soufari et al., 2020). Therefore there is one potentially catalytically active interface of the three interfaces present in the γ-CA trimeric domain of complex I. However, carbonic anhydrase activity of the complex I-attached γ-CAs still awaits experimental confirmation.

The function of the γ-CAs in complex I is not fully understood but there is experimental support in *Arabidopsis* for a role in recycling mitochondrial CO_2 released by matrix-localized catabolic processes (including glycine−serine conversion during photorespiration) for carbon fixation in the chloroplast (Eisenhut, Roell, & Weber, 2019; Fromm et al., 2016a). The γ-CA module is needed for complex I assembly, but this role does not require a presumably active trimer as variants lacking the Zn-coordinating histidines of the active interface are still able to support the establishment of wild-type levels of complex I in *Arabidopsis* (Formosa et al., 2018). *Polytomella* γ-CA is lacking all the catalytic residues and no bound Zn could be detected, an indication that this domain is probably enzymatically inactive (Fromm, Braun, & Peterhansel, 2016b). Since *Polytomella* is unable to grow photoautotrophically, a functional γ-CA domain in complex I might be linked to photosynthetically active eukaryotes. This view is reinforced by the finding that the zinc-coordinating histidines are also missing in the γCA domain of complex I in the nonphotosynthetic protist *Acanthamoeba castellanii* (Gawryluk & Gray, 2010). Cyanobacterial photosynthetic complex I, which is distinct from respiratory complex I, also exhibits a carbonic anhydrase module—with a few notable differences. This is not a γ-type CA and the module was shown to be active in the conversion of CO_2 to HCO_3^-. The module, structurally resolved by cryo-EM, is positioned at the distal end of the membrane, and shows connectivity to the proton-pumping subunits (Schuller et al., 2020).

Complex I assembly proceeds *via* the formation of several subunit-containing modules defining assembly intermediates. Such intermediates can be detected as subcomplexes in vivo when complex I does not accumulate or in some instances alongside the holoenzyme. The modules are formed independently by the incorporation of specific core and noncore subunits and further combined in a stepwise manner to yield the active holoenzyme. Plant complex I assembly intermediates have been best characterized in *Arabidopsis* (Braun et al., 2014; Meyer et al., 2019; Subrahmanian et al., 2016). While the modular mode of complex I assembly appears to be a common theme for

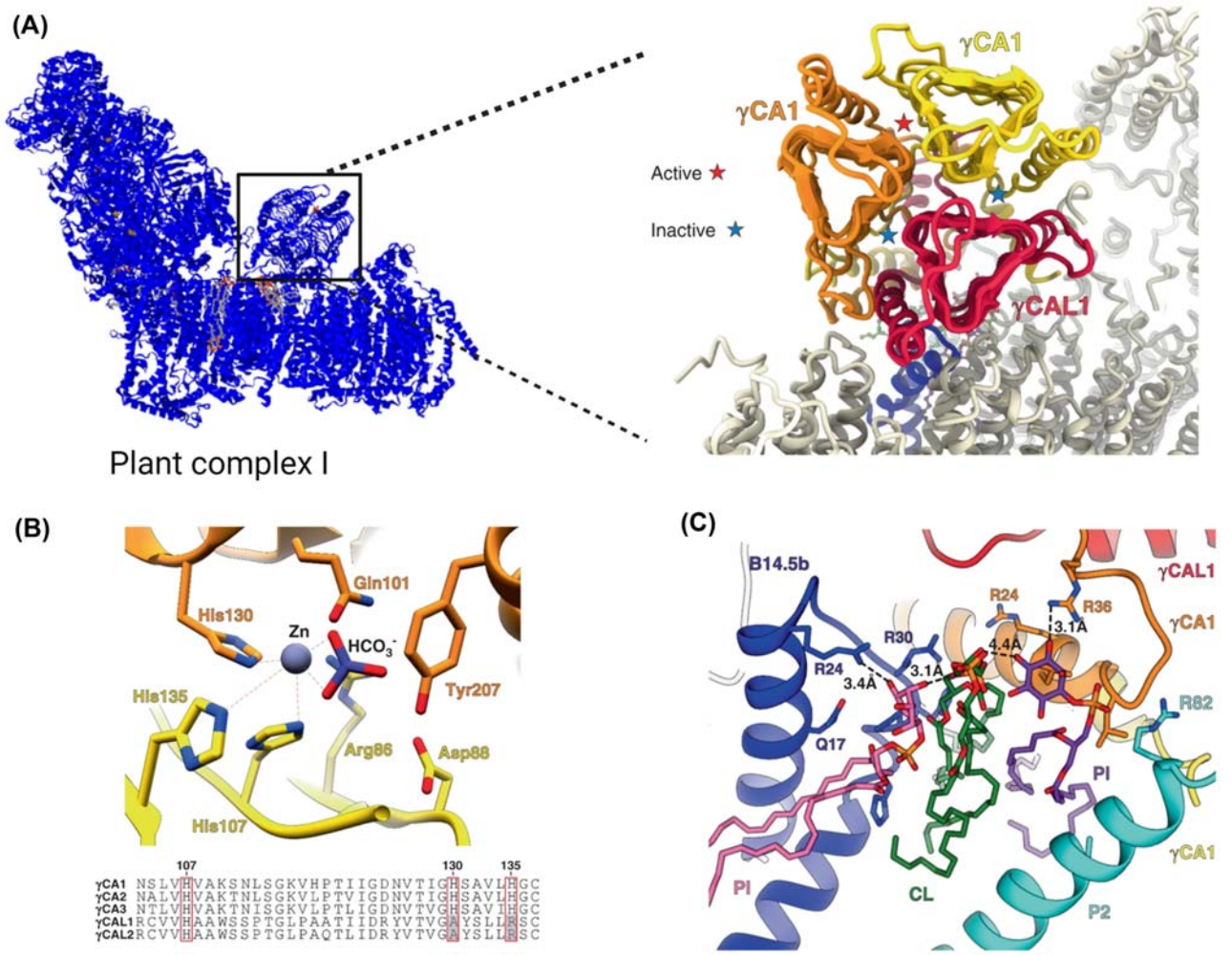

FIGURE 11.3 The carbonic anhydrase module of complex I modeled from cryo-electron microscopy of vascular plants. (A) Mitochondrial complex I 3D structure from *Brassica oleracea* (PDB ID: 7A23). The three carbonic anhydrase subunits form a canonical trimer. However, only one of the interfaces between each monomer potentially harbors an active site. (B) The single active site is bound by Zn^{2+} through coordination with three histidine residues. HCO_3^- has also been assigned to this site. (C) The carbonic anhydrase module is attached to the membrane arm through one cardiolipin (bright green molecule) and two phosphatidylinositol molecules (pink and purple, respectively). *Adapted from Soufari, H., Parrot, C., Kuhn, L., et al. (2020). Specific features and assembly of the plant mitochondrial complex I revealed by cryo-EM. Nat*ure *Commun*ications, 11*, 5195, based on the Creative Commons license (http://creativecommons.org/licenses/by/4.0/). Created with Biorender.com.*

holoenzyme formation across lineages, differences in the order in which the assembly modules are attached do exist. In animals, the N-module is assembled last onto a complex intermediate containing the Q module attached to the entire membrane arm (Formosa et al., 2018; Guerrero-Castillo et al., 2017; Stroud et al., 2016). In plant complex I, assembly is finalized by incorporation of the P_D extension onto an intermediate, already containing the N, Q, and P_P modules. The basis for such a difference remains obscure. In several plants, an N and Q module-containing complex I intermediate, but missing P_D, referred to as complex I* was identified as the last intermediate before final assembly (Ligas et al., 2019; Maldonado et al., 2020). The complex I* is missing two of the four proton channels but displays NADH-Q oxidoreductase activity in vitro. This form of complex I was hypothesized to function as an NADH-Q oxidoreductase with a lower H^+-pumping-to-electron-transfer ratio ($2H^+$:$2e^-$ ratio) than the complete holoenzyme ($4H^+$:$2e^-$ ratio) in vivo. The physiological relevance of this form of complex I awaits further experimental investigation (Maldonado et al., 2020).

In *Chlamydomonas*, modules (or subcomplexes) of 200 and 700 kDa are the only biochemically identified complex I intermediates (Subrahmanian et al., 2016). The 200 kDa module is soluble, displays NADH dehydrogenase activity and represents an early intermediate for assembly of the matrix arm (Cardol et al., 2002). The 700 kDa subcomplex is

loosely bound to the mitochondrial inner membrane and corresponds to a late intermediate in the assembly process that contains the entire soluble arm, the γ-CAs and the P_P modules (Cardol et al., 2008). The 700 kDa module is lacking the P_D extension of the membrane arm and its accumulation is diagnostic of a block in the assembly of the distal complex I arm (Barbieri et al., 2011; Cardol et al., 2002; Cardol et al., 2006). Some other assembly intermediates, such as the one that corresponds to the carbonic anhydrase domain, must exist but has still not been biochemically identified in *Chlamydomonas*.

Complex I assembly is a highly orchestrated process assisted by a plethora of assembly factors, which are not part of the final holoenzyme but can be found associated to some assembly intermediates (Alston et al., 2020; Formosa et al., 2018; Giachin et al., 2016). Twenty-three assembly factors have been identified to be required for assembly of mammalian complex I, out of which thirteen appear to be conserved in *Arabidopsis* and *Chlamydomonas* based on sequence similarity (Table 11.1). Conceivably, some of the assembly factors could have diverged considerably so that they fail to be recognized by bioinformatics analyses. Moreover, most of the candidate complex I assembly factors await experimental validation in plants. Elucidating the precise molecular function of these factors remains challenging. In the absence of motifs indicative of an activity, several of them are presumed to act as chaperones in the assembly process. However, biochemical activity has been determined for a few of the assembly components such as NDUFAF5, an arginine hydroxylase that catalyzes the addition of a hydroxyl group onto a specific arginine in NDUFS7, a subunit in the Q-module (Rhein et al., 2016). In *Arabidopsis*, only three assembly factors have been thus far confirmed to be involved in the formation of complex I: L-galactono-1,4-lactone dehydrogenase (GLDH) (Pineau et al., 2008; Schertl et al., 2012; Schimmeyer et al., 2016), the protein INDH (Wydro et al., 2013), and the LYR protein CIAF1 (Ivanova et al., 2019). Functional dissection of CIAF1 supports a role in the delivery of Fe-S clusters to subunits in the soluble arm of complex I. INDH appears to have a dual function, with a role in mitochondrial translation and the potential for transferring Fe-S clusters to complex I subunits during their maturation (Wydro et al., 2013). GLDH, the only plant-specific assembly factor, catalyzes the last enzymatic step of ascorbate biosynthesis (Millar et al., 2003). The enzyme associates with several membrane-bound complex I intermediates in the mitochondrial matrix (Ligas et al., 2019). Binding of GLDH to complex I*, the largest complex I intermediate, was evidenced in the resolved cryo-EM structure (Soufari et al., 2020). Comparison to the complete holoenzyme suggests that GLDH acts by preventing the binding of plant-specific P1 subunit (Table 11.1) to the P_P module. Following the release of GLDH, P1 binds and associates with the P_D module. Although the molecular mechanism of GLDH in assembly remains unclear, its function as an assembly factor is distinct from its enzymatic role in ascorbate synthesis (Schimmeyer et al., 2016). In *Chlamydomonas*, a P1-like protein does not appear to be present, and it is unclear from the limited proteomic analyses if the 700 kDa complex corresponds to the complex I* intermediate identified in vascular plants.

NDUFAF3 and AMC1 are the only two assembly factors known to function in complex I formation in *Chlamydomonas* (Massoz et al., 2017; Subrahmanian et al., 2020). NDUFAF3 is also conserved in humans and is associated from the early to the late assembly intermediates consisting of subunits from the Q module (Maio et al., 2017). Similar to mammalian complex I, loss of NDUFAF3 in *Chlamydomonas* results in decreased steady state levels of Q module subunits and decreased levels of fully assembled enzyme (Saada et al., 2009). On the other hand, AMC1 appears restricted to *Chlamydomonas* and is poorly conserved among the closest known relatives of *Chlamydomonas* (Subrahmanian et al., 2020). The absence of AMC1 results in a distal membrane arm assembly defect, evidenced by accumulation of the 700 kDa subcomplex. In addition, the loss of AMC1 yields decreased levels of the mitochondrial transcript *nad4*, which encodes a subunit required for the assembly of the distal end of the membrane arm. Although its exact mechanism of action remains to be determined, AMC1 is involved in complex I biogenesis through its role in mitochondrial *nad4* expression.

11.2.1.2 Complex II

Complex II or succinate dehydrogenase catalyzes the reversible conversion of succinate into fumarate and the reduction of ubiquinone to ubiquinol and is part of both the tricarboxylic acid cycle (TCA) cycle and the respiratory chain. It is a small heterotetrameric complex of approximately 110 kDa anchored in the inner mitochondrial membrane (IMM) by two small hydrophobic subunits (SDH3 and SDH4), with two soluble subunits (SDH1 and SDH2) protruding into the matrix. Crystallization and structure determination have been obtained for both bacterial and eukaryotic enzymes (Sun et al., 2005; Yankovskaya et al., 2003). SDH1 bears a FAD cofactor close to the succinate-binding site while SDH2 contains three Fe-S clusters (see Section 11.2.2.2). Two ubiquinone reduction sites are present on SDH3 and SDH4 with a *b*-type heme located at the interface between these two subunits. The subunit composition is conserved in

Chlamydomonas (Table 11.2) (Cardol et al., 2005; Cardol et al., 2009) but in land plants four additional subunits are found, one hydrophilic (SDH5) and the three others (SDH6−8) that are more hydrophobic (Eubel, Jänsch, & Braun, 2003; Millar et al., 2004; Schikowsky, Senkler, & Braun, 2017). SDH6−7 are thought to compensate for missing sequence stretches of SDH3 and SDH4 and contribute to anchoring the complex to the IMM (Schikowsky et al., 2017).

Two electrons from succinate are transferred to FAD, individually fueled by the three Fe-S clusters, and then to the membrane-located ubiquinone-binding site where ubiquinone (Q) is reduced to ubiquinol (QH_2). The *b*-type heme would not be required for catalysis (Oyedotun, Sit, & Lemire, 2007).

SDH1 and SDH2 are conserved proteins encoded in the nuclear genome of almost all eukaryotes. SDH3 and SDH4 have been transferred from the mitochondrial genome to the nuclear genome multiple times and are less well conserved (Huang et al., 2019). In *Chlamydomonas*, the four subunits are nucleus-encoded.

Regarding the assembly (Moosavi et al., 2019), two assembly factors, SDHAF1 and SDHAF2, participate in the insertion of the Fe-S clusters and of the FAD cofactor in SDH2 and SDH1, respectively. The role of SDHAF1 in Fe-S cluster insertion has been demonstrated in human but not in yeast. SDHAF3 is postulated to work together with SDHAF1 for maturation of SDH2 during oxidative metabolism and reactive oxygen species (ROS) production. SDHAF4 acts as a chaperone that binds to SDH1-FAD to prevent ROS formation that would likely be produced upon exposing FAD to the environment. The first step of assembly is the maturation of SDH1 and SDH2, which is followed by their dimerization and their insertion into the membrane through interactions with SDH3 and SDH4. TCM62 and FLX1 are specific to yeast; the former is a mitochondrial carrier of succinate and fumarate, and the latter would be

TABLE 11.2 Complex II subunits and biogenesis factors in *Chlamydomonas* and other organisms.

Complex II constituents and assembly factors					
Constituents (subunits)					
Chlamydomonas			Counterparts in other organisms		
Gene	Protein product	Phytozome accession [#]	*Homo sapiens*	Yeast	*Arabidopsis* accession [#,a]
SDH1	Succinate dehydrogenase flavoprotein subunit	Cre14.g619133	*SDHA*	*SDH1*	At5g66760, At2g18450
SDH2	Iron-sulfur protein of succinate dehydrogenase	Cre06.g264200	*SDHB*	*SDH2*	At3g27680, At5g40650, At5g65165
SDH3	Succinate dehydrogenase subunit b560	Cre01.g020350	*SDHC*	*SDH3*	At5g09600, At4g32210
SDH4	Succinate dehydrogenase (ubiquinone) membrane anchor subunit	Cre01.g020305	*SDHD*	*SDH4*	At2g46505
–	–	–	–	–	At1g47420 (*SDH5*)
–	–	–	–	–	At1g08480 (*SDH6*)
–	–	–	–	–	At3g47833, At5g62575 (*SDH7*)
–	–	–	–	–	At2g46390 (*SDH8*)
Assembly factors					
SDHAF1	SDHAF1	Cre13.g801514	*SDHAF1*	*SDH6*	At2g39725
SDHAF2	SDHAF2	Cre12.g550750	*SDHAF2*	*SDH5*	At5g51040
SDHAF3	SDHAF3	Cre06.g278242	*SDHAF3*	*SDH7*	At3g19508
–	–	–	*SDHAF4*	*SDH8*	At5g67490
–	–	–	–	*TCM62*	–

[a] *Accession numbers according to Meyer et al. (2019) and Salinas et al. (2014).*
[#] *# = number.*

involved in the flavination of SDH1, but their roles in complex II assembly are still debated. Two assembly factors have been characterized in *A. thaliana*: SDHAF2 and SDHAF4. Knockdown mutants of *SDHAF2* display reduced amounts of complex II and a decrease of SDH1-FAD, demonstrating the conserved role of SDHAF2 in flavination (Huang et al., 2013). Knockout mutants of SDHAF4 are missing the SDH1/SDH2 intermediate (Belt et al., 2018). SDHAF1 and SDHAF3 are LYRM proteins. In *Chlamydomonas* three (SDHAF1, EMI5, DC11) out of the four canonical assembly factors have been predicted based on genome analysis (Table 11.2), but nothing is known about the assembly steps of complex II.

11.2.1.3 Complex III

Complex III (or cytochrome bc_1), the third complex of the OXPHOS chain and the second proton pumping complex, catalyzes electron transfer from reduced ubiquinone to soluble cytochrome *c*. This complex is a symmetrical dimer, each monomer containing 10 and 11 subunits in yeast and mammals, respectively (Ndi et al., 2018) (Table 11.3). The additional subunit in human (Su9) is generated by cleavage of the N-terminal sequence of the UQCRCFS1 protein (Rieske Iron-Sulfur Protein). Crystal structures have been solved in many eukaryotic species

TABLE 11.3 Complex III subunits and biogenesis factors in *Chlamydomonas* and other organisms.

Complex III constituents and expression/assembly factors					
Constituents (subunits)					
Chlamydomonas			**Counterparts in other organisms**		
Gene	Protein product	Phytozome accession [#]	*Homo sapiens*	Yeast	*Arabidopsis* accession [#,a]
QCR1	Core 1	Cre12.g523850	*UQCR1*	*COR1*	At3g02090
QCR2	Core 2	Cre12.g509750	*UQCR2*	*COR2*	At3g16480, At1g51980 (Ryan et al., 1978)
Cob	Cytochrome *b*	CreMt.g802337	*MT-CYB*	*COB*	AtMg00220
CYT1	Cytochrome c_1	Cre15.g638500	*CYC1*	*CYT1*	At3g27240, At5g40810
RIP1	Rieske iron-sulfur protein	Cre01.g051900	*UQCRCFS1*	*ISP, RIP1*	At5g13440, At5g13430
QCR6[b]	QCR6[b]	Cre16.g801917[b]	*UQCRH*	*QCR6*	At2g01090, At1g15120
QCR7	QCR7	Cre06.g262700	*UQCRB*	*QCR7*	At4g32470, At5g25450
QCR8	QCR8	Cre03.g156950	*UQCRQ*	*QCR8*	At3g10860, At5g05370
QCR9	QCR9	Cre11.g468950	*UQCR10*	*QCR9*	At3g52730
QCR10	QCR10	Cre09.g409150	*UQCR11*	*QCR10*	At2g40765
Expression and assembly factors					
BCS1	BCS1	Cre05.g234661	*BCS1L*	*BCS1*	At5g17760, AtMg00570
–	–	–	–	*FMP25*	–
UCC1	CBP3, UCC1	Cre01.g052050	*UQCC1*	*CBP3*	At5g51220
–	–	–	*UQCC3*	*CBP4*	At1g79390
–	–	–	*UQCC2*	*CBP6*	–
–	–	–	*TTC19*	–	–
LYRM7	LYRM7	Cre07.g332150	*LYRM7*	*MZM1*	At3g62810

[a] *Accession numbers according to Meyer et al. (2019) and Salinas et al., (2014).*
[b] Chlamydomonas *QCR6 was missing in the previous* Chlamydomonas *genome annotations on Phytozome (v5.5), but has been restored in the newer v6.1 annotations as Cre16.g801917.*
[#] *# = number.*

(reviewed in Ndi et al. 2018). The three catalytic subunits which are of bacterial origin comprise: cytochrome *b* (*cob*), cytochrome c_1 (*CYC1*), and the Rieske iron-sulfur (Fe-S) protein (*RIP1*, see Section 11.2.2.2). Cytochrome *b* contains a ubiquinone oxidation site (Q_o) located at the IMS side and a ubiquinone reduction site (Q_i) located at the matrix side, separated by two *b*-type hemes. One heme (b_L) is close to the Q_o site and has a low redox potential and the other heme (b_H), located close to the Q_i site, has a higher potential (Crofts et al., 2017). The Rieske protein contains a (2Fe-2S) center allowing electron transfer from cytochrome *b* to cytochrome c_1. Cytochrome c_1 contains a *c*-type heme. The other proteins of eukaryotic origin are involved in maintaining the stability of the complex (Ndi et al., 2018).

The electron transfer from reduced ubiquinone to cytochrome *c* is accomplished by the Q cycle (reviewed in Crofts et al., 2017). In this cycle, QH_2 is oxidized in a bifurcated reaction at the Q_o site where one electron is transferred successively from the Rieske protein to cytochrome c_1, and then to soluble cytochrome *c*. The remaining semiquinone at the Q_o site is oxidized by hemes b_L and b_H, and the latter delivers the electron to reduce ubiquinone at the quinone-reducing site (Q_i -site). The cycle is repeated when a second ubiquinol enters and gets oxidized, leading to a second electron being transferred to cytochrome *c*, and the semiquinone to be fully reduced into ubiquinol at the Q_i site by the second electron. In this way, four protons are ejected into the IMS and two protons from the matrix are used to produce a ubiquinone on the Q_i site. Like in yeast and *A. thaliana* (reviewed in Meyer et al., 2019), *Chlamydomonas* complex III would possess 10 subunits (Cardol et al., 2005, 2009) (Table 11.3).

Complex III assembly is well studied in yeast and human (reviewed in Ndi et al., 2018) and will be here shortly described for yeast using the yeast nomenclature. The mitochondrion-encoded cytochrome *b* protein is cotranslationally inserted in the membrane. The assembly proteins CBP3-CBP6 bind to cytochrome *b* after its translation for stabilization. Heme b_L is inserted in cytochrome *b* with the assistance of CBP4, followed by insertion of heme b_H. At that stage, dimerization would occur although this is not yet clear. The CBP3-CBP6 cofactors are released and subunits QCR7 and 8 are attached to cytochrome *b*. Four additional subunits are then inserted (QCR6, cytochrome c_1, COR1 and COR2) while at the same time CBP4 is released. QCR9, QCR10, and ISP are finally incorporated. The incorporation of ISP requires MZM1, a LYR protein, which functions as a chaperone for stabilization of the holo-ISP (Fe-S cluster-bound form) in the matrix (Atkinson et al., 2011; Ndi et al., 2018). ISP is then incorporated into complex III by BCS1, an AAA-ATPase. BCS1 is responsible for the translocation of the holo-ISP from the matrix to the IMS side of complex III. FMP25 is a fungal-specific assembly factor anchored in the membrane that is proposed to be required before the insertion of ISP into complex III. TTC19 (tetratricopeptide domain 19) is a human-specific factor found in a high-molecular-weight complex at the IMM side that interacts with complex III (Ndi et al., 2018). Three assembly factors (BCS1, UCC1, LYRM7) are encoded in the nuclear genome of *Chlamydomonas*, but nothing is known about their participation in the assembly process. Notably CBP4, a factor required for insertion of the b_L, appears to be absent, an indication that the pathway for heme insertion might be different in *Chlamydomonas*.

11.2.1.4 Complex IV

Complex IV is the last proton pumping complex of the OXPHOS chain with a size of approximately 200 kDa. It catalyzes electron transfer from reduced cytochrome *c* to molecular oxygen in a process coupled to the transfer of four protons across the inner membrane. The COX1, COX2, and COX3 subunits are the core subunits of bacterial origin. COX1 bears two hemes (*a*, a_3) and a copper center (Cu_B), COX2 carries another copper center (Cu_A), COX3 does not harbor any prosthetic groups. Eukaryotic complex IV contains 14 subunits in mammals (Timón-Gómez et al., 2018), and 11 in yeast (Soto et al., 2012). It is the least characterized respiratory complex in *A. thaliana* where it is estimated to contain approximately 14 components (Mansilla et al., 2018; Meyer et al., 2019; Senkler et al., 2017b). In *Chlamydomonas* the holoenzyme is resolved in 10 subunits by 2D/BN-PAGE among which eight are identified (Table 11.4) (van Lis et al., 2003). In most organisms, COX1, COX2, and COX3 are encoded in the mitochondrial genome. The remaining subunits are encoded in the nuclear genome and play a role in the biogenesis or stability of the complex. However, *COX2* or *COX3* but never *COX1* can be found in the nuclear genome, in land plants (Daley, Clifton, & Whelan, 2002), and in Chlorophyceae, including *Chlamydomonas* (see Section 11.2.2.1).

For the electron flow inside the complex, cytochrome *c* interacts with a domain of COX2 which protrudes in the IMS and electrons are transferred to the Cu_A center of COX2. The electrons pass to heme *a* of COX1, which transfers the electrons to the heme a_3-Cu_B center where O_2 is reduced to water (Soto et al., 2012). In

TABLE 11.4 Complex IV subunits and biogenesis factors in *Chlamydomonas* and other organisms.

Complex IV constituents and expression/assembly factors						
Constituents (subunits)						
Chlamydomonas			**Counterparts in other organisms**			
Gene	**Protein product**	**Phytozome accession** [#]	***Homo sapiens***	**Yeast**	***Arabidopsis* accession** [#,a]	
cox1	Subunit 1	CreMt.g802340	*MT-CO1*	*COX1*	AtMg01360	
COX2A *COX2B*	Subunit 2A Subunit 2B	Cre03.g154350 Cre01.g049500	*MT-CO2*	*COX2*	AtMg00160	
COX3	Subunit 3	Cre04.g221700	*MT-CO3*	*COX3*	AtMg00730	
COX4	Subunit 5b, subunit 4	Cre13.g567600	*COX5b*	*COX4*	At3g15640, At1g80230, At1g52710	
COX5C	Subunit 5c	Cre03.g157700	–	–	At3g62400, At2g47380, At5g61310, At5g40382	
–	–	–	*COX4*	*COX5b*	At4g00860, At1g01170	
–	–	–	*COX5a*	*COX6*	–	
–	–	–	*COX7a*	*COX7*	At4g21105	
–	–	–	*COX6c*	*COX7a*	At2g47380, At5g40382, At5g61310	
–	–	–	*COX7c*	*COX8*	At1g72020	
–	–	–	*COX8*	–	–	
COX12	Subunit 12	Cre06.g304350	*COX6b*	*COX9*	At1g22450, At5g57815, At1g32710, At4g28060	
COX13	Subunit 13	Cre12.g537450	*COX6a*	*COX10*	At4g37830	
–	–	–	*COX7b*			
–	–	–	*COX8*			
–	–	–	–	–	At4g14570[b]	
–	–	–	–	–	At4g00960[b]	
–	–	–	–	–	At3g12150[b]	
Expression and assembly factors				Proposed role[c]	*Arabidopsis* Accession [#]	
OXA1 *OXA3*	OXA1 OXA3	Cre03.g198150 Cre16.g690200	*OXA family*		Membrane insertion of COX subunits	At5g62050 At2g46470
COX10	COX10	Cre12.g516350	*COX10*	*COX10*	Farnesylation of heme *a*	At2g44520
COX11	COX11	Cre01.g055550	*COX11*	*COX11*	Insertion of Cu_B in COX1	At1g02410
–	–	–	*COX14*	*COX14*	Interaction with COX1	–

(*Continued*)

TABLE 11.4 (Continued)

Complex IV constituents and expression/assembly factors

Constituents (subunits)						
Chlamydomonas			Counterparts in other organisms			
Gene	**Protein product**	**Phytozome accession #**	***Homo sapiens***	**Yeast**	***Arabidopsis* accession #,a**	
COX15	COX15	Cre02.g082700	*COX15*	*COX15*	Biosynthesis of heme *a*	At5g56090.1
COX16	COX16	Cre03.g165400	*COX16*	*COX16*	Interaction with COX1	At4g14145
COX17	COX17	Cre05.g232850	*COX17*	*COX17*	Binding of two copper ions and delivery to SCO1	At3g15352.1, At1g53030
COX19	COX19	Cre10.g454550	*COX19*	*COX19*	Transduction of a SCO1-dependent redox signal	At1g66590/ At1g69750
–	–	–	*COX20*	*COX20*	Maturation and assembly of COX2, interaction with SCO1/ SCO2	–
COX23	COX23	Cre03.g213425	–	*COX23*	Homolog of COX17	At4g12340, At1g02160/ At5g09570
SHY1	SHY1	Cre16.g664700	*SURF1*	*SHY1*	Interaction with COX1 (expression)	At3g17910/ At1g48510
SCO1	SCO1	Cre17.g732850	*SCO1*	*SCO1*	Copper chaperone, transport of copper to the Cu_A site of COX2	At3g08950
SCO2	SCO2	Cre07.g339200	*SCO2*	*SCO2*	Copper chaperone, transport of copper to the Cu_A site of COX2	At4g39740
–	–	–	*COA3*	*COA3*	Component of MITRAC (mitochondrial translation regulation assembly intermediate of cytochrome c oxidase complex)	–
COX191	COX191	Cre01.g069107	*PET191*	*PET191*	ND	At1g10865
CMC1	CMC1	Cre10.g440150	*CMC1*	*CMC1*	Component of MITRAC	At5g16060
CMCL1	CMC1-like	Cre06.g286400	–	–	–	–
CMC2	CMC2	Cre16.g682587	*CMC2*	*CMC2*	CMC1 homolog	At4g21192
–	–	–	*HIGD1A*	*RCF1*	Assembly of super complexes, COX12 and COX13 assembly	At3g48030
–	–	–	*HIGDA2*	*RCF2*	Assembly of super complexes, COX12 and COX13 assembly	–
COX90	COX90	Cre16.g691850	–	–	–	–

[a]*Accession numbers according to Meyer et al. (2019) and Salinas et al. (2014).*
[b]*Candidate complex IV subunits of* Arabidopsis.
[c]*Proposed roles according to UNIPROT (Mansilla et al., 2018; Meyer et al., 2019).*
[#]*# = number.*

Chlamydomonas, the COX2 subunit is encoded by two independent nuclear genes, *COX2A* and *COX2B*, and mitochondria import the cytosol-synthesized COX2A and COX2B subunits and integrate them into complex IV. COX2A is equivalent to the N-terminal, membrane-bound half of the typical COX2 subunit, while the COX2B corresponds to the hydrophilic, C-terminal half of a conventional COX2 protein (Perez-Martínez et al., 2001).

The assembly of complex IV is by far the best characterized and a detailed analysis of the assembly process is described in bacteria (Schimo et al., 2017), yeast (Soto & Barrientos, 2016), mammals (Timón-Gómez et al., 2018), and plants (Mansilla et al., 2018; Meyer et al., 2019). Many assembly factors have been found and analyzed in yeast and human. Table 11.4 presents a summary of their role. Most assembly factors appear to control the synthesis and delivery of the prosthetic groups (heme *a* and the three Cu atoms required for electron transfer). Some of them have also been characterized in plants (Meyer et al., 2019). The nuclear genome of *Chlamydomonas* encodes most of the known assembly factors (Table 11.4) as well as a specific assembly factor, COX90, which has no counterpart in other organisms (Lown, Watson, & Purton, 2001).

11.2.1.5 Complex V, F_1Fo-ATP synthase

Mitochondrial complex V (F_1Fo-ATP synthase, EC 3.6.1.3) catalyzes the phosphorylation of ADP by inorganic phosphate, using the proton motive force generated by the respiratory chain. One of the best characterized enzymes, both from the structural and functional point of view, is the one from bovine heart mitochondria. Two main sectors are present in the beef enzyme: the membrane-bound region Fo (*a*/A6L/*b*/DAPI/*e*/*f*/*g*/c_8-ring) and the extrinsic, more hydrophilic moiety F_1 ($\alpha_3/\beta_3/\gamma/\delta/\varepsilon$/oligomycin sensitivity conferral protein, OSCP/*b*/*d*/F6) (Alfonzo & Kandrach, 1981). F_1Fo-ATP synthase is also a molecular motor (Oster & Wang, 2003) with a central rotor ($\gamma/\delta/\varepsilon/c_8$-ring) and stator components: the membrane-bound subunit *a*, the catalytic core (α_3/β_3), the dimerization/oligomerization module (A6L/*b*/*DAPI*/*e*/*f*/*g*), and a peripheral stalk (OSCP/*b*/*d*/F6) (Arselin et al., 2004; Walker & Dickson, 2006). Proton-flux through subunit *a* along with a ring of eight *c* subunits drive the rotation of the central shaft ($\gamma/\delta/\varepsilon$), which induces conformational changes in the three catalytic sites of the α_3/β_3 core, allowing for successive ADP + Pi binding, ATP synthesis, and ATP release (Suzuki et al., 2014). In turn, the peripheral stalk (OSCP/*b*/*d*/F6) counteracts the torque generated by the central rotary shaft, allowing a flexible coupling of the F_1 sector to the Fo motor (Colina-Tenorio et al., 2018; Stewart et al., 2012; Wächter et al., 2011), that is, bending of the peripheral stalk contributes to elastic energy storage. Additional components, like the inhibitory protein IF_1 (Cabezón et al., 2003) prevent futile ATP hydrolysis. Nevertheless, subunits present in the bovine enzyme are not common to all mitochondrial ATP synthases, and several organisms including trypanosomatids (Zíková et al., 2009), euglenoids (Yadav et al., 2017), chlorophycean algae (Vazquez-Acevedo et al., 2006), and ciliates (Balabaskaran et al., 2010) exhibit atypical overall architecture and subunit composition.

An early preparation of the *Chlamydomonas* F_1Fo-ATP synthase exhibited 14 different polypeptides and an activity of 2.87 μmol ATP hydrolyzed/min/mg protein that was sensitive to the classical inhibitor oligomycin (Nurani & Franzén, 1996). Further characterization of the algal enzyme identified the α, β, γ, and δ subunits, plus eight polypeptides with no counterpart in the databases (Funes et al., 2002a). N-terminal sequencing of selected bands (van Lis et al., 2003) uncovered a novel 60-kDa protein with no known ortholog, later named ASA1, for ATP synthase-associated protein.

A highly purified mitochondrial F_1Fo-ATP synthase was obtained from *Polytomella parva*, a chlorophycean alga closely related to *Chlamydomonas* lacking a cell wall and a photosynthetic plastid. The enzyme had at least 10 polypeptides with apparent molecular masses from 6 to 63 kDa. The α and β subunits exhibited atypical N- and C-terminal extensions, respectively (Atteia, Dreyfus, & González-Halphen, 1997; Van Lis et al., 2007), like the ones in the *Chlamydomonas* enzyme (Franzén & Falk, 1992). Both algal F_1Fo-ATP synthases migrate in BN-PAGE in the presence of the detergent lauryl-maltoside with an apparent molecular mass of 1600 kDa (Atteia et al., 1997; Dudkina et al., 2005), suggesting that the algal enzymes are detergent-resistant dimers. The completion of the *Chlamydomonas* genome (Merchant et al., 2007) allowed identification of 14 subunits of the ATP synthase: the classical subunits α, β, γ, δ, ε, *a*, *c*, and OSCP plus seven atypical polypeptides with no counterpart in the databases, named ASA1 to ASA7 (Vazquez-Acevedo et al., 2006). In addition, no genes encoding homologs of the bovine *A6L, b, d, DAPI, e, f, g, IF_1*, and F6 subunits were found, suggesting that ASA subunits are the main constituents of the peripheral stalk in the algal enzyme. Based on different experimental approaches, successive models proposed the topological disposition of the ASA subunits in the enzymes from both the green and the colorless alga: these include

dissociation of the enzyme into subcomplexes by high temperature, or by high amphipol or detergent concentrations (Van Lis et al., 2007; Vazquez-Acevedo et al., 2006; Vázquez-Acevedo et al., 2016; Villavicencio-Queijeiro, Pardo, & González-Halphen, 2015); characterization of chemical cross-linked products in the purified native enzyme (Cano-Estrada et al., 2010); in vitro analysis of protein−protein interactions using recombinant subunits or in vivo studies using a yeast two-hybrid system (Colina-Tenorio et al., 2016; Miranda-Astudillo et al., 2014; Sánchez-Vásquez et al., 2017); and knockdown of ATP synthase subunits using RNA interference (Lapaille et al., 2010a; Lapaille et al., 2010b).

Electron-microscopy and single-particle analysis studies carried out with the *Polytomella* enzyme found that the peripheral stalks were extremely robust and that the Fo sectors formed an angle of 70 degrees with the stalk (Cano-Estrada et al., 2010; Dudkina et al., 2005). In *Polytomella* mitochondria subjected to ultrathin sectioning, ATP synthase oligomers were found to form helical arrangements along the tubular cristae (Dudkina et al., 2005) in rows with 12 nm intervals (Dudkina et al., 2010). Also, electron cryotomography studies of detergent-purified *Polytomella* ATP synthase reconstituted into liposomes revealed that the dimeric enzyme bends the lipid bilayer locally (Blum et al., 2019), as originally observed in yeast (Paumard et al., 2002). Similar row arrangements are expected in *Chlamydomonas* since RNA interference silencing of the *ATP2* gene (encoding subunit β) impeded enzyme assembly and mitochondrial cristae formation (Lapaille et al., 2010a, 2010b).

Cryo-microscopy studies revealed a structural map of the *Polytomella* dimeric ATP synthase at 6.2 Å resolution (Allegretti et al., 2015). The model shows a robust peripheral stalk constituted by many entwined α-helices that form a solid scaffold, in accordance with the high propensity of several ASA subunits to form coiled-coils (Miranda-Astudillo et al., 2014). Furthermore, both peripheral stalks of the dimer were found to be connected by a helix−turn−helix motif (of the ASA1 subunit), while another subunit (ASA3) with an Armadillo repeat-like structure was found to join the two F_1Fo-ATPase monomers. The model also revealed the almost horizontally membrane-embedded α-helices of subunit *a* that contains the two proton-translocating hemi-channels and that seems to embrace a 10-subunit *c*-ring. This atypical topology of subunit *a* was later found in F_1Fo-ATPases of other biological sources, including the bacterium *Paracoccus denitrificans* (Morales-Rios et al., 2015), the yeast *Yarrowia lipolytica* (Hahn et al., 2016), the protist *Euglena gracilis* (Mühleip et al., 2019), bovine mitochondria (Spikes, Montgomery, & Walker, 2020), and the apicomplexan parasite *Toxoplasma gondii* (Mühleip et al., 2021).

Further refinement of cryo-EM techniques allowed the construction of an image at 2.94 Å overall resolution of the *Polytomella* enzyme that revealed the complete disposition of all previously known subunits and novel structural and functional features (Murphy et al., 2019). In the Fo region, a novel bilayer-embedded subunit ASA10, which links the two ATP synthase monomers, was identified. Ordered water molecules that may facilitate proton translocation were present within the two hemi-channels of subunit *a*. A strong electron density, interpreted to be a metal ion ligated by two histidine residues, possibly zinc, was proposed to synchronize proton translocation with c_{10}-ring protonation and rotation. In the F_1 region, each long C-terminal extension of the β subunit appears to hold the adjacent α subunit, stabilizing the structure of the α_3/β_3 moiety. Also, one of the N-terminal extensions of the α subunits binds to the peripheral stalk, while the other two form a bundle that attaches OSCP to the α_3/β_3 core, enhancing the stability of the enzyme. The OSCP subunit has a hinge that joins the F_1 head to the peripheral stalk and that seems to play a dynamic role during catalysis, allowing the flexible coupling of the F_1 sector to the Fo motor. Thirteen independent rotary states could be identified in the *Polytomella* enzyme, providing molecular details of its movements during catalysis. The F_1 sector was found to rotate together with the central stalk and the c_{10} ring around 30 degrees at the beginning of each 120-degree step. Fig. 11.4A shows the structural maps for the ATP synthases of *Polytomella* and *Chlamydomonas*, the latter modeled based on the structure of the former. The main structural difference between the algal enzymes is the bridge that joins the middle part of the two peripheral stalks formed by the helix−turn−helix motif of the ASA1 subunits, which is present in the *Polytomella* enzyme but probably absent in its *Chlamydomonas* counterpart. The detailed model of the 1.6 MDa *Chlamydomonas* dimeric enzyme, showing the disposition of its 62 polypeptides, colored by subunit, is presented in Fig. 11.4B.

An inhibitor protein that may control the algal ATP synthase hydrolytic activity remains to be identified and characterized. Nevertheless, either one of the enzyme subunits or an independent polypeptide are expected to exert a regulatory role like subunit ε in gamma-proteobacteria (Lino et al., 2009), subunit ζ in α-proteobacteria (García-Trejo et al., 2016), or the IF_1 protein in mitochondrial enzymes (van Raaij et al., 1996).

Since all of the subunits of the chlorophycean mitochondrial ATP synthases are nucleus-encoded (Vazquez-Acevedo et al., 2006), it is of interest to learn how the precursors of the ASA subunits are imported into mitochondria and

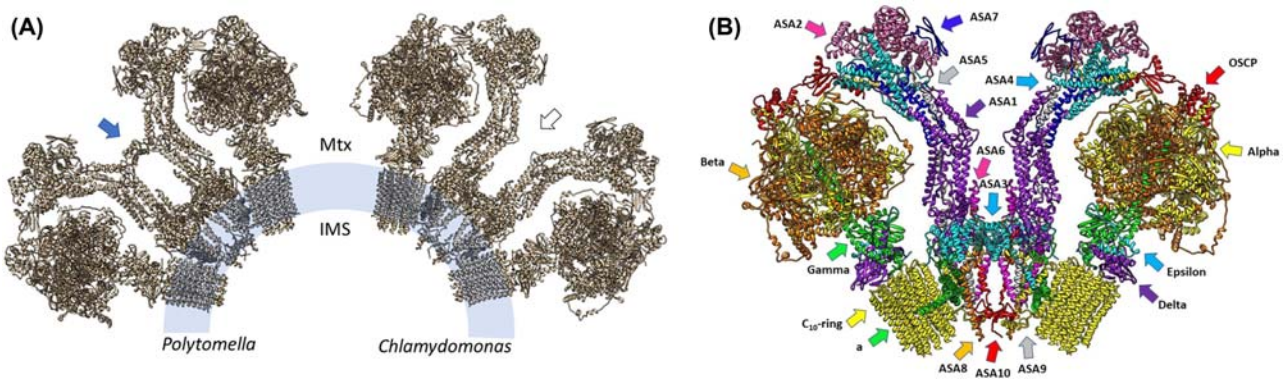

FIGURE 11.4 The mitochondrial F1Fo-ATPases from chlorophycean algae. (A) 3D structures of mitochondrial F1Fo-ATPases from chlorophycean algae. The map of the colorless algal (*Polytomella*) enzyme is shown [PDB 6rd4.1 (Murphy et al., 2019)]. The model of the *Chlamydomonas* dimeric enzyme exhibits a total of 62 polypeptides and was built with Swiss Modeler (Waterhouse et al., 2018) using as template the *Polytomella* map. The inner mitochondrial membrane, bent locally by the dimeric enzymes, is shown in light blue; IMS: intermembrane space; Mtx: mitochondrial matrix. The main structural difference between the algal enzymes is the bridge that joins the two peripheral stalks, present in the *Polytomella* enzyme (blue arrow) but probably absent in the *Chlamydomonas* structure (white arrow). (B) Model of the 3D structure of the mitochondrial F1Fo-ATPase from *Chlamydomonas*. The model of the *Chlamydomonas* dimeric enzyme was built using as template the *Polytomella* 3D map obtained by single-particle cryo-EM [PDB 6rd4.1 (Murphy et al., 2019)]. Each arrow indicates the name of the subunits depicted with a matching color.

assembled into a functional ATP synthase. Unfortunately, expression and assembly factors of the *Chlamydomonas* complex V constituents are yet to be characterized. By contrast, several have been identified in yeast: two chaperones for the F_1 domain, ATP11 and ATP12 (Ackerman & Tzagoloff, 1990; Wang, White, & Ackerman, 2001); FMC1, a soluble protein located in the mitochondrial matrix that is required for the proper folding/stability or functioning of ATP12p in heat stress conditions (Lefebvre-Legendre et al., 2001); ATP10 and ATP22, instrumental in assembly of Fo (Ackerman & Tzagoloff, 1990; Helfenbein et al., 2003; Tzagoloff et al., 2004); ATP23, a putative metalloprotease of the IMM needed for processing and assembly of ATP6 (Zeng, Neupert, & Tzagoloff, 2007); INA22 and INA17, two components of the INA complex located in the IMM that are involved in the assembly of the peripheral stalk (Lytovchenko et al., 2014); AEP1 and AEP2, which are instrumental for the correct expression of ATP9 (Finnegan et al., 1995; Payne, Schweizer, & Lukins, 1991); and AEP3, which stabilizes the mitochondrial dicistronic mRNA-encoding subunits 6 and 8 (Ellis et al., 2004). In mammals, the transmembrane protein 70 (TMEM70) of the inner mitochondrial membrane, interacts with subunit *c* to help it assemble into the membrane-embedded rotor of the enzyme (Kovalčíková et al., 2019; Sánchez-Caballero et al., 2020). Orthologs for four of these factors, ATP11, ATP12, ATP23, and TMEM70 could be identified in the *Chlamydomonas* genome, although their actual participation in complex V assembly remains to be demonstrated. Most probably, more ATP synthase biogenesis factors remain to be identified in the green alga. Table 11.5 lists all the subunits of the *Chlamydomonas* F_1Fo-ATP synthase and its putative expression and assembly factors.

11.2.1.6 Super complexes

Super complexes and the concept of respirasome have been described 20 years ago in mammals and yeast where association of complex III and complex IV or complexes I, III, and IV have been identified using digitonin for mild detergent solubilization of mitochondrial membranes followed by separation of the complexes by Blue Native PAGE (Schägger & Pfeiffer, 2000). Super complexes have also been detected in plants using the same technique (Eubel et al., 2004) and association $III_2 + I$ has been found in *Chlamydomonas* (Cardol et al., 2008). These super complexes can also be visualized by electron cryotomography (Davies, Blum, & Kühlbrandt, 2018). The actors regulating their organization and their biogenesis are still under intense investigation (Lobo-Jarne & Ugalde, 2018). A few factors have been isolated and the best known to date are the COX7A2L and RCFs. COX7A2L also named SCAF1 was first shown to be responsible for integration of complex IV into respirasome but this finding was later challenged by other groups. RCF factors in complex IV assembly are listed (Table 11.4) and their role in super complex formation is considered indirect (Lobo-Jarne & Ugalde, 2018).

TABLE 11.5 Complex V subunits and biogenesis factors in *Chlamydomonas* and other organisms.

F_1Fo-ATP synthase constituents and expression/assembly factors					
Constituents (subunits)					
Chlamydomonas			Counterparts in other organisms		
Gene	Protein product	Phytozome accession #	*Homo sapiens/Bos taurus*	Yeast	*Arabidopsis* accession #
ATP6	Subunit *a;* ATP6	Cre01.g018800	*ATP6/a*	*ATPA (ATP6)*	AtMg00410
ATP9A	Subunit c; subunit 9 (isoform A)	Cre17.g732000	*ATP5G3/c*	*ATPC (ATP9)*	At2g07671 AtMg01080
ATP9B	Subunit c; Subunit 9 (isoform B)	Cre17.g731950	*ATP5G3/c*	*ATPC (ATP9)*	At2g07671 AtMg01080
ATP1A	Alpha subunit	Cre02.g116750	*ATP5A1/α*	*α (ATP1)*	At2g07698 AtMg01190
ATP1B	Alpha subunit (isoform B)	Cre10.g419050	*ATP5A1/α*	*α (ATP1)*	At2g07698AtMg01190
ATP2	Beta subunit	Cre17.g698000	*ATP5B/β*	*β (ATP2)*	AtCg00480
ATP3	Gamma subunit	Cre15.g635850	*ATP5C1/γ*	*γ (ATP3)*	At2g33040
ATP16	Delta subunit	Cre11.g467707	*ATP5D/δ*	*δ (ATP16)*	At5g47030
ATP15	Epsilon subunit	Cre10.g420700	*ATP5E/ε*	*ε (ATP15)*	At1g51650
ATP5	OSCP subunit	Cre16.g680000	*ATP5O/OSCP*	*ATP5*	At5g13450
ASA1	ASA1 subunit	Cre07.g340350	–	–	–
ASA2	ASA2 subunit	Cre09.g415550	–	–	–
ASA3	ASA3 subunit	Cre07.g338050	–	–	–
ASA4	ASA4 subunit	Cre13.g581600	–	–	–
ASA5	ASA5 subunit	Cre17.g721300	–	–	–
ASA6	ASA6 subunit	Cre02.g079800	–	–	–
ASA7	ASA7 subunit	Cre09.g416150	–	–	–
ASA8	ASA8 subunit	Cre09.g402300	–	–	–
ASA9	ASA9 subunit	Cre09.g395350	–	–	–
ASA10	ASA10 subunit	Cre12.g499800	–	–	–
Expression and assembly factors					
ATP11	Assembly factor 1	Cre10.g437050	*ATPAF1*	*ATP11*	At2g34050
ATP12	Assembly factor 2a	Cre17.g726250	*ATPAF2*	*ATP12*	At5g40660
ATP23	Assembly factor	Cre17.g697934	–	–	At3g03420
TMEM70	Assembly factor	Cre12.g540051	*TMEM70*	–	–

#= number.

11.2.1.7 Other components related to oxidative phosphorylation

11.2.1.7.1 Alternative NAD(P)H dehydrogenases

In addition to the classical proton-pumping complex I, mitochondria of most eukaryotes contain several type II NAD(P)H dehydrogenases (NDH2) which transfer electrons from NAD(P)H to ubiquinone and are insensitive to rotenone

(Matus-Ortega et al., 2011). These simple one-subunit flavoenzymes are located on the surface of the mitochondrial inner membrane and face either the matrix (internal) or the IMS (external). Their activity results in the dissipation of the redox energy of the NADH/ubiquinone couple (Kerscher et al., 2008). The *Chlamydomonas* genome was found to code for six proteins sharing high level of similarity to known NDH2 type II NAD(P)H dehydrogenases (NDA1, 2, 3, 5, 6, and 7) (Cardol et al., 2005) (Table 11.6). NDA1 is located on the inner face of the inner mitochondrial membrane. Inactivation of its expression has almost no impact on growth in the dark and on respiration in a wild-type genetic background of *Chlamydomonas*. However, inactivation of *NDA1* expression decreases growth and respiration of *dum17* mitochondrial mutant, indicating that NDA1 participates in oxidizing reduced equivalents in the matrix along with complex I (Lecler et al., 2012). Although it belongs to the mitochondrial NDH2 family, *Chlamydomonas* NDA2 protein is targeted to the thylakoid membrane in the chloroplast and is involved chlororespiration, a process allowing nonphotochemical reduction of the plastoquinone (PQ) pool (Desplats et al., 2009; Jans et al., 2008) (see Chapter 18). In many other photosynthetic organisms, nonphotochemical reduction of PQ is performed by a bacterial-like NDH-1 complex whose many subunits are homologous to mitochondrial complex I (Strand, D'Andrea, & Bock, 2019), but such a complex is absent in *Chlamydomonas* plastids. In this respect, NDA3 has been identified with NDA2 in an enriched chloroplastic fraction by proteomic analysis, but its function is unknown (Terashima et al., 2010). The cellular location of the three other NDA proteins (NDA5−7) is unknown. NDA5 is homologous to Arabidopsis NDC1 and shares a common cyanobacterial origin (Dinant et al., 2001). Arabidopsis NDC1 associates with plastoglobules in the chloroplast and is essential for phylloquinone (vitamin K1) production (Piller, Besagni, & Ksas, 2011) by catalyzing the NADPH-dependent reduction of demethylphylloquinone, the ninth step of phylloquinone biosynthesis in the chloroplast (Fatihi et al., 2015). It was therefore suggested that NDA5 could perform the same enzymatic function in *Chlamydomonas* (Emonds-Alt et al., 2017). Finally, the *NDA6* and *NDA7* genes are adjacent to each other on chromosome 12, and therefore presumably arose through a duplication event. Their function is unknown but it can be speculated that at least one could serve as an external NADH dehydrogenase in mitochondria, similarly to AtNDB2 of *A. thaliana* (Sweetman et al., 2019).

11.2.1.7.2 Alternative oxidases

The mitochondrion from most eukaryotes also possesses an alternative oxidase (AOX) which bypasses the energy-conserving electron transport complexes III and IV by transferring electrons directly from the ubiquinol pool to molecular oxygen. The enzyme is thought to regulate the respiratory electron flow and protect plant cells from oxidative damage (Maxwell, Wang, & McIntosh, 1999). In *Chlamydomonas*, the presence of a carbon monoxide and cyanide-resistant alternative respiratory

TABLE 11.6 Other components related to oxidative phosphorylation (OXPHOS).

Gene	Protein product	Phytozome accession [#]
NDA1	Type-II NADH:ubiquinone oxidoreductase, mitochondrial	Cre16.g691552
NDA2	Type-II NAD(P)H:plastoquinone oxidoreductase, chloroplast	Cre19.g750547
NDA3	Putative type-II NAD(P)H dehydrogenase, chloroplast	Cre05.g232200
NDA5	Putative NADPH: demethylphylloquinone oxidoreductase, chloroplast**?**	Cre16.g671000
NDA6	Putative type-II NAD(P)H dehydrogenase, mitochondrial**?**	Cre12.g555803
NDA7	Putative type-II NAD(P)H dehydrogenase, mitochondrial**?**	Cre12.g556228
AOX1	Alternative oxidase 1, mitochondrial	Cre09.g395950
AOX2	Alternative oxidase 2, mitochondrial	Cre03.g169550
UCP1	Putative uncoupling protein	Cre06.g278750
UCP2A	Putative uncoupling protein	Cre06.g257550
UCP3	Putative uncoupling protein	Cre04.g218650
UCP2C	Putative uncoupling protein	Cre15.g641200

[#] *# = number.*

pathway was discovered very early (Hommersand & Thimann, 1965), and later shown to be salicylhydroxamic acid-sensitive (Matagne et al., 1989; Weger, Guy, & Turpin, 1990). All *Chlamydomonas* respiratory-deficient mutants with an impaired cyanide-sensitive cytochrome pathway still exhibit a fully functional alternative pathway (Salinas et al., 2014).

Two isoforms of the alternative oxidase are encoded in the nuclear genome of *Chlamydomonas*, *AOX1* and *AOX2* (Dinant et al., 2001) (Table 11.6) and are targeted to mitochondria (Kaye et al., 2019). The *AOX1* gene is more actively transcribed than *AOX2* (Dinant et al., 2001). Several studies performed in *Chlamydomonas* showed that a range of stress factors lead to induction of AOX mRNA or protein abundance, and enhanced AOX capacity. *AOX1* mRNA and protein levels are strongly dependent on the nitrogen source, being stimulated by nitrate and downregulated by ammonium (Baurain et al., 2003). In nitrate-grown cells, the alternative oxidase pathway may permit the export of reducing power out of mitochondria in the form of malate for nitrate and nitrite reduction (Gérin et al., 2010).

AOX1 mRNA level is also increased by the presence of H_2O_2, cold stress, and antimycin A (Molen et al., 2006). Nevertheless, unlike of what happens in flowering plants, even when *AOX* is transcriptionally activated by antimycin A, there is no accumulation of AOX protein, suggesting a posttranscriptional control of AOX levels (Zalutskaya, Ostroukhova, & Filina, 2017). *AOX1* transcript, protein amounts, and functional capacity, also increased upon heat stress (Zalutskaya, Lapina, & Ermilova, 2015), NO exposure (Zalutskaya et al., 2017), or sulfur deprivation (Zalutskaya et al., 2018). The expression of *AOX1* may thus be subjected to complex regulation, where among other factors NO can serve as a triggering signal (He, Van Breusegem, & Mhamdi, 2018). Several additional factors, including a heat-inducible Ca^{2+} influx, protein kinases, and the nitrate assimilation regulatory protein (NIT2) may also control its expression (Zalutskaya et al., 2017). Less is known about the expression of *AOX2* gene. It is also inducible, being increased by oxygen or copper deprivation and regulated at least by the copper response regulator 1 (CRR1) (Ostroukhova, Zalutskaya, & Ermilova, 2017).

The lack of *AOX1* expression in a *Chlamydomonas* mutant led to increased ROS accumulation, an increase of several enzymes involved in anabolic pathways and a concomitant general downregulation of several enzymes of the main catabolic pathways (Gérin et al., 2010). ROS accumulation was especially pronounced in very high light, with the *aox1* mutant being more sensitive than the *aox2* mutant; the accumulation of ROS correlated with damage of the photosynthetic machinery, ultimately resulting in cell death (Kaye et al., 2019). These results suggest that the alternative oxidase pathway participates in acclimation of *Chlamydomonas* cells to excess absorbed light energy (Kaye et al., 2019), that is when CO_2 fixation capacity is limited. In line with this proposal, the alternative respiratory pathway decreased considerably at high CO_2 concentrations (Goyal & Tolbert, 1989). This supports the idea that when photosynthetic electron carriers are highly reduced, the reduction of oxygen by AOX (especially AOX1) in the mitochondrion is an efficient electron sink for photosynthetically derived electrons (Kaye et al., 2019).

11.2.1.7.3 Uncoupling proteins

Found in most eukaryotes, uncoupling proteins (UCPs) are membrane-intrinsic proteins that compete with the F_1Fo-ATP synthase (complex V) for the proton−electron gradient established by the activity of complexes I, III, and IV. One of the main function for UCPs might be to protect the mitochondrion against ROS by diminishing the reduced state of the carriers of the respiratory chain (Sluse et al., 2006). In humans, UCPs belong to the mitochondrial carrier protein family 25, also called solute family SLC25, which includes 53 members (Ruprecht & Kunji, 2020). This family has 58 members in *A. thaliana* (Monné et al., 2018) and at least 36 genes in *Chlamydomonas* according to version 5.5 genome annotation. In the previous version of this book, based on their similarity to the mammalian protein UCP1, three *Chlamydomonas* proteins were proposed to be UCPs (UCP1−3) (Cardol et al., 2005). Since then, a fourth putative UCP has been identified (Table 11.6). The six putative UCP1 homologs in *A. thaliana* (AtUCP1−6) have been shown to be either dicarboxylate carriers, C4 metabolite carriers / inorganic phosphate carriers, or amino acid carriers (Monné et al., 2018; Palmieri et al., 2008; Vozza et al., 2014). The current annotations of the *Chlamydomonas* SLC25 family members must therefore be treated with great caution in the absence of experimental confirmation of function.

11.2.1.7.4 Reactive oxygen species production in the mitochondrial electron transport chain: scavenging and processing machinery

In addition to photosynthetic electron transport, mitochondrial respiration is a significant generator of ROS (Larosa & Remacle, 2018). Complexes I, II, and III are the main sources of superoxide (O_2^-) which is converted into hydrogen peroxide (H_2O_2). *Chlamydomonas* respiratory mutants of complexes I and IV exhibit reduced ROS production which is

correlated to decreased levels of ROS-detoxifying enzymes, at least in complex I mutants (Larosa & Remacle, 2018). The major scavenging enzymes in *Chlamydomonas*, like in other organisms, include superoxide dismutases (SODs), ascorbate peroxidases (APXs), peroxiredoxins (PRXs), glutathione peroxidases (GPXs), glutaredoxins (GRXs), thioredoxins (TRXs), and glutathione *S*-transferases (GSTs) (He et al., 2018). Table 11.7 reports the genes encoding predicted mitochondrial isoforms. In addition, ROS can also act as signaling molecules between organelles in anterograde signaling (i.e., from nucleus to mitochondria) or retrograde signaling (i.e., from mitochondria to nucleus) by modifying protein function and regulating the acclimation of the cells under different stress conditions (Ng et al., 2014). Mutants for some genes encoding scavenging enzymes mentioned above are available in the CLiP library (https://www.chlamylibrary.org/) and may be useful to study the mechanism of respiratory-dependent ROS production and signaling in *Chlamydomonas*.

Localization of ROS-scavenging enzymes was predicted using PredAlgo (Tardif et al., 2012), Target_P (Armenteros et al., 2019) and MitoFates (Fukasawa et al., 2015) with at least two positive results out of three for mitochondrial localization. That was not the case for TRXO1, but its localization to mitochondria is confirmed in Lemaire and Miginiac-Maslow (2004).

11.2.2 Import and maturation of the mitochondrial proteins

11.2.2.1 Import of mitochondrial proteins

Mitochondrial genomes encode a small number of hydrophobic proteins, usually participating in OXPHOS, that are cotranslationally inserted into the membrane (Szyrach et al., 2003). Chlorophycean algae such as *Chlamydomonas* lack several of the genes usually present in mitochondrial genomes: *ATP6*, *ATP8*, *COX2*, *COX3*, *NAD3*, and *NAD4L* (see Section 11.1.1). These genes have migrated to the nucleus and their protein products are imported into mitochondria (Cardol et al., 2006; Funes et al., 2002b; Perez-Martínez et al., 2000; Perez-Martínez et al., 2001). Another distinctive feature of some chlorophycean algae such as *Chlamydomonas* is that the *COX2* gene is split into two independent genes, *COX2A* and *COX2B* (Perez-Martinez et al., 2002; Rodríguez-Salinas, Remacle, & González-Halphen, 2012). In general, most mitochondrial proteins are nucleus-encoded and synthesized on cytosolic ribosomes (Neupert & Herrmann, 2007), usually as precursors carrying N-terminal extensions named mitochondrial targeting sequences (MTSs). These MTSs are required for import into the organelle and are usually removed by matrix-localized proteases shortly after internalization (Neupert, 1997). All MTSs contain regions that tend to form positively charged, amphiphilic

TABLE 11.7 Mitochondrial ROS scavenging and processing enzymes in *Chlamydomonas*.

Gene	Protein product	Phytozome accession [#]
(none)	Ascorbate peroxidase	Cre09.g401886
GPX1	Glutathione peroxidase	Cre02.g078300
GPX3	Glutathione peroxidase	Cre03.g197750
GRX5	Glutaredoxin	Cre07.g325600
GST8	Glutathione *S*-transferase	Cre12.g508850
PRX4	Peroxiredoxin	Cre02.g080900
PRX5	Peroxiredoxin	Cre01.g014350
PRX7	Peroxiredoxin	Cre17.g743897
MSD1	Superoxide dismutase	Cre02.g096150
MSD2	Superoxide dismutase	Cre13.g605150
TRXO1	Thioredoxin	Cre05.g248500

Localization of ROS scavenging enzymes was predicted using PredAlgo (Tardif et al., 2012), Target_P (Armenteros et al., 2019) and MitoFates (Fukasawa et al., 2015) with at least two positive results out of three for mitochondrial localization. That was not the case for TRXO1, but its localization in mitochondria is confirmed in Lemaire and Miginiac-Maslow (2004).
[#] *# = number.*

α-helices (von Heijne, Stepphuhn, & Herrmann, 1989) with a low number of acidic amino acids and a high proportion of alanine, leucine, serine, glycine, and arginine residues. NMR and circular dichroism studies of a synthetic peptide with the MTS sequence of the β subunit of the *Chlamydomonas* FoF_1-ATP synthase (Franzén & Falk, 1992), have shown that this presequence adopts an α-helical structure in 2,2,2-trifluoroethanol/water, a solvent believed to mimic biological membranes (Lancelin et al., 1996). *Chlamydomonas* MTSs range from relatively short (~30 residues) to unusually long (110−160 residues) (Funes et al., 2002a). The shorter ones usually direct soluble precursors to the mitochondrial matrix, while the larger ones exhibit bipartite structures, with N-terminal regions that direct the precursor to the mitochondrial matrix and C-terminal regions that may help integrate it into the IMM. Among the nucleus-encoded proteins that participate in OXPHOS, MTSs of the following lengths have been found: for the ND3 and ND4L subunits of complex I, 160 and 130 amino acids, respectively (Cardol et al., 2006), for complex III subunits Rieske RIP1 and cytochrome c_1, 54 (Atteia & Franzén, 1996) and 70 residues, respectively (Atteia et al., 2006); for complex IV subunits COX2A and COX3, 130 and 110 amino acids, respectively (Perez-Martínez et al., 2000, 2001); and for the α, β, and *a* subunits of complex V, 26 (Franzén & Falk, 1992), 45 (Nurani & Franzén, 1996) and 107 amino acids (Funes et al., 2002b), respectively. Thus bipartite *Chlamydomonas* MTSs seem to be atypically long in those precursors containing two or more transmembrane stretches, such as the products of nucleus-encoded *ATP6*, *ATP8*, *COX2*, *COX3*, *NAD3*, and *ND4L* genes. A long MTS could promote the interactions of the precursor with the mitochondrial import machinery (Claros & Vincens, 1996) or help to unfold the protein in order to increase its importability (Claros et al., 1995).

The main components of the mitochondrial protein import machinery have been well characterized in yeast: (1) the translocase of the outer membrane (TOM); (2) the sorting and assembly machinery of the outer mitochondrial membrane (SAM); (3) the proteins of mitochondrial IMS import and assembly pathway (MIA); (4) the intermembrane space-localized small TIMs; (5) the translocators of the inner membrane, TIM23; and (6) TIM22. Efforts have been made to reconstruct the *Chlamydomonas* mitochondrial protein import machinery (Figueroa-Martínez et al., 2008) using bioinformatic approaches (Fig. 11.5).

The TOM complex represents the main gateway for proteins being internalized into mitochondria. The complex typically contains seven subunits in yeast, TOM70, 40, 22, 20, 7, 6, and 5, although in *Chlamydomonas* and in several plants TOM70 is absent and TOM22 has been replaced by TOM9, a component structurally similar to yeast and mammalian TOM22 but lacking a cytosolic receptor domain (Carrie, Murcha, & Whelan, 2010; Matouschek, Pfanner, & Voos, 2000).

The SAM complex is required for insertion of outer membrane proteins that form β-barrels or α-helical bundles (Takeda et al., 2021). The β-barrel subunit SAM50, is instrumental in the insertion process, and four additional components of SAM have been characterized in yeast: SAM37, SAM35, MDM10, and MIM1. In *Chlamydomonas* and plants, only orthologs of SAM50 have been identified. In addition, Metaxin, an independent protein, not part of the SAM complex, with a conserved GST domain, may also be involved in the import of β-barrel proteins and their localization to the outer membrane.

In the mitochondrial IMS, the MIA pathway (Chacinska et al., 2004) consists of the MIA40, ERV1, and HOT13, components that catalyze the oxidative folding of proteins when they enter the IM (Finger & Riemer, 2020; Lu et al., 2004), and specifically those that contain conserved cysteine residues arranged in twin CX_9C or CX_3C motifs (Gabriel et al., 2007). Orthologs of MIA40 and ERV1 are present in *Chlamydomonas*. In contrast, the cysteine-rich protein HOT13 (Curran et al., 2004), involved in late stages of assembly of IMS proteins, seems to lack an ortholog in the green alga.

In the IMS, the small TIMs play an essential role as chaperones for importing carrier proteins that are directed toward TIM22 of the inner membrane, and in directing β-barrel proteins toward SAM in the outer membrane (Petrakis, Alcock, & Tokatlidis, 2009).

The TIM23 complex is responsible for the import of proteins that contain an MTS and that may be transferred across the IMM or inserted laterally into that same membrane. Its main components are TIM50, 23, 17, and 21, where TIM17 is a voltage sensor (Meier, Neupert, & Herrmann, 2005) and TIM23 forms a voltage-sensitive channel (Truscott et al., 2001). The TIM23 complex requires the function of the presequence translocase-associated motor (PAM) (Matouschek et al., 2000) that drives, in an ATP-dependent reaction, the unfolding and the translocation of the precursors. Its components are the heat-shock protein mtHSP70, TIM44, PAM18, PAM17, and PAM16. Except for PAM17, the subunits of the TIM23 complex are conserved in *Chlamydomonas*, yeast, humans, and plants. In addition, TIM17 of *Chlamydomonas* and plants contains a long extension of 158 residues at their C-terminal that seems to cross the IMS and the outer membrane, exposing it to the cytosol (Murcha et al., 2005). Since TIM17 is known to bind tRNAs and mRNAs, it was suggested to also participate in the import of nucleic acids into mitochondria.

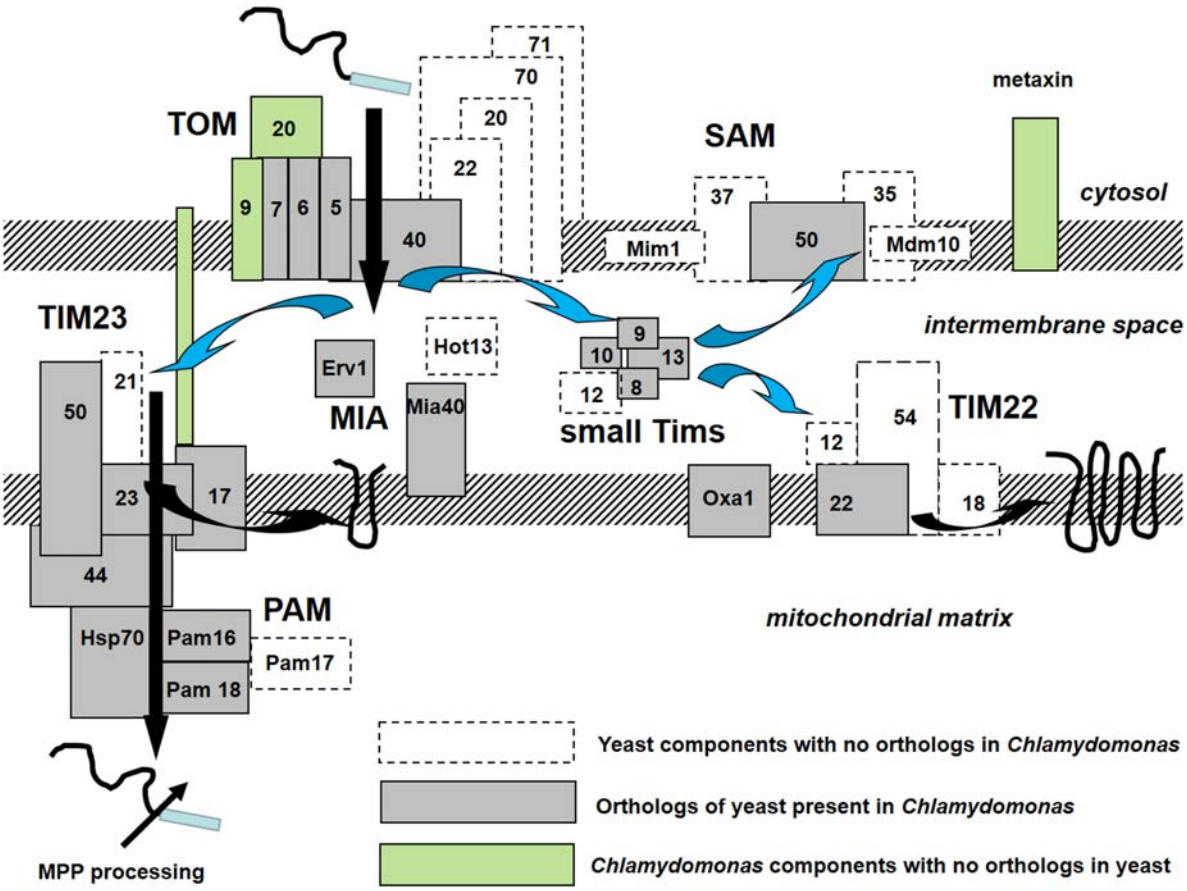

FIGURE 11.5 The mitochondrial protein import machinery of *Chlamydomonas*. The diagram shows the main components of the well-characterized mitochondrial protein import machinery of yeast, the yeast orthologs identified in *Chlamydomonas*, and the putative components that may be unique to green algae and plants.

In the IMM, another translocator, the TIM22 complex, is responsible for the import of proteins containing four or six-transmembrane stretches, such as the ADP/ATP translocator, the dicarboxylate carrier, and the phosphate carrier (Ramage et al., 1993). TIM22 also imports components of the mitochondrial pyruvate carrier, sideroflexins, and the translocase components TIM17, TIM22, and TIM23 (Horten, Colina-Tenorio, & Rampelt, 2020). Such proteins lack an MTS and seem to contain internal targeting signals, but details on the mechanism by which they are inserted in the IMM remain largely unknown. The yeast TIM22 complex is formed by TIM54, 22, 18, and 12, where TIM22 has been shown to exhibit a channel activity in the presence of its substrate proteins (Kerscher et al., 1997). In contrast to TIM23, the TIM22 components seem to be poorly conserved. TIM54, 18 and 12 are only found in yeast and not in other organisms such as *Chlamydomonas*. Clearly, more components of the green alga TIM22 complex remain to be identified.

Protein biogenesis in mitochondria involves several additional components: proteins and translocators that insert mitochondrial-synthesized proteins into the IMM, a series of chaperones that fold the proteins that arrive to the mitochondrial matrix, and several peptidases that remove the MTSs of the precursors, before or after they are assembled in their corresponding complex. All these additional mitochondrial components are not considered in detail but are shown in Table 11.8. Peptidases play different roles: some remove the MTSs, such as the mitochondrial processing peptidase (MPP) or the intermediate processing peptidase (IMP), others like the OCT1 protease, remove a single residue from proteins whose MTS has already been excised (Vögtle et al., 2009), while others, such as the presequence degrading peptidase (PreP), break down the detached MTS (Koppen & Langer, 2007). In most organisms, the MPP protease, formed by its α and β subunits, is a soluble enzyme (Neupert, 1997), but in plants MPP is bound to complex III as subunits QCR1 (β) and QCR2 (α) (Glaser & Dessi, 1999).

TABLE 11.8 The main constituents of the mitochondrial protein import machinery of yeast and its orthologs in *Chlamydomonas* and *Arabidopsis*.

Gene (*S. cerevisiae*)	Protein (*S. cerevisiae*)	*Chlamydomonas*	*Arabidopsis*
Translocase of the outer mitochondrial membrane (TOM)			
TOM20 (YGR082W)	Tom20	–	–
–	–	*TOM20* (Cre12.g534600)[a]	*TOM20–1* (At3g27070)[a] *TOM20–2* (At1g27390)[a] *TOM20–3* (At3g27080)[a] *TOM20–4* (At5g40930)[a]
TOM70 (YNL121C)	Tom70	–	mtOM64 (At5g09420)
TOM71 (YHR117W)	Tom71	–	–
TOM40 (YMR203W)	Tom40	*TOM40* (Cre10.g424450)	*TOM40–1* (At3g20000) *TOM40–2* (At1g50400)
TOM22 (YNL131W)	Tom22	*TOM9* (Cre06.g278345)[b]	*TOM9–1* (At1g04070)[b] *TOM9–2* (At5g43970)[b]
TOM7 (YNL070W)	Tom7	*TOM7* (Cre10.g437500)	*TOM7–1* (At5g41685) *TOM7–2* (At1g64220)
TOM6 (YOR045W)	Tom6	*TOM6* (Cre16.g670250)	*TOM6* (At1g49410)
TOM5 (YPR133W)	Tom5	*TOM5* (Cre06.g276001)	*TOM5* (At5g08040)
Sorting and assembly machinery of the outer mitochondrial membrane (SAM)			
SAM50 (YNL026W)	Sam50	*SAM50* (Cre06.g308900)	*SAM50–1* (At3g11070) *SAM50–2* (At5g05520)
SAM37 (YMR060C)	Sam37	–	–
SAM35 (YHR083W)	Sam35	–	–
MDM10 (YAL010C)	Mdm10	–	–
MIM1 (YOL026C)	Mim1	–	–
–	–	*MTX1* (Cre03.g177900)[a]	MTX (At2g19080)[a]
Mitochondrial intermembrane space import and assembly (MIA)			
MIA40 (YKL195W)	Mia40	*MIA40* (Cre03.g144827)	*MIA40* (At5g23395)
ERV1 (YGR029W)	Erv1	*ERV1A* (Cre14.g633000) *ERV1B* (Cre03.g173200)	*ERV1* (At1g49880)
HOT13 (YKL084W)	Hot13	–	–
Small Tims of the intermembrane space			
TIM13 (YGR181W)	Tim13	*TIM13* (Cre16.g650800)	*AtTIM13* (At1g61570)
TIM12 (YBR091C)	Tim12	–	–
TIM10 (YHR005C)	Tim10	*TIM10* (Cre12.g514900)	*AtTIM10* (At2g29530)
TIM9 (YEL020W)	Tim9	*TIM9* (Cre01.g033400)	*AtTIM9* (At3g46560)
TIM8 (YJR135W)	Tim8	*TIM8* (Cre03.g189750)	*AtTIM8* (At5g50810)
Translocase of the inner mitochondrial membrane (TIM22)			
TIM54 (YJL054W)	Tim54	–	–
TIM22 (YDL217C)	Tim22	*TIM22A* (Cre01.g021050) *TIM22B* (Cre03.g183100) *TIM22C* (Cre01.g050400)	*TIM22–1* (At3g10110) *TIM22–2* (At1g18320)

(*Continued*)

TABLE 11.8 (Continued)

Gene (*S. cerevisiae*)	Protein (*S. cerevisiae*)	*Chlamydomonas*	*Arabidopsis*
Translocase of the outer mitochondrial membrane (TOM)			
TIM18 (YOR297C)	Tim18	–	–
Translocase of the inner mitochondrial membrane (TIM23)			
TIM23–1 (YNR017W)	Tim23	*TIM23* (Cre10.g434250)	*TIM23–1* (At1g17530) *TIM23–2* (At1g72750) *TIM23–3* (At3g04800)
TIM17–1 (YJL143W)	Tim17	*TIM17* (Cre10.g452650)	*TIM17–1* (At1g20350) *TIM17–2* (At2g37410) *TIM17–3* (At5g11690)
TIM50 (YPL063W)	Tim50	*TIM50* (Cre12.g505950)	*TIM50* (At1g55900)
TIM21 (YGR033C)	Tim21	*TIM21* (Cre09.g405550)	*TIM21* (At4g00026)
Presequence translocase-associated motor (PAM)			
TIM44 (YIL022W)	Tim44	*TIM44* (Cre16.g660800)	*TIM44–1* (At2g20510) *TIM44–2* (At2g36070)
mtHSP70–1 (YJR045C) *mtHSP70–2* (YLR369W)	mtHsp70	*HSP70C* (Cre09.g393200)*HSP70D* (Cre12.g535700)*HSP70F* (Cre09.g412880)	*mtHSP70–1* (At5g09590) *mtHSP70–2* (At4g37910)
PAM18 (YLR008C)	Pam18	*PAM18* (Cre02.g133000)	*PAM18–1* (At2g35795) *PAM18–2* (At3g09700) *PAM18–3* (At5g03030)
MDJ2 (YNL328C)	Mdj2	–	–
PAM16 (YJL104W)	Pam16	*PAM16* (Cre09.g412300)	*PAM16–1* (At5g61880) *PAM16–2* (At3g59280)
PAM17 (YKR065C)	Pam17	–	–
Mitochondrial processing peptidases			
MAS2 (YHR024C)	α-MPP	*MPPA1* (Cre17.g722800) –	*α-MPP-1* (At3g16480) *α-MPP-2* (At1g51980)
MAS1 (YLR163C)	β-MPP	–	*β-MPP* (At3g02090)
OCT1 (YKL134C)	Oct	–	–
IMP1 (YMR150C)	Imp1	*IMP1* (Cre18.g746000)	*IMP1–1* (At1g53530) *IMP1–2* (At1g29960) *IMP1–3* (At1g23465)
IMP2 (YMR035W)	Imp2	*IMP2* (Cre01.g027100)	*IMP2* (At3g08980)
SOM1 (YEL059C)	Som1	–	–
YTA12 (YMR089C)	Yta12	–	–
YTA10 (YER017C)	Yta10	*FTSH3* (Cre01.g019850)	*FTSH3* (At2g29080) *FTSH10* (At1g07510)
YME1 (YPR024W)	Yme1	*FTSH4* (Cre13.g568400)	*FTSH4* (At2g26140) *FTSH11* (At5g53170)
MGR1 (YCL044C)	Mgr1	–	–
MGR3 (YMR115W)	Mgr3	–	–
PCP1 (YGR101W)	Pcp1	–	–
ICP55 (YER078C)	Icp55	*ICP55* (Cre01.g046150)	*ICP55* (At1g09300)

(*Continued*)

TABLE 11.8 (Continued)

Gene (*S. cerevisiae*)	Protein (*S. cerevisiae*)	*Chlamydomonas*	*Arabidopsis*
Translocase of the outer mitochondrial membrane (TOM)			
PREP1 (YDR430C)	Prep	*PREP1* (Cre01.g020900)	*PREP1* (At3g19170) *PREP2* (At1g49630)
Components that insert mitochondrial-synthesized proteins			
OXA1 (YER154W)	Oxa1	*OXA1* (Cre03.g198150). *OXA3* (Cre16.g690200)	*OXA1−1* (At5g62050) *OXA1−2* (At2g46470)
MBA1 (YBR185C)	Mba1	–	–
MDM38 (YOL027C)	Mdm38	*MDM38* (Cre15.g639150)	*MDM38−1* (At3g59820) *MDM38−2* (At1g65540)
COX18 (YGR062C)	Cox18	–	–
PNT1 (YOR266W)	Pnt1	–	–
MSS2 (YDL107W)	Mss2	–	–
Matrix chaperones that fold proteins			
MDJ1 (YFL016C)	Mdj1	*MDJ1A* (Cre12.g551500)[c] *MDJ1B* (Cre12.g560700)	*MDJ1* (At5g48030)
MGE1 (YOR232W)	Mge1	*MGE1* (Cre08.g370450)	*MGE1−1* (At4g26780) *MGE1−2* (At5g55200)
HSP60 (YLR259C)	Hsp60	*CPN60C* (Cre06.g309100)	*HSP60−1* (At3g23990) *HSP60−2* (At2g33210) *HSP60−3* (At3g13860)
HSP10 (YOR020C)	Hsp10	*CPN10* (Cre03.g178450)	*HSP10−1* (At1g14980) *HSP10−2* (At1g23100)
HSP78 (YDR258C)	Hsp78	–	–
ZIM17 (YNL310C)	Zim17	*ZIM17* (Cre07.g334850)	*ZIM17* (At3g54826)

[a] *TOM20 and MTX1 are unique to plant and algal lineages, without orthologs in yeast.*
[b] *TOM9 is an ortholog of yeast TOM22 that lacks the cytosolic receptor domain.*
[c] *MDJ1A and MDJ1B (Willmund et al., 2008) are similar to At5g48030.*

11.2.2.2 Mitochondrial iron-sulfur proteins and their maturation pathways

Fe-S clusters/proteins have major functions in electron transfer or catalytic reactions, but they are also used as redox sensors, allowing for the perception of variations in the intracellular concentrations of iron or Fe-S clusters, oxygen, or nitric oxide (Lill, 2009; Miller & Auerbuch, 2015). In mitochondria, Fe-S clusters are crucial for the activity of respiratory chain complexes I, II, and III, and for several matrix-located proteins required, for instance, for the synthesis of lipoic acid, biotin, or molybdenum cofactors (Przybyla-Toscano et al., 2021a). The de novo Fe-S cluster assembly, trafficking and insertion into mitochondrial proteins rely on the iron-sulfur cluster (ISC) machinery formed by *ca* 15−20 proteins depending on the organisms (Braymer et al., 2020). Since this machinery provides a sulfur moiety required for maturation of essential cytosolic and nuclear Fe-S proteins and is one of the few pathways retained in mitochondria-related organelles such as mitosomes and hydrogenosomes, it is part of the core functions ensured by mitochondria (Braymer et al., 2020). Although a limited number of studies have been performed using *Chlamydomonas*, we discuss in this section the Fe-S protein-dependent pathways that are present in algal mitochondria and their maturation by the ISC machinery based on data gained in algae but also in cyanobacteria and in other eukaryotes, notably *Arabidopsis*. The mitochondrial ISC machineries present in these organisms display similarities owing to their common ancestral origin.

As with chloroplasts (Przybyla-Toscano et al., 2018), the demand for Fe-S clusters in mitochondria is high (Table 11.9), notably because they are present in the highly abundant respiratory complexes and aconitases

TABLE 11.9 Iron-sulfur cluster (ISC) proteins in *Chlamydomonas* mitochondria and counterparts in *Arabidopsis*.

Chlamydomonas			Counterparts in other organisms
Gene names	**Protein product**	**Phytozome accession [#]**	***Arabidopsis***
NUO8	Subunit of the NADH:ubiquinone oxidoreductase complex	Cre12.g496750	At1g16700 (TYKY), At1g79010
NUO10	Subunit of the NADH:ubiquinone oxidoreductase complex	Cre12.g492300	At5g11770
NUO5	Subunit of the NADH:ubiquinone oxidoreductase complex	Cre10.g450400	At4g02580
NUO6	Subunit of the NADH:ubiquinone oxidoreductase complex	Cre10.g422600	At5g08530
NUOS1	Subunit of the NADH:ubiquinone oxidoreductase complex	Cre12.g535950	At5g37510
SDH2	Subunit 2 of the succinate dehydrogenase complex	Cre06.g264200	At3g27380 (*SDH2.1*), At5g40650 (*SDH2.2*), At5g65165 (*SDH2.3*)
FUO1	Electron-transfer flavoprotein:ubiquinone oxidoreductase	Cre02.g094300	At2g43400
RIP1	Rieske protein of the ubiquinol-cytochrome *c* reductase	Cre01.g051900	At5g13430, At5g13440
ACH1	Aconitase	Cre01.g042750	At4g35830 (*ACO1*), At4g26970 (*ACO2*), At2g05710 (*ACO3*)
LAS1	lipoate synthase	Cre08.g359700	At2g20860
BIO2	biotin synthase	Cre06.g261150	At2g43360
CNX2	Cofactor of nitrate reductase and xanthine dehydrogenase 2	Cre13.g602900	At2g31955
HEMN1[a]	Radical SAM superfamily protein, possible implication in heme synthesis	Cre03.g171461	At5g63290
NCP1	Radical SAM superfamily protein, wybutosine biosynthesis	Cre14.g623300	At1g75200
PFLA1	Pyruvate-formate lyase activase	Cre05.g234636	None

[a]*Named based on sequence identity with the* Arabidopsis *ortholog.*
[#]*# = number.*

(Fuchs et al., 2020; Przybyla-Toscano et al., 2021a). In complex I, eight Fe-S clusters are present in the matrix arm, one (2Fe-2S) cluster bound to NUO5, one (4Fe-4S) cluster to NUO10, one (4Fe-4S) cluster to NUO6, two (4Fe-4S) clusters to NUO8, and one (2Fe-2S) cluster, and two (4Fe-4S) clusters to the NUOS1. In complex II, three Fe-S clusters [one (2Fe-2S) cluster, one (3Fe-4S) cluster and one (4Fe-4S) cluster] are bound to the SDH2 subunit. A single (2Fe-2S) cluster is present in complex III, bound by the Rieske protein. By analogy with the situation in *Arabidopsis*, an additional (4Fe-4S)-containing protein, the electron-transfer flavoprotein:ubiquinone oxidoreductase, FUO1, should be important as an alternative respiratory pathway by transferring electrons from several flavoprotein dehydrogenases present in the matrix to ubiquinone under certain stress situations (Hildebrandt et al., 2015). All these proteins function in electron transfer, receiving electrons from organic substrates or proteins and transferring them to acceptor molecules, either ubiquinone or proteins.

The biosynthesis of molybdenum cofactor (Moco) has been well characterized in plants and the first step in its synthesis is catalyzed by the radical SAM Fe-S protein, CNX2 (cofactor for nitrate reductase and xanthine dehydrogenase 2) in the mitochondria (Mendel, 2013). Surprisingly, most Moco-containing enzymes are not present in mitochondria; these include nitrate reductase, xanthine dehydrogenase, and aldehyde oxidase, which are all cytosolic proteins, as well as the

ortholog of the mitochondrial amidoxime-reducing component (mARC) (van Lis et al., 2020). Only the sulfite oxidase is present in mitochondria of *Chlamydomonas* unlike the land plant counterpart of this protein, which is in the peroxisomes (Gérin et al., 2010). Noteworthy, xanthine dehydrogenase and aldehyde oxidase also bind an Fe-S cluster, the synthesis of which is ensured by the cytosolic CIA machinery. The latter biogenesis system depends on the mitochondrial ISC machinery (see below). A few other metabolic processes in plant mitochondria may depend on Fe-S proteins but evidence is sometimes scarce or uncertain and we direct the reader to the following recent overview for more information and details (Przybyla-Toscano et al., 2021a; Przybyla-Toscano et al., 2021b).

A notable difference between algae and land plants is the existence of a developed fermentative metabolism in *Chlamydomonas*. Among the Fe-S proteins involved in fermentation, the hydrogenases (HYDA1 and HYDA2) and pyruvate-ferredoxin oxidoreductase are located in the chloroplast, but the pyruvate formate lyase PFL1 seems dually targeted to the chloroplast and mitochondrion (Atteia et al., 2006). Other proteins that likely have roles in oxic conditions are the hybrid cluster proteins 1−4 (HCP1−4) which are expressed during darkness but also on nitrate-containing media (van Lis et al., 2020). These proteins, which are not present in land plants, bind a (4Fe-4S)-cluster as well as an atypical (4Fe-2O-2S)-hybrid cluster. Among these four proteins, HCP2 is assumed to be present in mitochondria (van Lis et al., 2020).

Other pathways rely on Fe-S proteins and particularly on radical SAM Fe-S enzymes. These enzymes usually incorporate a (4Fe-4S)-cluster that is commonly coordinated by a conserved Cx_3Cx_2C motif and used for the reductive cleavage of SAM, producing a 5′-deoxyadenosyl radical required for certain biochemical reactions (Lanz & Booker, 2015). In addition, radical SAM enzymes often incorporate a so-called auxiliary Fe-S cluster, notably providing sulfur atoms for the synthesis of biotin and lipoic acid upon destruction of the cluster (Lanz & Booker, 2015). Radical SAM superfamily proteins are often involved in posttranscriptional modification of tRNAs and by analogy to the described role of TYW1 in wybutosine biosynthesis; we assume that the *Chlamydomonas* ortholog NCP1 likely performs a similar role (Przybyla-Toscano et al., 2021a). In biotin and lipoate synthases, the auxiliary cluster is of the (2Fe-2S) and (4Fe-4S) cluster forms, respectively (Przybyla-Toscano et al., 2021b). Since several mitochondrial and extra-mitochondrial enzymatic complexes depend on lipoic acid or biotin for their activity, these Fe-S protein-dependent biosynthetic pathways also represent key functions of mitochondria even though lipoic acid is also synthesized in chloroplasts (Przybyla-Toscano et al., 2018). Accordingly, two lipoate synthase-coding genes (LAS1, Cre08.g359700 and LAS2, Cre02.g114400) and one biotin synthase-coding gene (BIO2, Cre06.g261150) are present in the *Chlamydomonas* genome. In addition to aconitase and SDH, which themselves bind Fe-S cluster(s), two other enzymes of the TCA cycle rely indirectly on the correct functioning of the lipoate synthase, the pyruvate dehydrogenase complex (PDC) and α-ketoglutarate dehydrogenase (KGDH) (Rébeillé et al., 2007). Indeed, the E2 subunit of the PDC and KGDH complexes binds lipoic acid. Lipoic acid is also bound to the E2 subunit of the branched chain α-ketoacid dehydrogenase and the GDC-H subunit of the glycine decarboxylase/glycine cleavage system complex (Rébeillé et al., 2007). In photosynthetic organisms, a single biotin-dependent enzyme should reside in mitochondria, the methylcrotonyl-CoA carboxylase (MCCase) which is involved in leucine degradation, while other biotin-dependent complexes are present in the cytosol and chloroplast, notably the acetyl-CoA carboxylases that catalyze carboxylation of acetyl-CoA to produce malonyl-CoA, the first committed step in the synthesis of fatty acid (Przybyla-Toscano et al., 2021a; Rébeillé et al., 2007).

There is also growing information about the molecular mechanisms involved in Fe-S cluster biogenesis and trafficking from maturation factors to the above-mentioned client apo-proteins, based on the current model established from studies in other eukaryotes (Lill & Freibert, 2020). Hence, we provide a list of *Chlamydomonas* ISC orthologs (Table 11.10) that expands the previous *Chlamydomonas* genome analysis (Godman & Balk, 2008). The Fe-S cluster biogenesis process can be divided into several steps, the first being de novo synthesis of a (2Fe-2S) cluster on the ISU1 scaffold protein (Fig. 11.6). This requires an assembly complex with the core-forming proteins being the pyridoxal phosphate-dependent cysteine desulfurase NFS1, the LYRM (Leu-Tyr-Arg Motif) family protein ISD11 and the acyl-carrier protein 1 (ACP1) (Braymer et al., 2020). The NFS1 protein provides the required sulfur atoms while ISD11 and ACP1 stabilize NFS1. The so-called frataxin (FTX1) protein is known to regulate iron entry into the complex and to stimulate the cysteine desulfurase activity of NFS1 (Colin et al., 2013; Gervason et al., 2019). How and under which form iron atoms are routed to the complex is not yet known. A ferredoxin (MFDX1) is also required at this stage to reduce the sulfane sulfur present on NFS1 as a persulfide to sulfide upon transfer of the sulfur to the scaffold protein (Gervason et al., 2019). The oxidized MFDX1 is recycled by a NADPH-dependent ferredoxin reductase (ARH1).

The second step is the transfer of the preformed (2Fe-2S) cluster to a glutaredoxin (GRX), referred to as GRX5 in *Chlamydomonas* (or GRXS15 in land plants), the first so-called Fe-S cluster transfer/carrier protein. This transfer is

TABLE 11.10 Iron-sulfur machinery in *Chlamydomonas* mitochondria and counterparts in other organisms.

Chlamydomonas			Counterparts in other organisms		
Gene	**Protein product**	**Phytozome accession [#]**	**Human**	**Yeast**	***Arabidopsis***
NIFS1	Cysteine desulfurase, sulfur donor	Cre02.g146250	*NFS1*	*NFS1*	At5g65720 (*NFS1*)
ISD11	Stabilization and activation of NFS1	Cre08.g382850	*LYRM4*	*ISD11*	At5g61220 (*ISD11*)
ACP1	Acyl-carrier protein, regulator of NFS1	Cre16.g673109	*ACP1*	*ACP1*	At2g44620 (*ACP1*) At1g65290 (*ACP2*) At5g47630 (*ACP3*)
ISU1	Scaffold protein, *de novo* Fe-S cluster assembly	Cre13.g568850	*ISCU2*	*ISU1, ISU2*	At4g22220 (*ISU1*) At3g01020 (*ISU2*) At4g04080 (*ISU3*)
FTX1	Frataxin, regulation of iron entry and cysteine desulfurase activity	Cre12.g538350	*FXN*	*YFH1*	At4g03240 (*FH*)
MFDX1	Ferredoxin, electron donor for sulfane sulfur reduction and reductive coupling of (2Fe-2S) cluster in (4Fe-4S) cluster	Cre12.g559950	*FDX2*	*YAH1*	At4g05450 (*mFDX1*) At4g21090 (*mFDX2*)
ARH1	NADPH dependent-ferredoxin reductase	Cre13.g562550	*ADXR*	*ARH1*	At4g32360 (*mFDR*)
HSP70C	HSP70 chaperone, implicated in the Fe-S cluster release	Cre09.g393200	*HSPA9*	*SSQ1*	At4g37910 (*HSCA1*) At5g09590 (HSCA2)
HSC20	J-type cochaperone, implicated in the Fe-S cluster release	Cre12.g507559	*HSC20*	*JAQ1*	At5g06410 (*HSCB*)
MGE1	Nucleotide exchange factor, implicated in the Fe-S cluster release	Cre08.g370450	*GRPEL1/2*	*MGE1*	At4g26780 (*MGE1a*) At5g55200 (*MGE1b*)
GRX5	Carrier protein, involved in Fe-S cluster trafficking	Cre07.g325600	*GLRX5*	*GRX5*	At3g15660 (*GRXS15*)
BOLA3	Targeting factor, involved in Fe-S cluster trafficking	Cre08.g385900	*BOLA3*	*BOL3*	–
BOLA4[a]	Targeting factor, involved in Fe-S cluster trafficking	Cre09.g394701[a]	–	–	At5g17560 (*BOLA4*)
ISCA1	Carrier protein, involved in Fe-S cluster trafficking	Cre09.g400775	*ISCA1*	*ISA1*	At2g16710 (*ISCA1a*) At2g36260 (*ISCA1b*)
ISCA2	Carrier protein, involved in Fe-S cluster trafficking	Cre07.g349600	*ISCA2*	*ISA2*	At5g03905 (*ISCA2*)
IBA57	Targeting factor, involved in Fe-S cluster trafficking	Cre10.g459000	*CAF17/ IBA57*	*IBA57*	At4g12130 (*IBA57.1*)
NFU4	Carrier protein, involved in Fe-S cluster trafficking	Cre12.g504150	*NFU1*	*NFU1*	At3g20970 (*NFU4*) At1g51390 (*NFU5*)
INDH1	Carrier protein, involved in Fe-S cluster trafficking	Cre10.g427050	*NUBPL*	–	At4g19540 (*INDH*)

The names and functional annotations have been modified when inadequate/inappropriate. Orthologs present in *Arabidopsis*, *H. sapiens*, and *S. cerevisiae* have been indicated.
[a]*The gene is missing in v6.1 due to a gap in the assembly.*
[#]*# = number.*

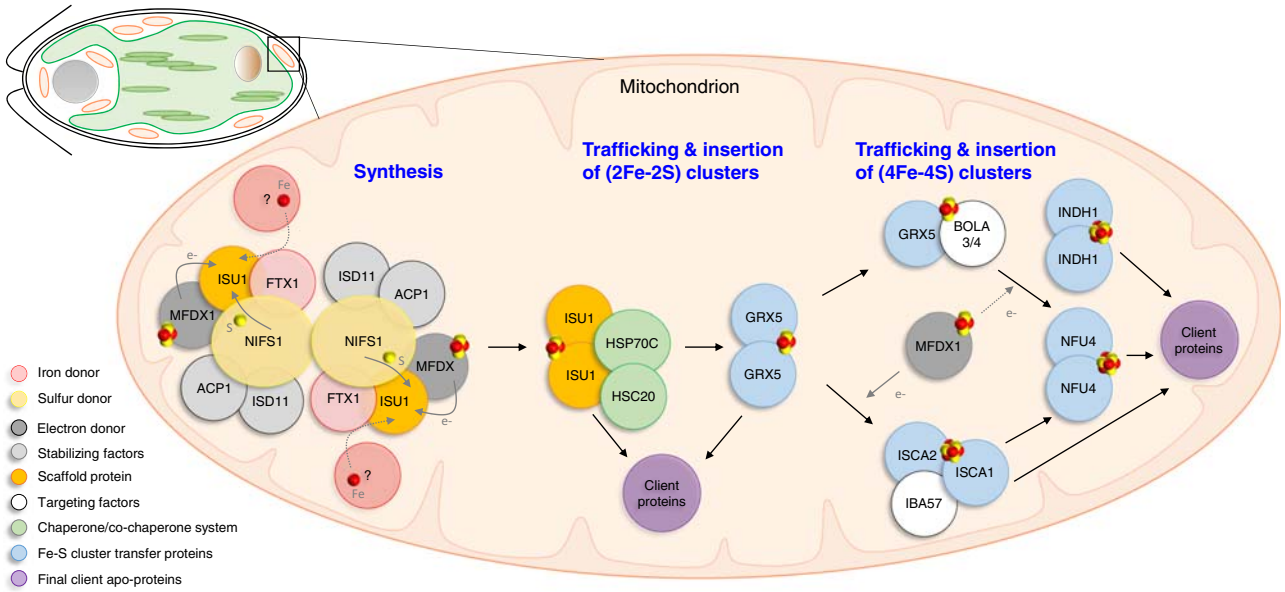

FIGURE 11.6 Model for the iron-sulfur cluster machinery in *Chlamydomonas*. The de novo synthesis of (2Fe-2S) clusters on the scaffold protein ISU requires the orchestrated action of six proteins constituting the early-acting ISC assembly complex. Afterward, the maturation of (2Fe-2S) proteins is ensured either directly by ISU or by the transfer protein GRX5 after a chaperone-assisted (2Fe-2S) cluster transfer from ISU. The maturation of (4Fe-4S) proteins requires additional Fe-S cluster conversion and transfer steps involving the Fe-S cluster transfer proteins ISCA, NFU, and INDH1 with the assistance of some companion maturation factors BOLA, IBA57, and of the electron donor MFDX1. More details about the roles of the respective maturation factors and underlying molecular mechanisms are provided in the text. The *Chlamydomonas* protein nomenclature is used.

assisted by a chaperone/cochaperone system consisting of HSC70C/HSC20B proteins and possibly the nucleotide exchange factor MGE1, although this remains to be demonstrated in photosynthetic organisms (Braymer et al., 2020). At this step, the (2Fe-2S) cluster can be delivered to acceptor proteins as shown for MFDX1 in *Arabidopsis* (Moseler et al., 2015) and possibly directly to respiratory complexes *via* HSC20 and additional LYRM assembly factors as proposed for the human HCSB ortholog (Maio et al., 2014, 2017). In yeast, GRX5 is the last protein necessary for feeding the cytosolic Fe-S protein assembly (CIA) machinery (Uzarska et al., 2013). Currently, it is proposed that the export of a sulfur (and possibly iron)-containing compound (likely a glutathione moiety) from mitochondria by an ABC transporter, ATM3 in Arabidopsis and *Chlamydomonas* (Schaedler et al., 2014; Srinivasan, Pierik, & Lill, 2014), compensates for the absence of cysteine desulfurase in the cytosol of eukaryotes. As such, this step is essential in most studied organisms because it is necessary for the functioning of the CIA machinery which provides Fe-S clusters for key DNA repair and replication enzymes or enzymes involved in cytosolic ribosome biogenesis; for a review see Paul and Lill (2015).

The subsequent mitochondrial ISC steps are the conversion of the (2Fe-2S) cluster into a (4Fe-4S) cluster, and (4Fe-4S) cluster trafficking and insertion into client apo-proteins. This is achieved by additional Fe-S cluster transfer proteins. The conversion is thought to occur in the presence of GSH *via* the reductive coupling of two (2Fe-2S) clusters during the transfer between GRX5 and an ISCA1−2 heterodimer, as shown in vitro using *Arabidopsis* proteins (Azam et al., 2020a) which also are present in *Chlamydomonas*. In human, it was shown in vitro that FDX2, but not FDX1, provides the electrons required for this reductive coupling (Weiler et al., 2020). In *Chlamydomonas*, this step should be performed by GSH and/or the sole MFDX1. The IBA57 seems also required at this step (Weiler et al., 2020) and could also be important for Fe-S cluster trafficking as shown from interaction and cellular studies performed with yeast and human proteins or cells (Gelling et al., 2008; Sheftel et al., 2012). The mitochondrial IBA57 protein is also present in *Chlamydomonas*. In *Arabidopsis* this protein is essential (Waller et al., 2012). In the next step, the NFU4 protein should receive its (4Fe-4S) cluster from the ISCA1/2 complex, as shown for the *Arabidopsis* proteins (Azam et al., 2020b). However, based on the reported in vitro Fe-S cluster transfer between a (2Fe-2S) cluster-bridging GRX5-BOLA3 complex and human NFU1 (Nasta et al., 2020), a similar reductive Fe-S cluster

coupling may be hypothesized in *Chlamydomonas* as well as a pathway to bypass ISCA-IBA57 proteins for the maturation of a specific subset of (4Fe-4S) proteins. The interaction of the mitochondrial Arabidopsis GRXS15 and BOLA4 proteins is well described (Couturier et al., 2014). It is noticeable that *Chlamydomonas* possesses generally the minimal set of ISC genes whereas *Arabidopsis* often has multiple genes (Couturier et al., 2013) (Table 11.10). This is the case for NFUs, for which *Chlamydomonas* only has a single representative referred to as NFU4 (newly adopted nomenclature). A notable exception to this rule is the BOLA family; the *Chlamydomonas* genome contains the three BOLA-encoding genes (BOLA1, BOLA2, BOLA4) classically present in terrestrial plants, but also possesses an animal-type mitochondrial BOLA3 representative (Couturier et al., 2014). The last protein currently known as being involved in Fe-S cluster biogenesis is INDH1. The mutation/depletion of the IND1/INDH ortholog in human, *Yarrowia lipolityca* or *Arabidopsis* leads to a specific decrease in complex I activity, but not in other respiratory complexes (Bych et al., 2008; Sheftel et al., 2009; Wydro et al., 2013). Since these proteins incorporate a (4Fe-4S) cluster, the results suggest a requirement for maturation of one or several (4Fe-4S) clusters present in complex I, although plant INDH has been proposed to play a role in protein translation (Wydro et al., 2013) (see also Section 11.2.1.1).

In conclusion, it is striking that such a complex ISC machinery, formed by $\sim$ 20 proteins including 8 different late-acting Fe-S cluster transfer proteins, is necessary for maturation of $\sim$15 mitochondrial Fe-S proteins. Despite the conservation of this system, there is still little information concerning the route(s) by which the Fe-S cluster(s) are acquired by their diverse set client proteins. Hence, considering its particular physiology and nutrition modes, *Chlamydomonas* remains an excellent model among photosynthetic organisms for studying genes encoding ISC components or Fe-S client proteins that are essential for mitochondrial functions in embryophytes (Couturier et al., 2013), as well as the atypical proteins such as the HCPs.

Acknowledgments

CR acknowledges FNRS-FWO EOS Project 30829584, FNRS CDR J.0175.20 and Action de Recherche Concertée from the University of Liege (DARKMET ARC grant 17/21−08). NR acknowledges the French Programme Investissement d'Avenir (PIA) "Lorraine Université d'Excellence" (reference no. ANR-15-IDEX-04-LUE) for the partial financial support of the work on Fe-S protein maturation. DG-H acknowledges grants PAPIIT IN209220 (DGAPA, UNAM), CONACyT-FONCICyT 279125, CONACyT-Frontera 21856, and the technical support of Miriam Vázquez-Acevedo (IFC, UNAM).

References

Ackerman, S. H., & Tzagoloff, A. (1990). Identification of two nuclear genes (ATP11, ATP12) required for assembly of the yeast F1-ATPase. *Proceedings of the National Academy of Sciences of the United States of America*, *87*, 4986−4990.

Alfonzo, M., Kandrach, M. A., & Racker, E. (1981). Isolation, characterization, and reconstitution of a solubilized fraction containing the hydrophobic sector of the mitochondrial proton pump. *Journal of Bioenergetics and Biomembranes*, *13*, 375−391.

Allegretti, M., Klusch, N., Mills, D. J., et al. (2015). Horizontal membrane-intrinsic α-helices in the stator a-subunit of an F-type ATP synthase. *Nature*, *521*, 237−240.

Alston, C. L., Veling, M. T., Heidler, J., et al. (2020). Pathogenic bi-allelic mutations in NDUFAF8 cause Leigh syndrome with an isolated complex I deficiency. *American Journal of Human Genetics*, *106*, 92−101.

Armenteros, J. J. A., Salvatore, M., Emanuelsson, O., et al. (2019). Detecting sequence signals in targeting peptides using deep learning. *Life Science Alliance*, *2*, e201900429.

Arselin, G., Vaillier, J., Salin, B., et al. (2004). The modulation in subunits e and g amounts of yeast ATP synthase modifies mitochondrial cristae morphology. *The Journal of Biological Chemistry*, *279*, 40392−40399.

Atkinson, A., Smith, P., Fox, J. L., et al. (2011). The LYR protein Mzm1 functions in the insertion of the Rieske Fe/S protein in yeast mitochondria. *Molecular and Cellular Biology*, *31*, 3988−3996.

Atteia, A., Adrait, A., Brugière, S., et al. (2009). A proteomic survey of *Chlamydomonas reinhardtii* mitochondria sheds new light on the metabolic plasticity of the organelle and on the nature of the alpha-proteobacterial mitochondrial ancestor. *Molecular Biology and Evolution*, *26*, 1533−1548.

Atteia, A., Dreyfus, G., & González-Halphen, D. (1997). Characterization of the α and β-subunits of the F0F1-ATPase from the alga *Polytomella* spp., a colorless relative of *Chlamydomonas reinhardtii*. *Biochimica et Biophysica Acta*, *1320*, 275−284.

Atteia, A., & Franzén, L. G. (1996). Identification, cDNA sequence and deduced amino acid sequence of the mitochondrial Rieske iron-sulfur protein from the green alga *Chlamydomonas reinhardtii* implications for protein targeting and subunit interaction. *European Journal of Biochemistry*, *237*, 792−799.

Atteia, A., van Lis, R., Gelius-Dietrich, G., et al. (2006). Pyruvate formate-lyase and a novel route of eukaryotic ATP synthesis in *Chlamydomonas* mitochondria. *The Journal of Biological Chemistry*, *281*, 9909−9918.

Azam, T., Przybyla-Toscano, J., Vignols, F., et al. (2020a). The *Arabidopsis* mitochondrial glutaredoxin GRXS15 provides [2Fe-2S] clusters for ISCA-mediated [4Fe-4S] cluster maturation. *International Journal of Molecular Sciences*, *21*, E9237.

Azam, T., Przybyla-Toscano, J., Vignols, F., et al. (2020b). [4Fe-4S] cluster trafficking mediated by *Arabidopsis* mitochondrial ISCA and NFU proteins. *The Journal of Biological Chemistry*, *295*, 18367−18378.

Babot, M., Birch, A., Labarbuta, P., et al. (2014). Characterisation of the active/de-active transition of mitochondrial complex I. *Biochimica et Biophysica Acta*, *1837*, 1083−1092.

Balabaskaran, N. P., Dudkina, N. V., Kane, L. A., et al. (2010). Highly divergent mitochondrial ATP synthase complexes in *Tetrahymena thermophila*. *PLoS Biology*, *8*, e1000418−e1000418.

Baradaran, R., Berrisford, J. M., Minhas, G. S., et al. (2013). Crystal structure of the entire respiratory complex I. *Nature*, *494*, 443−448.

Barbieri, R. M., Larosa, V., Nouet, C., et al. (2011). A forward genetic screen identifies mutants deficient for mitochondrial complex I assembly in *Chlamydomonas reinhardtii*. *Genetics*, *188*, 349−358.

Baurain, D., Dinant, M., Coosemans, N., et al. (2003). Regulation of the alternative oxidase Aox1 gene in *Chlamydomonas reinhardtii*. Role of the nitrogen source on the expression of a reporter gene under the control of the Aox1 promoter. *Plant Physiology*, *131*, 1418−1430.

Belt, K., Van Aken, O., Murcha, M., et al. (2018). An assembly factor promotes assembly of flavinated SDH1 into the succinate dehydrogenase complex. *Plant Physiology*, *177*, 1439−1452.

Bennoun, P., & Delosme, M. (1999). Chloroplast suppressors that act on a mitochondrial mutation in *Chlamydomonas reinhardtii*. *Molecular and General Genetics*, *262*, 85−89.

Berrisford, J. M., Baradaran, R., & Sazanov, L. A. (2016). Structure of bacterial respiratory complex I. *Biochimica et Biophysica Acta 2004*, *1857*, 892−901.

Blum, T. B., Hahn, A., Meier, T., et al. (2019). Dimers of mitochondrial ATP synthase induce membrane curvature and self-assemble into rows. *Proceedings of the National Academy of Sciences of the United States of America*, *116*, 4250−4255.

Boer, P. H., & Gray, M. W. (1988a). Genes encoding a subunit of respiratory NADH dehydrogenase (ND1) and a reverse transcriptase-like protein (RTL) are linked to ribosomal RNA gene pieces in *Chlamydomonas reinhardtii* mitochondrial DNA. *The EMBO Journal*, *7*, 3501−3508.

Boer, P. H., & Gray, M. W. (1988b). Transfer RNA genes and the genetic code in *Chlamydomonas reinhardtii* mitochondria. *Current Genetics*, *14*, 583−590.

Boer, P. H., & Gray, M. W. (1988c). Scrambled ribosomal RNA gene pieces in *Chlamydomonas reinhardtii* mitochondrial DNA. *Cell*, *55*, 399−411.

Bonnard, G., Gobert, A., Arrivé, M., et al. (2016). Transfer RNA maturation in *Chlamydomonas* mitochondria, chloroplast and the nucleus by a single RNase P protein. *The Plant Journal*, *87*, 270−280.

Boulouis, A., Drapier, D., Razafimanantsoa, H., et al. (2015). Spontaneous dominant mutations in *Chlamydomonas* highlight ongoing evolution by gene diversification. *The Plant Cell*, *27*, 984−1001.

Braun, H. P., Binder, S., Brennicke, A., et al. (2014). The life of plant mitochondrial complex I. *Mitochondrion*, *19*(Pt B), 295−313.

Braymer, J. J., Freibert, S. A., Rakwalska-Bange, M., et al. (2020). Mechanistic concepts of iron-sulfur protein biogenesis in biology. *Biochimica Biophysica Acta. Molecular Cell Research*, 118863.

Bych, K., Kerscher, S., Netz, D. J. A., et al. (2008). The iron-sulphur protein Ind1 is required for effective complex I assembly. *The EMBO Journal*, *27*, 1736−1746.

Cabezón, E., Montgomery, M. G., Leslie, A. G. W., et al. (2003). The structure of bovine F1-ATPase in complex with its regulatory protein IF1. *Nature Structural Biology*, *10*, 744−IF750.

Cabrera-Orefice, A., Yoga, E. G., Wirth, C., et al. (2018). Locking loop movement in the ubiquinone pocket of complex I disengages the proton pumps. *Nature Communications*, *9*, 4500−4500.

Cahoon, A. B., & Qureshi, A. A. (2018). Leaderless mRNAs are circularized in *Chlamydomonas reinhardtii* mitochondria. *Current Genetics*, *64*, 1321−1333.

Cano-Estrada, A., Vázquez-Acevedo, M., Villavicencio-Queijeiro, A., et al. (2010). Subunit-subunit interactions and overall topology of the dimeric mitochondrial ATP synthase of *Polytomella* sp. *Biochimica et Biophysica Acta*, *1797*, 1439−1448.

Cardol, P., Boutaffala, L., Memmi, S., et al. (2008). In *Chlamydomonas*, the loss of ND5 subunit prevents the assembly of whole mitochondrial complex I and leads to the formation of a low abundant 700 kDa subcomplex. *Biochimica et Biophysica Acta*, *1777*, 388−396.

Cardol, P., Figueroa, F., Remacle, C., et al. (2009). Oxidative phosphorylation: Building blocks and related components. In D. B. Stern (Ed.), *The Chlamydomonas sourcebook, organellar and metabolic processes* (pp. 469−502). San Diego: Elsevier Inc.

Cardol, P., Gloire, G., Havaux, M., et al. (2003). Photosynthesis and state transitions in mitochondrial mutants of *Chlamydomonas reinhardtii* affected in respiration. *Plant Physiology*, *133*, 2010−2020.

Cardol, P., González-Halphen, D., Reyes-Prieto, A., et al. (2005). The mitochondrial oxidative phosphorylation proteome of *Chlamydomonas reinhardtii* deduced from the Genome Sequencing Project. *Plant Physiology*, *137*, 447−459.

Cardol, P., Lapaille, M., Minet, P., et al. (2006). ND3 and ND4L subunits of mitochondrial complex I, both nucleus encoded in *Chlamydomonas reinhardtii*, are required for activity and assembly of the enzyme. *Eukaryotic Cell*, *5*, 1460−1467.

Cardol, P., Matagne, R. F., & Remacle, C. (2002). Impact of mutations affecting ND mitochondria-encoded subunits on the activity and assembly of complex I in *Chlamydomonas*. Implication for the structural organization of the enzyme. *Journal of Molecular Biology*, *319*, 1211−1221.

Cardol, P., & Remacle, C. (2009). The mitochondrial genome. *The Chlamydomonas sourcebook, organellar and metabolic processes*, 445−467, San Diego: Elsevier Inc..

Cardol, P., Vanrobaeys, F., Devreese, B., et al. (2004). Higher plant-like subunit composition of mitochondrial complex I from *Chlamydomonas reinhardtii*: 31 conserved components among eukaryotes. *Biochimica et Biophysica Acta*, *1658*, 212−224.

Carrie, C., Murcha, M. W., & Whelan, J. (2010). An in silico analysis of the mitochondrial protein import apparatus of plants. *BMC Plant Biology*, *10*, 249.

Carroll, J., Fearnley, I. M., Shannon, R. J., et al. (2003). Analysis of the subunit composition of complex I from bovine heart mitochondria. *Molecular & Cellular Proteomics*, *2*, 117−126.

Carroll, J., He, J., Ding, S., et al. (2021). TMEM70 and TMEM242 help to assemble the rotor ring of human ATP synthase and interact with assembly factors for complex I. *Proceedings of the National Academy of Sciences of the United States of America*, *118*, e2100558118.

Chacinska, A., Pfannschmidt, S., Wiedemann, N., et al. (2004). Essential role of Mia40 in import and assembly of mitochondrial intermembrane space proteins. *The EMBO Journal*, *23*, 3735−3746.

Claros, M. G., Perea, J., Shu, Y., et al. (1995). Limitations to in vivo import of hydrophobic proteins into yeast mitochondria: The case of a cytoplasmically synthesized apocytochrome b. *European Journal of Biochemistry*, *228*, 762−771.

Claros, M. G., & Vincens, P. (1996). Computational method to predict mitochondrially imported proteins and their targeting sequences. *European Journal of Biochemistry*, *241*, 779−786.

Cognat, V., Deragon, J.-M., Vinogradova, E., et al. (2008). On the evolution and expression of *Chlamydomonas* reinhardtii nucleus-encoded transfer RNA genes. *Genetics*, *179*, 113−123.

Cognat, V., Pawlak, G., Duchêne, A. M., et al. (2013). PlantRNA, a database for tRNAs of photosynthetic eukaryotes. *Nucleic Acids Research*, *41*, 273−279.

Colin, F., Martelli, A., Clémancey, M., et al. (2013). Mammalian frataxin controls sulfur production and iron entry during de novo Fe4S4 cluster assembly. *Journal of the American Chemical Society*, *135*, 733−740.

Colina-Tenorio, L., Dautant, A., Miranda-Astudillo, H., et al. (2018). The peripheral stalk of rotary ATPases. *Frontiers in Physiology*, *9*, 1243.

Colina-Tenorio, L., Miranda-Astudillo, H., Cano-Estrada, A., et al. (2016). Subunit Asa1 spans all the peripheral stalk of the mitochondrial ATP synthase of the chlorophycean alga Polytomella sp. *Biochimica et Biophysica Acta*, *1857*, 359−369.

Colleaux, L., Michel-Wolwertz, M. R., Matagne, R. F., et al. (1990). The apocytochrome b gene of *Chlamydomonas smithii* contains a mobile intron related to both *Saccharomyces* and *Neurospora* introns. *Molecular and General Genetics*, *223*, 288−296.

Couturier, J., Touraine, B., Briat, J.-F., et al. (2013). The iron-sulfur cluster assembly machineries in plants: current knowledge and open questions. *Frontiers in Plant Science*, *4*, 259.

Couturier, J., Wu, H.-C., Dhalleine, T., et al. (2014). Monothiol glutaredoxin-BolA interactions: redox control of *Arabidopsis thaliana* BolA2 and SufE1. *Molecular Plant*, *7*, 187−205.

Crofts, A. R., Rose, S. W., Burton, R. L., et al. (2017). The Q-cycle mechanism of the bc1 complex: A biologist's perspective on atomistic studies. *The Journal of Physical Chemistry. B*, *121*, 3701−3717.

Curran, S. P., Leuenberger, D., Leverich, E. P., et al. (2004). The role of Hot13p and redox chemistry in the mitochondrial TIM22 import pathway. *The Journal of Biological Chemistry*, *279*, 43744−43751.

Daley, D. O., Clifton, R., & Whelan, J. (2002). Intracellular gene transfer: Reduced hydrophobicity facilitates gene transfer for subunit 2 of cytochrome c oxidase. *Proceedings of the National Academy of Sciences of the United States of America*, *99*, 10510−10515.

Dang, Q. L., Phan, D. H., Johnson, A. N., et al. (2020). Analysis of human mutations in the supernumerary subunits of complex I. *eLife*, *10*, 1−35.

Davies, K. M., Blum, T. B., & Kühlbrandt, W. (2018). Conserved in situ arrangement of complex I and III2 in mitochondrial respiratory chain supercomplexes of mammals, yeast, and plants. *Proceedings of the National Academy of Sciences of the United States of America*, *115*, 3024−3029.

Denovan-Wright, E. M., & Lee, R. W. (1995). Evidence that the fragmented ribosomal RNAs of *Chlamydomonas* mitochondria are associated with ribosomes. *FEBS Letters*, *370*, 222−226.

Desplats, C., Mus, F., Cuiné, S., et al. (2009). Characterization of Nda2, a plastoquinone-reducing type II NAD(P)H dehydrogenase in *Chlamydomonas* chloroplasts. *The Journal of Biological Chemistry*, *284*, 4148−4157.

Dinant, M., Baurain, D., Coosemans, N., et al. (2001). Characterization of two genes encoding the mitochondrial alternative oxidase in *Chlamydomonas reinhardtii*. *Current Genetics*, *39*, 101−108.

Duby, F., Cardol, P., Matagne, R. F., et al. (2001). Structure of the telomeric ends of mt DNA, transcriptional analysis and complex I assembly in the dum24 mitochondrial mutant of *Chlamydomonas reinhardtii*. *Molecular Genetics and Genomics*, *266*, 109−114.

Duchêne, A.-M., Pujol, C., & Maréchal-Drouard, L. (2009). Import of tRNAs and aminoacyl-tRNA synthetases into mitochondria. *Current Genetics*, *55*, 1−18.

Dudkina, N. V., Heinemeyer, J., Keegstra, W., et al. (2005). Structure of dimeric ATP synthase from mitochondria: An angular association of monomers induces the strong curvature of the inner membrane. *FEBS Letters*, *579*, 5769−5772.

Dudkina, N. V., Oostergetel, G. T., Lewejohann, D., et al. (2010). Row-like organization of ATP synthase in intact mitochondria determined by cryo-electron tomography. *Biochimica et Biophysica Acta*, *1797*, 272−277.

Durante, L., Hübner, W., Lauersen, K. J., et al. (2019). Characterization of the GPR1/FUN34/YaaH protein family in the green microalga *Chlamydomonas* suggests their role as intracellular membrane acetate channels. *Plant Direct*, *3*, e00148.

Ehara, T., Osafune, T., & Hase, E. (1995). Behavior of mitochondria in synchronized cells of *Chlamydomonas reinhardtii* (Chlorophyta). *Journal of Cell Science*, *108*(Pt 2), 499−507.

Eisenhut, M., Roell, M.-S., & Weber, A. P. M. (2019). Mechanistic understanding of photorespiration paves the way to a new green revolution. *The New Phytologist*, *223*, 1762−1769.

Ellis, T. P., Helfenbein, K. G., Tzagoloff, A., et al. (2004). Aep3p stabilizes the mitochondrial bicistronic mRNA encoding subunits 6 and 8 of the H + -translocating ATP synthase of Saccharomyces cerevisiae. *The Journal of Biological Chemistry*, *279*, 15728−15733.

Elurbe, D. M., & Huynen, M. A. (2016). The origin of the supernumerary subunits and assembly factors of complex I: A treasure trove of pathway evolution. *Biochimica et Biophysica Acta*, *1857*, 971–979.

Emonds-Alt, B., Coosemans, N., Gerards, T., et al. (2017). Isolation and characterization of mutants corresponding to the MENA, MENB, MENC and MENE enzymatic steps of 5′-monohydroxyphylloquinone biosynthesis in *Chlamydomonas reinhardtii*. *The Plant Journal*, *89*, 141–154.

Eubel, H., Heinemeyer, J., Sunderhaus, S., et al. (2004). Respiratory chain supercomplexes in plant mitochondria. *Plant Physiology and Biochemistry*, *42*, 937–942.

Eubel, H., Jänsch, L., & Braun, H. P. (2003). New insights into the respiratory chain of plant mitochondria. Supercomplexes and a unique composition of complex II. *Plant Physiology*, *133*, 274–286.

Fatihi, A., Latimer, S., Schmollinger, S., et al. (2015). A dedicated type II NADPH dehydrogenase performs the penultimate step in the biosynthesis of vitamin K1 in *Synechocystis* and *Arabidopsis*. *The Plant Cell*, *27*, 1730–1741.

Ferry, J. G. (2010). The gamma class of carbonic anhydrases. *Biochimica et Biophysica Acta*, *1804*, 374–381.

Fiedorczuk, K., Letts, J. A., Degliesposti, G., et al. (2016). Atomic structure of the entire mammalian mitochondrial complex I. *Nature*, *538*, 406–410.

Figueroa-Martínez, F., Funes, S., Franzén, L. G., et al. (2008). Reconstructing the mitochondrial protein import machinery of *Chlamydomonas reinhardtii*. *Genetics*, *179*, 149–155.

Finger, Y., & Riemer, J. (2020). Protein import by the mitochondrial disulfide relay in higher eukaryotes. *Biological Chemistry*, *401*, 749–763.

Finnegan, P. M., Ellis, T. P., Nagley, P., et al. (1995). The mature AEP2 gene product of *Saccharomyces cerevisiae*, required for the expression of subunit 9 of ATP synthase, is a 58 kDa mitochondrial protein. *FEBS Letters*, *368*, 505–508.

Formosa, L. E., Dibley, M. G., Stroud, D. A., et al. (2018). Building a complex complex: Assembly of mitochondrial respiratory chain complex I. *Seminars in Cell & Developmental Biology*, *76*, 154–162.

Formosa, L. E., Muellner-Wong, L., Reljic, B., et al. (2020). Dissecting the roles of mitochondrial complex I intermediate assembly complex factors in the biogenesis of complex I. *Cell Rep*, *31*, 107541.

Formosa, L. E., Reljic, B., Sharpe, A. J., et al. (2021). Optic atrophy–associated TMEM126A is an assembly factor for the ND4-module of mitochondrial complex I. *Proceedings of the National Academy of Sciences of the United States of America*, *118*, e2019665118.

Franzén, L. G., & Falk, G. (1992). Nucleotide sequence of cDNA clones encoding the β subunit of mitochondrial ATP synthase from the green alga *Chlamydomonas reinhardtii*: The precursor protein encoded by the cDNA contains both an N-terminal presequence and a C-terminal extension. *Plant Molecular Biology*, *19*, 771–780.

Fromm, S., Braun, H. P., & Peterhansel, C. (2016b). Mitochondrial gamma carbonic anhydrases are required for complex I assembly and plant reproductive development. *The New Phytologist*, *211*, 194–207.

Fromm, S., Senkler, J., Zabaleta, E., et al. (2016a). The carbonic anhydrase domain of plant mitochondrial complex I. *Physiologia Plantarum*, *157*, 289–296.

Fuchs, P., Rugen, N., Carrie, C., et al. (2020). Single organelle function and organization as estimated from Arabidopsis mitochondrial proteomics. *The Plant Journal*, *101*, 420–441.

Fukasawa, Y., Tsuji, J., Fu, S. C., et al. (2015). MitoFates: Improved prediction of mitochondrial targeting sequences and their cleavage sites. *Molecular and Cellular Proteomics*, *14*, 1113–1126.

Funes, S., Davidson, E., Gonzalo Claros, M., et al. (2002b). The typically mitochondrial DNA-encoded ATP6 subunit of the F1F0-ATPase is encoded by a nuclear gene in *Chlamydomonas reinhardtii*. *The Journal of Biological Chemistry*, *277*, 6051–6058.

Funes, S., Perez-Martínez, X., Antaramian, A., et al. (2002a). Transfer of mitochondrial genes to the nucleus in chlamydomonad algae: Perspectives for the allotopic expression of OXPHOS proteins and future human therapies. In J. J. García-Trejo (Ed.), *Recent research developments in bioenergetics* (pp. 173–194). Research Signpost.

Gabriel, K., Milenkovic, D., Chacinska, A., et al. (2007). Novel mitochondrial intermembrane space proteins as substrates of the MIA import pathway. *Journal of Molecular Biology*, *365*, 612–620.

Gallaher, S. D., Fitz-Gibbon, S. T., Strenkert, D., et al. (2018). High-throughput sequencing of the chloroplast and mitochondrion of *Chlamydomonas reinhardtii* to generate improved *de novo* assemblies, analyze expression patterns and transcript speciation, and evaluate diversity among laboratory strains and wild isolates. *The Plant Journal*, *93*, 545–565.

García-Trejo, J. J., Zarco-Zavala, M., Mendoza-Hoffmann, F., et al. (2016). The inhibitory mechanism of the ζ subunit of the F1FO-ATPase nanomotor of *Paracoccus denitrificans* and related α-proteobacteria. *The Journal of Biological Chemistry*, *291*, 538–546.

Gawryluk, R. M. R., & Gray, M. W. (2010). Evidence for an early evolutionary emergence of gamma-type carbonic anhydrases as components of mitochondrial respiratory complex I. *BMC Evolutionary Biology*, *10*, 176.

Gelling, C., Dawes, I. W., Richhardt, N., et al. (2008). Mitochondrial Iba57p is required for Fe/S cluster formation on aconitase and activation of radical SAM enzymes. *Molecular and Cellular Biology*, *28*, 1851–1861.

Gérin, S., Mathy, G., Blomme, A., et al. (2010). Plasticity of the mitoproteome to nitrogen sources (nitrate and ammonium) in *Chlamydomonas reinhardtii*: The logic of Aox1 gene localization. *Biochimica et Biophysica Acta*, *1797*, 994–1003.

Gervason, S., Larkem, D., Mansour, A. B., et al. (2019). Physiologically relevant reconstitution of iron-sulfur cluster biosynthesis uncovers persulfide-processing functions of ferredoxin-2 and frataxin. *Nature Communications*, *10*, 3566.

Giachin, G., Bouverot, R., Acajjaoui, S., et al. (2016). Dynamics of human mitochondrial complex I assembly: Implications for neurodegenerative diseases. *Frontiers in Molecular Biosciences*, *3*, 43.

Glaser, E., & Dessi, P. (1999). Integration of the mitochondrial-processing peptidase into the cytochrome bc1 complex in plants. *Journal of Bioenergetics and Biomembranes*, *31*, 259−274.

Godman, J., & Balk, J. (2008). Genome analysis of *Chlamydomonas reinhardtii* reveals the existence of multiple, compartmentalized iron-sulfur protein assembly machineries of different evolutionary origins. *Genetics*, *179*, 59−68.

Goyal, A., & Tolbert, N. E. (1989). Variations in the alternative oxidase in *Chlamydomonas* grown in air or high CO_2. *Plant Physiology*, *89*, 958−962.

Grant, D., & Chiang, K. S. (1980). Physical mapping and characterization of *Chlamydomonas* mitochondrial DNA molecules: Their unique ends, sequence homogeneity, and conservation. *Plasmid*, *4*, 82−96.

Gray, M. W., & Boer, P. H. (1988). Organization and expression of algal (*Chlamydomonas reinhardtii*) mitochondrial DNA. *Philosophical Transactions of the Royal Society of London. Series B, Biological Sciences*, *319*, 135−147.

Guerrero-Castillo, S., Baertling, F., Kownatzki, D., et al. (2017). The assembly pathway of mitochondrial respiratory chain complex I. *Cell Metabolism*, *25*, 128−139.

Hahn, A., Parey, K., Bublitz, M., et al. (2016). Structure of a complete ATP synthase dimer reveals the molecular basis of inner mitochondrial membrane morphology. *Molecular Cell*, *63*, 445−456.

He, H., Van Breusegem, F., & Mhamdi, A. (2018). Redox-dependent control of nuclear transcription in plants. *Journal of Experimental Botany*, *69*, 3359−3372.

Helfenbein, K. G., Ellis, T. P., Dieckmann, C. L., et al. (2003). ATP22, a nuclear gene required for expression of the F0 sector of mitochondrial ATPase in Saccharomyces cerevisiae. *The Journal of Biological Chemistry*, *278*, 19751−19756.

Hildebrandt, T. M., Nunes Nesi, A., Araújo, W. L., et al. (2015). Amino acid catabolism in plants. *Molecular Plant*, *8*, 1563−1579.

Hiramatsu, T., Nakamura, S., Misumi, O., et al. (2006). Morphological changes in mitochondrial and chloroplast nucleoids and mitochondria during the *Chlamydomonas reinhardtii* (Chlorophyceae) cell cycle. *Journal of Phycology*, *42*, 1048−1058.

Hommersand, M. H., & Thimann, K. V. (1965). Terminal respiration of vegetative cells and zygospores in *Chlamydomonas reinhardi*. *Plant Physiology*, *40*, 1220−1227.

Horten, P., Colina-Tenorio, L., & Rampelt, H. (2020). Biogenesis of mitochondrial metabolite carriers. *Biomolecules*, *10*, 1−13.

Huang, S., Braun, H. P., Gawryluk, R. M. R., et al. (2019). Mitochondrial complex II of plants: Subunit composition, assembly, and function in respiration and signaling. *The Plant Journal*, *98*, 405−417.

Huang, S., Taylor, N. L., Ströher, E., et al. (2013). Succinate dehydrogenase assembly factor 2 is needed for assembly and activity of mitochondrial complex II and for normal root elongation in Arabidopsis. *The Plant Journal*, *73*, 429−441.

Ivanova, A., Gill-Hille, M., Huang, S., et al. (2019). A mitochondrial LYR protein is required for complex I assembly. *Plant Physiology*, *181*, 1632−1650.

Jans, F., Mignolet, E., Houyoux, P.-A., et al. (2008). A type II NAD(P)H dehydrogenase mediates light-independent plastoquinone reduction in the chloroplast of *Chlamydomonas*. *Proceedings of the National Academy of Sciences of the United States of America*, *105*, 20546−20551.

Kampjut, D., & Sazanov, L. A. (2020). The coupling mechanism of mammalian respiratory complex I. *Science*, *370*, eabc4209−eabc4209.

Kaye, Y., Huang, W., Clowez, S., et al. (2019). The mitochondrial alternative oxidase from *Chlamydomonas reinhardtii* enables survival in high light. *The Journal of Biological Chemistry*, *294*, 1380−1395.

Kerscher, O., Holder, J., Srinivasan, M., et al. (1997). The Tim54p-Tim22p complex mediates insertion of proteins into the mitochondrial inner membrane. *The Journal of Cell Biology*, *139*, 1663−1675.

Kerscher, S., Dröse, S., Zickermann, V., et al. (2008). The three families of respiratory NADH dehydrogenases. *Results and Problems in Cell Differentiation*, *45*, 185−222.

Klusch, N., Senkler, J., Yildiz, Ö., et al. (2021). A ferredoxin bridge connects the two arms of plant mitochondrial complex I. *The Plant Cell*, *33*, 2072−2091.

Koppen, M., & Langer, T. (2007). Protein degradation within mitochondria: Versatile activities of AAA proteases and other peptidases. *Critical Reviews in Biochemistry and Molecular Biology*, *42*, 221−242.

Kovalčíková, J., Vrbacký, M., Pecina, P., et al. (2019). TMEM70 facilitates biogenesis of mammalian ATP synthase by promoting subunit c incorporation into the rotor structure of the enzyme. *The FASEB Journal*, *33*, 14103−14117.

Kück, U., & Neuhaus, H. (1986). Universal genetic code evidenced in mitochondria of *Chlamydomonas reinhardii*. *Applied Microbiology and Biotechnology*, *23*, 462−469.

Lancelin, J. M., Gans, P., Bouchayer, E., et al. (1996). NMR structures of a mitochondrial transit peptide from the green alga *Chlamydomonas reinhardtii*. *FEBS Letters*, *391*, 203−208.

Lanz, N. D., & Booker, S. J. (2015). Auxiliary iron-sulfur cofactors in radical SAM enzymes. *Biochimica et Biophysica Acta*, *1853*, 1316−1334.

Lapaille, M., Escobar-Ramirez, A., Degand, H., et al. (2010a). Atypical subunit composition of the chlorophycean mitochondrial F1FO-ATP synthase and role of Asa7 protein in stability and oligomycin resistance of the enzyme. *Molecular Biology and Evolution*, *27*, 1630−1644.

Lapaille, M., Thiry, M., Perez, E., et al. (2010b). Loss of mitochondrial ATP synthase subunit beta (Atp2) alters mitochondrial and chloroplastic function and morphology in *Chlamydomonas*. *Biochimica et Biophysica Acta*, *1797*, 1533−1539.

Larosa, V., Coosemans, N., Motte, P., et al. (2012). Reconstruction of a human mitochondrial complex I mutation in the unicellular green alga *Chlamydomonas*. *The Plant Journal*, *70*, 759−768.

Larosa, V., & Remacle, C. (2018). Insights into the respiratory chain and oxidative stress. *Bioscience Reports*, 38, BSR20171492.

Lauersen, K. J., Willamme, R., Coosemans, N., et al. (2016). Peroxisomal microbodies are at the crossroads of acetate assimilation in the green microalga *Chlamydomonas reinhardtii*. *Algal Research*, *16*, 266–274.
Lecler, R., Vigeolas, H., Emonds-Alt, B., et al. (2012). Characterization of an internal type-II NADH dehydrogenase from *Chlamydomonas reinhardtii* mitochondria. *Current Genetics*, *58*, 205–216.
Lefebvre-Legendre, L., Vaillier, J., Benabdelhak, H., et al. (2001). Identification of a nuclear gene (FMC1) required for the assembly/stability of yeast mitochondrial F(1)-ATPase in heat stress conditions. *The Journal of Biological Chemistry*, *276*, 6789–6796.
Lemaire, S. D., & Miginiac-Maslow, M. (2004). The thioredoxin superfamily in *Chlamydomonas reinhardtii*. *Photosynthesis Research*, *82*, 203–220.
Levy, S., & Schuster, G. (2016). Polyadenylation and degradation of RNA in the mitochondria. *Biochemical Society Transactions*, *44*, 1475–1482.
Ligas, J., Pineau, E., Bock, R., et al. (2019). The assembly pathway of complex I in *Arabidopsis thaliana*. *The Plant Journal*, *97*, 447–459.
Lill, R. (2009). Function and biogenesis of iron-sulphur proteins. *Nature*, *460*, 831–838.
Lill, R., & Freibert, S.-A. (2020). Mechanisms of mitochondrial iron-sulfur protein biogenesis. *Annual Review of Biochemistry*, *89*, 471–499.
Lino, R., Hasegawa, R., Tabata, K. V., et al. (2009). Mechanism of inhibition by C-terminal alpha-helices of the epsilon subunit of *Escherichia coli* FoF1-ATP synthase. *The Journal of Biological Chemistry*, *284*, 17457–17464.
Lobo-Jarne, T., & Ugalde, C. (2018). Respiratory chain supercomplexes: Structures, function and biogenesis. *Seminars in Cell & Developmental Biology*, *76*, 179–190.
Lown, F. J., Watson, T., & Purton, S. (2001). *Chlamydomonas* nuclear mutants that fail to assemble respiratory or photosynthetic electron transfer complexes. *Biochemical Society Transactions*, *29*, 452–455.
Lu, H., Allen, S., Wardleworth, L., et al. (2004). Functional TIM10 chaperone assembly is redox-regulated in vivo. *The Journal of Biological Chemistry*, *279*, 18952–1895810.
Lytovchenko, O., Naumenko, N., Oeljeklaus, S., et al. (2014). The INA complex facilitates assembly of the peripheral stalk of the mitochondrial F1Fo-ATP synthase. *The EMBO Journal*, *33*, 1624–1638.
Ma, D. P., King, Y. T., Kim, Y., et al. (1992). Amplification and characterization of an inverted repeat from the *Chlamydomonas reinhardtii* mitochondrial genome. *Gene*, *119*, 253–257.
Maio, N., Kim, K. S., Singh, A., et al. (2017). A single adaptable cochaperone-scaffold complex delivers nascent iron-sulfur clusters to mammalian respiratory chain complexes I-III. *Cell Metabolism*, *25*, 945–953, e6.
Maio, N., Singh, A., Uhrigshardt, H., et al. (2014). Cochaperone binding to LYR motifs confers specificity of iron sulfur cluster delivery. *Cell Metabolism*, *19*, 445–457.
Maldonado, M., Padavannil, A., Zhou, L., et al. (2020). Atomic structure of a mitochondrial complex I intermediate from vascular plants. *eLife*, *9*, e56664.
Mansilla, N., Racca, S., Gras, D. E., et al. (2018). The complexity of mitochondrial complex iv: An update of cytochrome c oxidase biogenesis in plants. *International Journal of Molecular Sciences*, *19*, 662.
Martin, G., & Keller, W. (2007). RNA-specific ribonucleotidyl transferases. *RNA*, *13*, 1834–1849.
Massoz, S., Hanikenne, M., Bailleul, B., et al. (2017). In vivo chlorophyll fluorescence screening allows the isolation of a *Chlamydomonas* mutant defective for NDUFAF3, an assembly factor involved in mitochondrial complex I assembly. *The Plant Journal*, *92*, 584–595.
Massoz, S., Larosa, V., Horrion, B., et al. (2015). Isolation of *Chlamydomonas reinhardtii* mutants with altered mitochondrial respiration by chlorophyll fluorescence measurement. *Journal of Biotechnology*, *215*, 27–34.
Massoz, S., Larosa, V., Plancke, C., et al. (2014). Inactivation of genes coding for mitochondrial Nd7 and Nd9 complex I subunits in *Chlamydomonas reinhardtii*. Impact of complex I loss on respiration and energetic metabolism. *Mitochondrion*, *19*, 365–374.
Matagne, R. F., Michel-Wolwertz, M. R., Munaut, C., et al. (1989). Induction and characterization of mitochondrial DNA mutants in *Chlamydomonas reinhardtii*. *The Journal of Cell Biology*, *108*, 1221–1226.
Matouschek, A., Pfanner, N., & Voos, W. (2000). Protein unfolding by mitochondria: The Hsp70 import motor. *EMBO Reports*, *1*, 404–410.
Matus-Ortega, M. G., Salmerón-Santiago, K. G., Flores-Herrera, O., et al. (2011). The alternative NADH dehydrogenase is present in mitochondria of some animal taxa. *Comparative Biochemistry and Physiology. Part D, Genomics & Proteomics*, *6*, 256–263.
Maxwell, D. P., Wang, Y., & McIntosh, L. (1999). The alternative oxidase lowers mitochondrial reactive oxygen production in plant cells. *Proceedings of the National Academy of Sciences of the United States of America*, *96*, 8271–8276.
Meier, S., Neupert, W., & Herrmann, J. M. (2005). Conserved N-terminal negative charges in the Tim17 subunit of the TIM23 translocase play a critical role in the import of preproteins into mitochondria. *The Journal of Biological Chemistry*, *280*, 7777–7785.
Mendel, R. R. (2013). The molybdenum cofactor. *The Journal of Biological Chemistry*, *288*, 13165–13172.
Merchant, S. S., Prochnik, S. E., Vallon, O., et al. (2007). The *Chlamydomonas* genome reveals the evolution of key animal and plant functions. *Science*, *318*, 245–251.
Meyer, E. H., Welchen, E., & Carrie, C. (2019). Assembly of the complexes of the oxidative phosphorylation system in land plant mitochondria. *Annual Review of Plant Biology*, *70*, 23–50.
Michaelis, G., Vahrenholz, C., & Pratje, E. (1990). Mitochondrial DNA of *Chlamydomonas reinhardtii*: The gene for apocytochrome b and the complete functional map of the 15.8 kb DNA. *Molecular & General Genetics: MGG*, *223*, 211–216.
Millar, A. H., Eubel, H., Jänsch, L., et al. (2004). Mitochondrial cytochrome c oxidase and succinate dehydrogenase complexes contain plant specific subunits. *Plant Molecular Biology*, *56*, 77–90.
Millar, A. H., Mittova, V., Kiddle, G., et al. (2003). Control of ascorbate synthesis by respiration and its implications for stress responses. *Plant Physiology*, *133*, 443–447.

Miller, H. K., & Auerbuch, V. (2015). Bacterial iron-sulfur cluster sensors in mammalian pathogens. *Metallomics*, *7*, 943−956.
Miranda-Astudillo, H., Cano-Estrada, A., Vázquez-Acevedo, M., et al. (2014). Interactions of subunits Asa2, Asa4 and Asa7 in the peripheral stalk of the mitochondrial ATP synthase of the chlorophycean alga *Polytomella* sp. *Biochimica et Biophysica Acta*, *1837*, 1−13.
Molen, T. A., Rosso, D., Piercy, S., et al. (2006). Characterization of the alternative oxidase of *Chlamydomonas reinhardtii* in response to oxidative stress and a shift in nitrogen source. *Physiologia Plantarum*, *127*, 74−86.
Monné, M., Daddabbo, L., Gagneul, D., et al. (2018). Uncoupling proteins 1 and 2 (UCP1 and UCP2) fromArabidopsis thaliana are mitochondrial transporters of aspartate, glutamate, and dicarboxylates. *The Journal of Biological Chemistry*, *293*, 4213−4227.
Moosavi, B., Berry, E. A., Zhu, X. L., et al. (2019). The assembly of succinate dehydrogenase: A key enzyme in bioenergetics. *Cellular and Molecular Life Sciences: CMLS*, *76*, 4023−4042.
Morales-Rios, E., Montgomery, M. G., Leslie, A. G. W., et al. (2015). Structure of ATP synthase from *Paracoccus denitrificans* determined by X-ray crystallography at 4.0 Å resolution. *Proceedings of the National Academy of Sciences of the United States of America*, *112*, 13231−13236.
Moseler, A., Aller, I., Wagner, S., et al. (2015). The mitochondrial monothiol glutaredoxin S15 is essential for iron-sulfur protein maturation in *Arabidopsis thaliana*. *Proceedings of the National Academy of Sciences of the United States of America*, *112*, 13735−13740.
Mühleip, A., Kock Flygaard, R., Ovciarikova, J., et al. (2021). ATP synthase hexamer assemblies shape cristae of *Toxoplasma* mitochondria. *Nature Communications*, *12*, 120.
Mühleip, A., McComas, S. E., & Amunts, A. (2019). Structure of a mitochondrial ATP synthase with bound native cardiolipin. *eLife*, *8*, e51179.
Murcha, M. W., Elhafez, D., Millar, A. H., et al. (2005). The C-terminal region of TIM17 links the outer and inner mitochondrial membranes in *Arabidopsis* and is essential for protein import. *The Journal of Biological Chemistry*, *280*, 16476−16483.
Murphy, B. J., Klusch, N., Langer, J., et al. (2019). Rotary substates of mitochondrial ATP synthase reveal the basis of flexible F1-Fo coupling. *Science*, *364*, eaaw9128.
Nasta, V., Suraci, D., Gourdoupis, S., et al. (2020). A pathway for assembling [4Fe-4S]2 + clusters in mitochondrial iron-sulfur protein biogenesis. *The FEBS Journal*, *287*, 2312−2327.
Ndi, M., Marin-Buera, L., Salvatori, R., et al. (2018). Biogenesis of the bc1 complex of the mitochondrial respiratory chain. *Journal of Molecular Biology*, *430*, 3892−3905.
Nedelcu, A. M. (1997). Fragmented and scrambled mitochondrial ribosomal RNA coding regions among green algae: A model for their origin and evolution. *Molecular Biology and Evolution*, *14*, 506−517.
Neupert, W. (1997). Protein import into mitochondria. *Annual Review of Biochemistry*, *66*, 863−917.
Neupert, W., & Herrmann, J. M. (2007). Translocation of proteins into mitochondria. *Annual Review of Biochemistry*, *76*, 723−749.
Ng, S., De Clercq, I., Van., Aken, O., et al. (2014). Anterograde and retrograde regulation of nuclear genes encoding mitochondrial proteins during growth, development, and stress. *Molecular Plant*, *7*, 1075−1093.
Nishimura, Y., Higashiyama, T., Suzuki, L., et al. (1998). The biparental transmission of the mitochondrial genome in *Chlamydomonas reinhardtii* visualized in living cells. *European Journal of Cell Biology*, *77*, 124−133.
Nurani, G., & Franzén, L. G. (1996). Isolation and characterization of the mitochondrial ATP synthase from *Chlamydomonas reinhardtii*. cDNA sequence and deduced protein sequence of the alpha subunit. *Plant Molecular Biology*, *31*, 1105−1116.
Ojala, D., Merkel, C., Gelfand, R., et al. (1980). The tRNA genes punctuate the reading of genetic information in human mitochondrial DNA. *Cell*, *22*, 393−403.
Oster, G., & Wang, H. (2003). Rotary protein motors. *Trends in Cell Biology*, *13*, 114−121.
Ostroukhova, M., Zalutskaya, Z., & Ermilova, E. (2017). New insights into AOX2 transcriptional regulation in *Chlamydomonas reinhardtii*. *European Journal of Protistology*, *58*, 1−8.
Oyedotun, K. S., Sit, C. S., & Lemire, B. D. (2007). The *Saccharomyces cerevisiae* succinate dehydrogenase does not require heme for ubiquinone reduction. *Biochimica et Biophysica Acta*, *1767*, 1436−1445.
Palmieri, L., Picault, N., Arrigoni, R., et al. (2008). Molecular identification of three Arabidopsis thaliana mitochondrial dicarboxylate carrier isoforms: Organ distribution, bacterial expression, reconstitution into liposomes and functional characterization. *The Biochemical Journal*, *410*, 621−629.
Parey, K., Brandt, U., Xie, H., et al. (2018). Cryo-EM structure of respiratory complex I at work. *eLife*, *7*, e39213.
Parey, K., Haapanen, O., Sharma, V., et al. (2019). High-resolution cryo-EM structures of respiratory complex I: Mechanism, assembly, and disease. *Science Advances*, *5*, eaax9484.
Paul, V. D., & Lill, R. (2015). Biogenesis of cytosolic and nuclear iron-sulfur proteins and their role in genome stability. *Biochimica et Biophysica Acta*, *1853*, 1528−1539.
Paumard, P., Vaillier, J., Coulary, B., et al. (2002). The ATP synthase is involved in generating mitochondrial cristae morphology. *The EMBO Journal*, *21*, 221−230.
Payne, M. J., Schweizer, E., & Lukins, H. B. (1991). Properties of two nuclear pet mutants affecting expression of the mitochondrial oli1 gene of Saccharomyces cerevisiae. *Current Genetics*, *19*, 343−351.
Perez-Martínez, X., Antaramian, A., Vazquez-Acevedo, M., et al. (2001). Subunit II of cytochrome c oxidase *in Chlamydomonad algae* is a heterodimer encoded by two independent nuclear genes. *The Journal of Biological Chemistry*, *276*, 11302−11309.
Perez-Martinez, X., Funes, S., Tolkunova, E., et al. (2002). Structure of nuclear-localized cox3 genes in *Chlamydomonas reinhardtii* and in its colorless close relative *Polytomella* sp. *Current Genetics*, *40*, 399−404.

Perez-Martínez, X., Vázquez-Acevedo, M., Tolkunova, E., et al. (2000). Unusual location of a mitochondrial gene. Subunit III of cytochrome c oxidase is encoded in the nucleus of *Chlamydomonad algae*. *The Journal of Biological Chemistry*, *275*, 30144−30152.

Peters, K., Belt, K., & Braun, H. P. (2013). 3D Gel map of *Arabidopsis* complex I. *Frontiers in Plant Science*, *4*, 153.

Petrakis, N., Alcock, F., & Tokatlidis, K. (2009). Mitochondrial ATP-independent chaperones. *IUBMB Life*, *61*, 909−914.

Piller, L., Besagni, C., Ksas, B., et al. (2011). Chloroplast lipid droplet type II NAD(P)H quinone oxidoreductase is essential for prenylquinone metabolism and vitamin K1 accumulation. *Proceedings of the National Academy of Sciences of the United States of America*, *108*, 14354−14359.

Pineau, B., Layoune, O., Danon, A., et al. (2008). L-galactono-1,4-lactone dehydrogenase is required for the accumulation of plant respiratory complex I. *The Journal of Biological Chemistry*, *283*, 32500−32505.

Plancke, C., Vigeolas, H., Höhner, R., et al. (2014). Lack of isocitrate lyase in *Chlamydomonas* leads to changes in carbon metabolism and in the response to oxidative stress under mixotrophic growth. *The Plant Journal*, *77*, 404−417.

Przybyla-Toscano, J., Boussardon, C., Law, S. R., et al. (2021b). Gene atlas of iron-containing proteins in *Arabidopsis* thaliana. *The Plant Journal*, *106*, 258−274.

Przybyla-Toscano, J., Christ, L., Keech, O., et al. (2021a). Iron-sulfur proteins in plant mitochondria: roles and maturation. *Journal of Experimental Botany*, *72*, 2014−2044.

Przybyla-Toscano, J., Roland, M., Gaymard, F., et al. (2018). Roles and maturation of iron-sulfur proteins in plastids. *Journal of Biological Inorganic Chemistry: JBIC: a Publication of the Society of Biological Inorganic Chemistry*, *23*, 545−566.

Ramage, L., Junne, T., Hahne, K., et al. (1993). Functional cooperation of mitochondrial protein import receptors in yeast. *The EMBO Journal*, *12*, 4115−4123.

Rébeillé, F., Alban, C., Bourguignon, J., et al. (2007). The role of plant mitochondria in the biosynthesis of coenzymes. *Photosynthesis Research*, *92*, 149−162.

Remacle, C., Baurain, D., Cardol, P., et al. (2001). Mutants of *Chlamydomonas reinhardtii* deficient in mitochondrial complex I: Characterization of two mutations affecting the nd1 coding sequence. *Genetics*, *158*, 1051−1060.

Remacle, C., Cardol, P., Coosemans, N., et al. (2006). High-efficiency biolistic transformation of *Chlamydomonas* mitochondria can be used to insert mutations in complex I genes. *Proceedings of the National Academy of Sciences of the United States of America*, *103*, 4771−4776.

Remacle, C., Coosemans, N., Jans, F., et al. (2010). Knock-down of the COX3 and COX17 gene expression of cytochrome c oxidase in the unicellular green alga *Chlamydomonas reinhardtii*. *Plant Molecular Biology*, *74*, 223−233.

Rhein, V. F., Carroll, J., Ding, S., et al. (2016). NDUFAF5 hydroxylates NDUFS7 at an early stage in the assembly of human complex I. *The Journal of Biological Chemistry*, *291*, 14851−14860.

Rodríguez-Salinas, E., Remacle, C., & González-Halphen, D. (2012). *Green Algae Genomics. A Mitochondrial Perspective. Epub ahead of print*. Available from https://doi.org/10.1016/B978-0-12-394279-1.00008-9.

Ruprecht, J. J., & Kunji, E. R. S. (2020). The SLC25 mitochondrial carrier family: Structure and mechanism. *Trends in Biochemical Sciences*, *45*, 244−258.

Ryan, R., Grant, D., Chiang, K. S., et al. (1978). Isolation and characterization of mitochondrial DNA from *Chlamydomonas reinhardtii*. *Proceedings of the National Academy of Sciences of the United States of America*, *75*, 3268−3272.

Saada, A., Vogel, R. O., Hoefs, S. J., et al. (2009). Mutations in NDUFAF3 (C3ORF60), encoding an NDUFAF4 (C6ORF66)-interacting complex I assembly protein, cause fatal neonatal mitochondrial disease. *American Journal of Human Genetics*, *84*, 718−727.

Salinas, T., Duby, F., Larosa, V., et al. (2012). Co-evolution of mitochondrial tRNA import and codon usage determines translational efficiency in the green alga *Chlamydomonas*. *PLoS Genetics*, *8*, e1002946.

Salinas, T., Larosa, V., Cardol, P., et al. (2014). Respiratory-deficient mutants of the unicellular green alga *Chlamydomonas*: A review. *Biochimie*, *100*, 207−218.

Salinas-Giegé, T., Cavaiuolo, M., Cognat, V., et al. (2017). Polycytidylation of mitochondrial mRNAs in *Chlamydomonas reinhardtii*. *Nucleic Acids Research*, *45*, 12963−12973.

Sánchez-Caballero, L., Elurbe, D. M., Baertling, F., et al. (2020). TMEM70 functions in the assembly of complexes I and V. *Biochimica et Biophysica Acta*, *1861*, 148202.

Sánchez-Vásquez, L., Vázquez-Acevedo, M., de la Mora, J., et al. (2017). Near-neighbor interactions of the membrane-embedded subunits of the mitochondrial ATP synthase of a chlorophycean alga. *Biochimica et Biophysica Acta*, *1858*, 497−509.

Schaedler, T. A., Thornton, J. D., Kruse, I., et al. (2014). A conserved mitochondrial ATP-binding cassette transporter exports glutathione polysulfide for cytosolic metal cofactor assembly. *The Journal of Biological Chemistry*, *289*, 23264−23274.

Schägger, H., & Pfeiffer, K. (2000). Supercomplexes in the respiratory chains of yeast and mammalian mitochondria. *The EMBO Journal*, *19*, 1777−1783.

Schertl, P., Sunderhaus, S., Klodmann, J., et al. (2012). L-galactono-1,4-lactone dehydrogenase (GLDH) forms part of three subcomplexes of mitochondrial complex I in Arabidopsis thaliana. *The Journal of Biological Chemistry*, *287*, 14412−14419.

Schikowsky, C., Senkler, J., & Braun, H. P. (2017). SDH6 and SDH7 contribute to anchoring succinate dehydrogenase to the inner mitochondrial membrane in Arabidopsis thaliana. *Plant Physiology*, *173*, 1094−1108.

Schimmeyer, J., Bock, R., & Meyer, E. H. (2016). l-Galactono-1,4-lactone dehydrogenase is an assembly factor of the membrane arm of mitochondrial complex I in *Arabidopsis*. *Plant Molecular Biology*, *90*, 117−126.

Schimo, S., Wittig, I., Pos, K. M., et al. (2017). Cytochrome c oxidase biogenesis and metallochaperone interactions: Steps in the assembly pathway of a bacterial complex. *PLoS One*, *12*, e0170037.

Schönfeld, C., Wobbe, L., Borgstädt, R., et al. (2004). The nucleus-encoded protein MOC1 is essential for mitochondrial light acclimation in *Chlamydomonas reinhardtii*. *The Journal of Biological Chemistry*, *279*, 50366−50374.

Schuller, J. M., Saura, P., Thiemann, J., et al. (2020). Redox-coupled proton pumping drives carbon concentration in the photosynthetic complex I. *Nature Communications*, *11*, 494.

Senkler, J., Senkler, M., & Braun, H. P. (2017a). Structure and function of complex I in animals and plants - a comparative view. *Physiologia Plantarum*, *161*, 6−15.

Senkler, J., Senkler, M., Eubel, H., et al. (2017b). The mitochondrial complexome of *Arabidopsis thaliana*. *The Plant Journal*, *89*, 1079−1092.

Sheftel, A. D., Stehling, O., Pierik, A. J., et al. (2009). Human ind1, an iron-sulfur cluster assembly factor for respiratory complex I. *Molecular and Cellular Biology*, *29*, 6059−6073.

Sheftel, A. D., Wilbrecht, C., Stehling, O., et al. (2012). The human mitochondrial ISCA1, ISCA2, and IBA57 proteins are required for [4Fe-4S] protein maturation. *Molecular Biology of the Cell*, *23*, 1157−1166.

Sluse, F. E., Jarmuszkiewicz, W., Navet, R., et al. (2006). Mitochondrial UCPs: New insights into regulation and impact. *Biochimica et Biophysica Acta*, *1757*, 480−485.

Smith, D. R., & Craig, R. J. (2021). Does mitochondrial DNA replication in *Chlamydomonas* require a reverse transcriptase? *The New Phytologist*, *229*, 1192−1195.

Soto, I. C., & Barrientos, A. (2016). Mitochondrial cytochrome c oxidase biogenesis is regulated by the redox state of a heme-binding translational activator. *Antioxidants & Redox Signaling*, *24*, 281−298.

Soto, I. C., Fontanesi, F., Liu, J., et al. (2012). Biogenesis and assembly of eukaryotic cytochrome c oxidase catalytic core. *Biochimica et Biophysica Acta*, *1817*, 883−897.

Soufari, H., Parrot, C., Kuhn, L., et al. (2020). Specific features and assembly of the plant mitochondrial complex I revealed by cryo-EM. *Nature Communications*, *11*, 5195.

Spikes, T. E., Montgomery, M. G., & Walker, J. E. (2020). Structure of the dimeric ATP synthase from bovine mitochondria. *Proceedings of the National Academy of Sciences of the United States of America*, *117*, 23519−23526.

Srinivasan, V., Pierik, A. J., & Lill, R. (2014). Crystal structures of nucleotide-free and glutathione-bound mitochondrial ABC transporter Atm1. *Science*, *343*, 1137−1140.

Stewart, A. G., Lee, L. K., Donohoe, M., et al. (2012). The dynamic stator stalk of rotary ATPases. *Nature Communications*, *3*, 687.

Strand, D. D., D'Andrea, L., & Bock, R. (2019). The plastid NAD(P)H dehydrogenase-like complex: structure, function and evolutionary dynamics. *The Biochemical Journal*, *476*, 2743−2756.

Stroud, D. A., Surgenor, E. E., Formosa, L. E., et al. (2016). Accessory subunits are integral for assembly and function of human mitochondrial complex I. *Nature*, *538*, 123−126.

Subrahmanian, N., Castonguay, A. D., Remacle, C., et al. (2020). Assembly of mitochondrial complex I requires the low-complexity protein AMC1 in *Chlamydomonas reinhardtii*. *Genetics*, *214*, 895−911.

Subrahmanian, N., Remacle, C., & Hamel, P. P. (2016). Plant mitochondrial complex I composition and assembly: A review. *Biochimica et Biophysica Acta*, *1857*, 1001−1014.

Sun, F., Huo, X., Zhai, Y., et al. (2005). Crystal structure of mitochondrial respiratory membrane protein complex II. *Cell*, *121*, 1043−1057.

Sunderhaus, S., Dudkina, N. V., Jansch, L., et al. (2006). Carbonic anhydrase subunits form a matrix-exposed domain attached to the membrane arm of mitochondrial complex I in plants. *The Journal of Biological Chemistry*, *281*, 6482−6488.

Suzuki, T., Tanaka, K., Wakabayashi, C., et al. (2014). Chemomechanical coupling of human mitochondrial F1-ATPase motor. *Nature Chemical Biology*, *10*, 930−936.

Sweetman, C., Waterman, C. D., Rainbird, B. M., et al. (2019). AtNDB2 is the main external NADH dehydrogenase in mitochondria and is important for tolerance to environmental stress. *Plant Physiology*, *181*, 774−788.

Szyrach, G., Ott, M., Bonnefoy, N., et al. (2003). Ribosome binding to the Oxa1 complex facilitates co-translational protein insertion in mitochondria. *The EMBO Journal*, *22*, 6448−6457.

Takeda, H., Tsutsumi, A., Nishizawa, T., et al. (2021). Mitochondrial sorting and assembly machinery operates by β-barrel switching. *Nature*, *12*, 1−7.

Tardif, M., Atteia, A., Specht, M., et al. (2012). Predalgo: A new subcellular localization prediction tool dedicated to green algae. *Molecular Biology and Evolution*, *29*, 3625−3639.

Terashima, M., Specht, M., Naumann, B., et al. (2010). Characterizing the anaerobic response of *Chlamydomonas reinhardtii* by quantitative proteomics. *Molecular & Cellular Proteomics*, *9*, 1514−1532.

Thompson, K., Mai, N., Oláhová, M., et al. (2018). *OXA 1L* mutations cause mitochondrial encephalopathy and a combined oxidative phosphorylation defect. *EMBO Molecular Medicine*, *10*, e9060.

Timón-Gómez, A., Nývltová, E., Abriata, L. A., et al. (2018). Mitochondrial cytochrome c oxidase biogenesis: Recent developments. *Seminars in Cell & Developmental Biology*, *76*, 163−178.

Truscott, K. N., Kovermann, P., Geissler, A., et al. (2001). A presequence- and voltage-sensitive channel of the mitochondrial preprotein translocase formed by Tim23. *Nature Structural & Molecular Biology*, *8*, 1074−1082.

Tzagoloff, A., Barrientos, A., Neupert, W., et al. (2004). Atp10p assists assembly of Atp6p into the F0 unit of the yeast mitochondrial ATPase. *The Journal of Biological Chemistry*, *279*, 19775−19780.

Uzarska, M. A., Dutkiewicz, R., Freibert, S.-A., et al. (2013). The mitochondrial Hsp70 chaperone Ssq1 facilitates Fe/S cluster transfer from Isu1 to Grx5 by complex formation. *Molecular Biology of the Cell*, *24*, 1830−1841.

Vahrenholz, C., Riemen, G., Pratje, E., et al. (1993). Mitochondrial DNA of *Chlamydomonas reinhardtii*: The structure of the ends of the linear 15.8-kb genome suggests mechanisms for DNA replication. *Current Genetics*, *24*, 241−247.

van Lis, R., Atteia, A., Mendoza-Hernández, G., et al. (2003). Identification of novel mitochondrial protein components of *Chlamydomonas reinhardtii*. A proteomic approach. *Plant Physiology*, *132*, 318−330.

van Lis, R., Brugière, S., Baffert, C., et al. (2020). Hybrid cluster proteins in a photosynthetic microalga. *The FEBS Journal*, *287*, 721−735.

Van Lis, R., Mendoza-Hernández, G., Groth, G., et al. (2007). New insights into the unique structure of the F0F 1-ATP synthase from the chlamydomonad algae Polytomella sp. and *Chlamydomonas reinhardtii*. *Plant Physiology*, *144*, 1190−1199.

van Raaij, M. J., Orriss, G. L., Montgomery, M. G., et al. (1996). The ATPase inhibitor protein from bovine heart mitochondria: The minimal inhibitory sequence. *Biochemistry*, *35*, 15618−15625.

Vazquez-Acevedo, M., Cardol, P., Cano-Estrada, A., et al. (2006). The mitochondrial ATP synthase of chlorophycean algae contains eight subunits of unknown origin involved in the formation of an atypical stator-stalk and in the dimerization of the complex. *Journal of Bioenergetics and Biomembranes*, *38*, 271−282.

Vázquez-Acevedo, M., Vega-deLuna, F., Sánchez-Vásquez, L., et al. (2016). Dissecting the peripheral stalk of the mitochondrial ATP synthase of chlorophycean algae. *Biochimica et Biophysica Acta*, *1857*, 1183−1190.

Villavicencio-Queijeiro, A., Pardo, J. P., & González-Halphen, D. (2015). Kinetic and hysteretic behavior of ATP hydrolysis of the highly stable dimeric ATP synthase of Polytomella sp. *Archives of Biochemistry and Biophysics*, *575*, 30−37.

Vinogradova, E., Salinas, T., Cognat, V., et al. (2009). Steady-state levels of imported tRNAs in *Chlamydomonas* mitochondria are correlated with both cytosolic and mitochondrial codon usages. *Nucleic Acids Research*, *37*, 1521−1528.

Vinothkumar, K. R., Zhu, J., & Hirst, J. (2014). Architecture of mammalian respiratory complex I. *Nature*, *515*, 80−84.

Vögtle, F. N., Wortelkamp, S., Zahedi, R. P., et al. (2009). Global analysis of the mitochondrial N-proteome identifies a processing peptidase critical for protein stability. *Cell*, *139*, 428−439.

von Heijne, G., Stepphuhn, J., & Herrmann, R. G. (1989). Domain structure of mitochondrial and chloroplast targeting peptides. *European Journal of Biochemistry*, *180*, 535−545.

Vozza, A., Parisi, G., De Leonardis, F., et al. (2014). UCP2 transports C4 metabolites out of mitochondria, regulating glucose and glutamine oxidation. *Proceedings of the National Academy of Sciences of the United States of America*, *111*, 960−965.

Wächter, A., Bi, Y., Dunn, S. D., et al. (2011). Two rotary motors in F-ATP synthase are elastically coupled by a flexible rotor and a stiff stator stalk. *Proceedings of the National Academy of Sciences of the United States of America*, *108*, 3924−3929.

Walker, J. E., & Dickson, V. K. (2006). The peripheral stalk of the mitochondrial ATP synthase. *Biochimica et Biophysica Acta*, *1757*, 286−296.

Waller, J. C., Ellens, K. W., Alvarez, S., et al. (2012). Mitochondrial and plastidial COG0354 proteins have folate-dependent functions in iron-sulphur cluster metabolism. *Journal of Experimental Botany*, *63*, 403−411.

Waltz, F., & Giegé, P. (2020). Striking diversity of mitochondria-specific translation processes across eukaryotes. *Trends in Biochemical Sciences*, *45*, 149−162.

Waltz, F., Salinas-Giegé, T., Englmeier, R., et al. (2021). How to build a ribosome from RNA fragments in *Chlamydomonas* mitochondria. *Nature Communications*, *12*, 7176.

Wang, Z. G., White, P. S., & Ackerman, S. H. (2001). Atp11p and Atp12p are assembly factors for the F(1)-ATPase in human mitochondria. *The Journal of Biological Chemistry*, *276*, 30773−30778.

Waterhouse, A., Bertoni, M., Bienert, S., et al. (2018). SWISS-MODEL: Homology modelling of protein structures and complexes. *Nucleic Acids Research*, *46*, W296−W303.

Weger, H. G., Guy, R. D., & Turpin, D. H. (1990). Cytochrome and alternative pathway respiration in green algae : measurements using inhibitors and o(2) discrimination. *Plant Physiology*, *93*, 356−360.

Weiler, B. D., Brück, M.-C., Kothe, I., et al. (2020). Mitochondrial [4Fe-4S] protein assembly involves reductive [2Fe-2S] cluster fusion on ISCA1-ISCA2 by electron flow from ferredoxin FDX2. *Proceedings of the National Academy of Sciences of the United States of America*, *117*, 20555−20565.

Willmund, F., Dorn, K. V., Schulz-Raffelt, M., et al. (2008). The chloroplast DnaJ homolog CDJ1 of *Chlamydomonas reinhardtii* is part of a multichaperone complex containing HSP70B, CGE1, and HSP90C. *Plant Physiology*, *148*, 2070−2082.

Wobbe, L., & Nixon, P. J. (2013). The mTERF protein MOC1 terminates mitochondrial DNA transcription in the unicellular green alga *Chlamydomonas reinhardtii*. *Nucleic Acids Research*, *41*, 6553−6567.

Wydro, M. M., Sharma, P., Foster, J. M., et al. (2013). The evolutionarily conserved iron-sulfur protein INDH is required for complex I assembly and mitochondrial translation in *Arabidopsis* [corrected]. *The Plant Cell*, *25*, 4014−4027.

Yadav, K. N. S., Miranda-Astudillo, H. V., Colina-Tenorio, L., et al. (2017). Atypical composition and structure of the mitochondrial dimeric ATP synthase from *Euglena gracilis*. *Biochimica et Biophysica Acta*, *1858*, 267−275.

Yankovskaya, V., Horsefield, R., Törnroth, S., et al. (2003). Architecture of succinate dehydrogenase and reactive oxygen species generation. *Science*, *299*, 700−704.

Zalutskaya, Z., Filina, V., Ostroukhova, M., et al. (2018). Regulation of alternative oxidase 1 in *Chlamydomonas reinhardtii* during sulfur starvation. *European Journal of Protistology*, *63*, 26−33.

Zalutskaya, Z., Lapina, T., & Ermilova, E. (2015). The *Chlamydomonas reinhardtii* alternative oxidase 1 is regulated by heat stress. *Plant Physiology and Biochemistry*, *97*, 229–234.

Zalutskaya, Z., Ostroukhova, M., Filina, V., et al. (2017). Nitric oxide upregulates expression of alternative oxidase 1 in *Chlamydomonas reinhardtii*. *Journal of Plant Physiology*, *219*, 123–127.

Zeng, X., Neupert, W., & Tzagoloff, A. (2007). The metalloprotease encoded by ATP23 has a dual function in processing and assembly of subunit 6 of mitochondrial ATPase. *Molecular Biology of the Cell*, *18*, 617–626.

Zhu, J., Vinothkumar, K. R., & Hirst, J. (2016). Structure of mammalian respiratory complex I. *Nature*, *536*, 354–358.

Zickermann, V., Wirth, C., Nasiri, H., et al. (2015). Mechanistic insight from the crystal structure of mitochondrial complex I. *Science*, *5*, 4–10.

Zíková, A., Schnaufer, A., Dalley, R. A., et al. (2009). The F0F1-ATP synthase complex contains novel subunits and is essential for procyclic *Trypanosoma brucei*. *PLoS Pathogens*, *5*, e1000436.

Zimmer, S. L., Fei, Z., & Stern, D. B. (2008). Genome-based analysis of *Chlamydomonas reinhardtii* exoribonucleases and poly(A) polymerases predicts unexpected organellar and exosomal features. *Genetics*, *179*, 125–136.

Zimmer, S. L., Schein, A., Zipor, G., et al. (2009). Polyadenylation in *Arabidopsis* and *Chlamydomonas* organelles: The input of nucleotidyltransferases, poly(A) polymerases and polynucleotide phosphorylase. *The Plant Journal*, *59*, 88–99.

Further reading

Mimaki, M., Wang, X., McKenzie, M., et al. (2012). Understanding mitochondrial complex I assembly in health and disease. *Biochimica et Biophysica Acta*, *1817*, 851–862.

Vogel, R. O., Smeitink, J. A. M., & Nijtmans, L. G. J. (2007). Human mitochondrial complex I assembly: A dynamic and versatile process. *Biochimica et Biophysica Acta*, *1767*, 1215–1227.

Zhu, J., King, M. S., Yu, M., et al. (2015). Structure of subcomplex Ibeta of mammalian respiratory complex I leads to new supernumerary subunit assignments. *Proceedings of the National Academy of Sciences of the United States of America*, *112*, 12087–12092.